Article:
Terkes, Musa, Demirci, Alpaslan, Gokalp, Erdin et al. (1 more author) (2024) Battery Passport for Second-Life Batteries:Potential Applications and Challenges. IEEE Access. pp. 128424-128467. ISSN 2169-3536

https://doi.org/10.1109/ACCESS.2024.3450790

IEEE Access
Multidisciplinary | Rapid Review | Open Access Journal

Received 5 August 2024, accepted 21 August 2024, date of publication 30 August 2024, date of current version 19 September 2024.

Digital Object Identifier 10.1109/ACCESS.2024.3450790

TOPICAL REVIEW

Battery Passport for Second-Life Batteries: Potential Applications and Challenges

MUSA TERKES[1], ALPASLAN DEMIRCI[1], (Member, IEEE), ERDIN GOKALP[1], AND UMIT CALI[2,3], (Senior Member, IEEE)

[1]Department of Electrical Engineering, Yildiz Technical University, 34349 Istanbul, Türkiye
[2]Department of Electric Energy, Norwegian University of Science and Technology, 7034 Trondheim, Norway
[3]School of Physics, Engineering and Technology, University of York, YO10 5DD York, U.K.

Corresponding author: Umit Cali (umit.cali@ntnu.no)

ABSTRACT The capacity of electric vehicle batteries degrades depending on users' driving and charging behaviors and operating conditions. Degraded batteries can provide energy and power to second-use applications as energy storage. However, the feasibility of a second-life battery strongly depends on price and technical properties such as the remaining capacity, temperature, and cycle life. Besides, new battery production needs intensive mining, leading to extensive water and electricity consumption and carbon emissions. Therefore, second-life applications can extend existing storage and balance the needs of numerous new batteries, whose prices are intensively related to political, economic, ethnic, and social factors. This review investigates the critical phases, economics, market, problems, future importance of new production, second life, and recycling, and reveals potential challenges and solutions. Moreover, battery chemistries are compared using comprehensive terminology. Three selected battery models commonly used in research are mathematically described and compared. Recent advances in thermal modeling are mathematically discussed, and the experimental methodology for state of health estimation and battery model parameterization is detailed. End-of-life estimation methods are discussed, and the often neglected state of function phenomenon is expressed mathematically. Standards, regulations, second-life application areas, recycling process, and precious metal market are briefly explained. In addition, a blockchain perspective is suggested for untraceable raw data in the cradle-to-grave battery cycle. Developing artificial intelligence-based data processing empowered by blockchain to enhance battery features further may help sustainable development and clean energy utilization.

INDEX TERMS Second-life battery, recycling, battery technology, electric vehicles, energy storage systems.

NOMENCLATURE

i_{bat}	DC current provided to the battery.
i_{bat}^{+}	The charge current.
i_{bat}^{-}	The discharge current.
υ_1	The $1^s t$ order model voltage.
R_1	Equivalent circuit resistor parameter.
C_1	Equivalent circuit capacitor parameter.
υ_2	The $2^n d$ order model voltage.
R_2	Equivalent circuit resistor parameter.
C_2	Equivalent circuit capacitor parameter.
υ_{oc}	Open circuit voltage.
R_0	Equivalent circuit resistor parameter.
a_{0-5}	Equivalent circuit model sensitivity parameter.
R_S	Series internal resistance.
b_{0-5}	Equivalent circuit model sensitivity parameter.
R_{ts}	First component estimated to determine the total internal resistance.
R_{tl}	Second component estimated to determine the total internal resistance.
R_{tot}	Total internal resistance of the battery.
P_e	Electrical power of the battery.
c_0, c_1, c_2	Equivalent circuit model sensitivity parameter.

The associate editor coordinating the review of this manuscript and approving it for publication was Atri Bera.

d_0, d_1, d_2	Equivalent circuit model sensitivity parameter.
η_{chr}	Battery charge efficiency.
η_{disch}	Battery discharge efficiency.
T_i	The time to discharge at constant current.
K	A fixed constant.
C_i	The battery capacity in ampere-hour.
C_n	Battery capacity.
I_n^*	Conjugate of discharge rate.
I_i	The battery capacity in ampere-hour at a given discharge rate.
Δt	Time interval.
c_i^s	The solid phase lithium concentration.
r	ButlerVolmer kinetics constant.
$D_{s,i}$	The diffusion coefficient for the electrode.
k_i	The reaction rate constant for intercalation or deintercalation.
$c_{max,i}^s$	The maximum solid phase concentration of the electrode.
F	Faraday constant.
ϕ_1	The solid phase potential.
ϕ_2	The liquid phase potential.
U_i	The open circuit potential.
j_i	The flux into the electrode particle.
$P(t)$	Power to/from the battery at time t.
E_{wh}	Battery energy capacity.
$u(t)$	Control variables in optimization n at time t.
$x(t)$	State variables at time t.
$\lambda(t)$	Wholesale electricity price at time t.
N	Number of cells in the battery.
$E_{lost,Wh}$	Lost battery energy capacity.
T_{end}	Total simulation time.
$\lambda_{degrad,Wh}$	Cost of battery charge degradation.
R_p	Parallel resistor in the equivalent circuit model.
C_p	Parallel capacitor in equivalent circuit model.
$I_r(t)$	Current through the parallel resistor in the equivalent circuit model.
$I(t)$	Battery current at time t.
$z(t)$	State of charge at time t.
E_{Ah}	Battery charge capacity.
V_{mean}	Mean battery voltage.
$\phi_{s,1}$	The initial solid potential.
β	Degradation parameter in equivalent circuit model.
$\lambda_{degrad,Ah}$	Cost of battery charge degradation.
υ_n	The effective electrode volume.
δ_n	The negative electrode thickness.
$\varepsilon_{s;n}$	The solid-phase volume fraction of negative electrode.
R_S	Series resistor in the equivalent circuit model.
A	The electrode plate area.
$\varepsilon_{s;p}$	The solid-phase volume fraction of positive electrode.
υ_p	The volume of a single sphere.
$\upsilon_n^{\Delta x}, \upsilon_p^{\Delta x}$	Number of spherical particles of the electrodes.
n, p	A battery constant determined by the battery technology.
N_n	The cell is discretized along x for the negative electrode.
N_p	The cell is discretized along x for the positive electrode.
δ_p	The positive electrode thickness.
j_m^{Li}	The molar flux.
α_s	The seperator transfer coefficient.
j_0	The exchange current density.
P_{max}^{disch}	Maximum discharge power of the battery.
$P_d(t)$	Instantaneous demanded power.
P_{max}	Maximum battery output power.
$P(t)$	Instantaneous battery output power.
υ_{bat}	Battery terminal voltage.
V_{oc}	The open collector voltage.
SOF_{safety}	The state of function based on safety.
SOF_{Ri}	The state of function based on internal resistance.
$I_{max,cur}^{disch}$	The maximum discharge current of the maximum battery current.
P_{max}^{chr}	Maximum charge power of the battery.
α_c	The cathodic transfer coefficient.
$\phi_{s,m}$	Solid potential.
$\phi_{e,m}$	Electrolyte potential.
$c_{s,(m,N_r)}$	A nonlinear function of the surface concentration.
$i_{s,m}$	The electronic current in solid phase.
$i_{e,m}$	The ionic current in electrolyte phase.
Δx_m	A collection of active material spherical particles.
R_f	The electrode surface film resistance.
N_r	The cell is discretized along r for any type of the electrode.
r_p	The radius of the p$^t h$ discretized element.
$\psi(T)$	The generic parameter.
ψ_{act}	The value of the parameter at the reference temperature.
E_{act}^{ψ}	The activation energy for the parameter ψ.
T_{act}	The actual temperature.
C_{EOL}	The battery capacity at the end-of-life.
C	Instantaneous battery capacity considering aging.
α_a	The anodic transfer coefficient.
η_m	The reaction overpotential.
Ri_{EOL}	The end-of-life value of the internal resistance.
Ri_{BOL}	The beginning of life value of the internal resistance.
Ri, R_0	The current value of the internal resistance.
X_i	The current value of the safety indicators.
$X_{i,EOL}$	The end-of-life value of the safety indicators.
$X_{i,BOL}$	The beginning of life value of the safety indicators.
P_{min}^{chr}	The minimum charge power of the battery.

P_{max}^{disch}	The maximum discharge power of the battery.
P_{min}	The power design limits of the battery.
P_{max}	The power design limits of the battery.
$U_{t,k+L}$	The predicted terminal voltage at index k+L.
I_{min}^{chr}	The minimum continuous charging current.
I_{max}^{disch}	The maximum continuous discharging current.
$I_{max,vol}^{chr}$	The maximum charge current of the maximum battery voltage.
$I_{max,vol}^{disch}$	The maximum discharge current of the maximum battery voltage.
U_{min}	The minimum terminal voltage of the battery.
U_{max}	The maximum terminal voltage of the battery.
I_{max}^{chr}	Maximum charge current of the battery.
I_{max}^{disch}	Maximum discharge current of the battery.
$I_{max,cur}^{chr}$	The maximum charge current of the maximum battery current.
SOF_{cap}	The state of function based on battery capacity.

ABBREVIATIONS

SEI	Solid electrolyte interphase layer.
HEV	Hybrid electric vehicle.
OCV	Open circuit voltage.
DOD	Depth of discharge (%).
P2D	The pseudo-two-dimensional or partial differential battery model.
SOC	State of charge (%).
EV	Electric vehicle.
ECM	The equivalent circuit battery model.
BMS	Battery energy management system.
SLB	Second-life battery.
FB	Fresh battery.
ESS	Energy storage systems.
LCO	Lithium cobalt oxide.
LFP	Lithium iron phosphate.
LTO	Lithium titanium-oxide.
NCM	Nickel-cadmium manganese.
NCA	Nickel cobalt aluminum oxide.
LLI	The loss of lithium-ion inventory.
LAM	The loss of active materials.
SOH	State of health.
RUL	Remaining useful life.
OEM	Original equipment manufacturer.
EOL	End-of-life.
SOF	State of function.
EIS	Electrochemical impedance spectroscopy.
ICA	Incremental capacity analysis.
TIG	Tungsten inert gas.
SVM	Support vector machine.
HI	Health indicators.
SOT	State of temperature.
RES	Renewable energy system.
RTO	Recovery time objective.
COE	Cost of energy ($/kWh).
NiMh	Nickel metal hydride.
LMO	Lithium manganese oxide.
LMT	Light means of transport.
UL	Underwriters Laboratories.
HESS	Hybrid energy storage system.
BOL	Beginning of lifetime.

I. INTRODUCTION

To achieve net zero emission targets, transportation, residences, and other areas, incentives and interest in clean energy alternatives are increasing daily. Adopting electric vehicles (EVs) in significant polluting transportation is promising. Additionally, the share of EVs in the automobile market has risen to 18% with the technology developing day by day. Conventional power plants supply the grid and are responsible for 73% of air pollution. Thus, renewable technologies have reduced grid dependency by up to 42% [1], [2], [3]. Considering that primary electricity demand will have increased by 50% by 2050, its 88% share of renewables in power generation is likely to be supported by the growing EV market [4]. More precisely, energy storage systems (ESS), which can also use dismounted EV batteries, support clean energy technologies that increase system performance and reduce overall costs. Also, ESS use is expanding daily due to its improving performance. Thus, an increase of 787.5 billion $ is expected by 2050 in batteries, which currently have a market of 44.5 billion $ [3], [4], [5], [6]. Also, the production of EV batteries is increasing by 3% yearly [7]. EV batteries, whose market volumes are growing significantly, will not be able to satisfy users in terms of performance due to aging over time. The pile of batteries removed from vehicles can be a severe problem. While precious metals can be recovered in recycling, the battery landfill must be managed appropriately. Battery production volumes will increase due to the popularity of EV fleets in transportation electrification. Therefore, mining, carbon emissions, and electricity consumption in production will increase, and a large battery landfill cannot be avoided. Today's initial focus is to allow retired vehicle batteries to be used in reuse applications to address many more issues. After the first life for power performance, EV batteries can be evaluated for their energy performance in less demanding second-life applications. Production volume pressure can be reduced by extending the circular supply chain for batteries. Useful lifetimes will increase the return on investment for many investors and delay inefficient business models regarding recycling costs.

A. PROBLEM FORMULATION

The cradle-to-grave journey of EV batteries encounters many uncertainties. The uncertain aging development process in the internal structure of different chemistries prevents the formation of a clear idea. For this reason, the reuse processes of EV battery cells, which will be considered second life, vary. Labor efforts, testing, and balancing procedures lead to different selling prices. In addition, the purchase prices of robust cells are relatively higher. Financial uncertainty

also creates an environment of insecurity in stationary storage investments. Initial capacities and increased internal resistance are unpredictable and may not guarantee the desired supply-demand match. Sensitive aspects such as ambient temperature, charging and discharging current, state of charge (SOC), and thus depth of discharge (DOD) are under user control during the first use. Therefore, it may be utilized less than desired as it directly impacts the second use due to the circular chain. A similar process of technical and economic uncertainty is encountered in the transition to recycling. Is this idea of technological development in reuse worth implementing? Is it necessary to stop producing and give life another chance? Is this just an expectation or a reality that will shape the future? While existing projects and commercial products are already on the market, many challenges need to be overcome, and the many advantages of second life have been repeatedly proven in the literature. However, there are still vague ideas, and this is not yet a mature issue. The first and second-use processes in the circular battery chain and the subsequent recycling business models must be managed and appropriately evaluated by many stakeholders in the sector. Creating a large pool of ideas is essential, especially for investors and researchers interested in joining this sector. This review article is inspired by the pros and cons, current situation, technological developments, market, and future directions at each stage of the EV battery journey without going into the production process.

B. LITERATURE REVIEW

Batteries are removed from EVs when driving performance declines and customer dissatisfaction begins, depending on the initial usage profile. After being removed from EV and separated into cells, they are repackaged by removing heterogeneity using various methods for second-life applications. It is predicted that second-life batteries (SLBs), whose application area is gradually expanding, can reduce the global temperature concern. For example, battery production of 1 kWh causes about 55 kg of emission of CO_2 and electricity consumption of 50-65 kWh [8]. For producing 1 ton of lithium-ion, approximately 250 tons of mineral ore or 750 tons of mineral-rich brine is collected [9], and 1,900 tons of water is consumed [10]. Thus, recycling high precious metal content at the cathode of SLBs is critical when the lifespan ends in 8-15 years. In this context, it is estimated that 250,000 metric tons of EV lithium-ion batteries will be recycled by 2025 [11]. Although high-volume recycling is thought to make the circular economy profitable, only 40-50% of the investment is recovered [12]. However the technical and financial return of recycling is relatively low, these reasons will make it worthwhile. Researchers have repeatedly proven that SLBs provide useful outputs, with developed new strategies in large-scale and small-scale networks depending on the variety of use cases. Furthermore, the well-known advantages of SLB over fresh battery (FB) may not always be valid. Therefore, the general advantages and limitations of SLB need to be discussed and, contrary to popular belief, the advantages of FB need to be emphasized. Thus, Table 1 summarizes SLB's unpredictable behavior and details the results of studies arguing that SLB has an advantage or disadvantage over FB or that its advantage is conditional. The table shows that the trade-off between first and second use will directly affect recycling processes and investment ideas. Therefore, carefully reviewing each stage of the circular chain is critical.

C. RESEARCH ELABORATION

Recently, many studies have focused on the immature second-life issue and, more broadly, on the battery circular economy and supply chain. Table 2 summarizes the subject matter and content of the (reputable) publications selected by the authors. Many critical topics, such as technological developments, problems and solutions, business models, future directions, market forecasts, and labor-related reuse preparation processes, are addressed in these studies. However, many of these issues have yet to be considered at each stage of the battery circular chain (first use, second life, and recycling). In particular, there are cases where these issues have been addressed superficially. Regarding proposed solutions, the battery passport needs to be addressed. Also, it can be emphasized that the feasibility trade-offs between FB and SLB should be addressed. Another shortcoming is that the technological superiority in battery chemistries is not considered an issue that needs to be addressed, even though it is a known fact. Other neglected issues are the state of function (SOF) phenomenon, which needs to be discussed in end-of-life forecasts, the lack of support for market forecasts by reputable global reports, and the lack of explanation of the precious metals market in recycling. The lack of detailed explanation of the most reputable models proposed by researchers for batteries and the subsequent mention of the aging mechanism also creates an unreliable opinion environment. The life cycle of EV battery is briefly summarized in Figure 1. Accordingly, the original contributions of this paper are as follows:

- SLB research should address the cradle-to-grave journey of EV batteries, completing the chain from first life to recycling. For each stage, the scope was detailed with technical, economic, and environmental developments, potential markets, and future projections.
- Different battery technologies and first-life markets are considered, and battery models that can be used to characterize and degrade batteries are examined.
- Recent advances in thermal modeling are mathematically discussed, and the experimental methodology for SOH estimation and battery model parameterization is detailed.
- Commonly used definitions and standards for second-life batteries are given, as are details of the preparation process.
- Precise parameters and predictions for the degradation process and detecting the second-life transition are also

TABLE 1. SLB's changeable behavior.

Reference	What is claiming?			Notable details of the study results
	1^{st}	2^{nd}	3^{rd}	
[13]	✓			Reducing peak demand in power systems
[14]	✓			Ensuring economic network resilience
[15]	✓			Troubleshooting networked challenges
[16]	✓			Increasing self-sufficiency in behind-the-meter
[17]	✓			Increasing self-consumption for small prosumers
[18, 19]	✓			Reducing the investment payback period in rural islands
[20]	✓			Reducing total cost and carbon footprint in smart homes
[21]	✓			Reducing electricity bill
[22]	✓			Reducing total cost in smart microgrids
[23]	✓			Providing economic EV charge control
[24]	✓			Reducing carbon emissions
[25]	✓			Reducing grid dependency
[26, 27]	✓			Reducing global warming
[28, 29]	✓			Extending EV battery life
[30]	✓			Reducing capacity loss and improving economic performance via energy management strategies
[31–33]	✓			Reducing levelized cost of energy (LCOE) and increasing revenue
[34]	✓			Reducing total cost even at low DODs
[35]	✓			Reducing carbon emissions in a sustainable future vision
[36]	✓			Reducing the total cost of charging at hybrid battery swapping stations
[37]	✓			Increasing throughput in residential and commercial buildings
[38]		✓		More rapid decrease in battery prices compared to wind energy
[39]		✓		Carbon emissions must remain below 113 tCO_2eq/kWh
[40]		✓		Reducing the cost of the plug-in hybrid EV (PHEV) battery to 5.71 \$/kWh or increasing the carbon penalty to 70.34 \$/tonne
[41]		✓		Wind speed, solar radiation and FIT values lower than 4.7 m/s, 3 kWh/m^2/day and 0.035 \$/kWh
[42]		✓		Providing reuse costs ranging from 27.2-38.3 €/kWh
[43]		✓		In the electricity market, renewable buildings should cost less than 214 \$/kWh compared to the FB of 400 \$/kWh
[44]		✓		Planning DOD around 85% for residential buildings with EVs
[45]		✓		Subsidising CAPEX or OPEX
[46]		✓		Implementing a 60 $/tCO_2eq penalty for carbon emissions in payment for lower electricity prices
[47]			✓	Higher levelized cost of storage (LCOS)
[48]			✓	Negative purchasing costs and higher payback periods
[49]			✓	Inability to reduce the peak voltage in the network despite the increase in capacity
[50]			✓	Low economic returns in P2P energy trading including degradation costs

1^{st}: SLB has superiority against FB ; **2^{nd}:** SLB's superiority in feasibility performance depends on specific conditions ; **3^{rd}:** SLB is not superior against FB.

under discussion. Second-life application areas, barriers and market are other issues included in the review.
- In recycling, the methods by which the chemical components are to be obtained are analyzed and their market value is examined as in the other stages.
- Discussing critical obstacles in the basic battery supply chain, proposals are made to overcome them, including blockchain, hybrid energy storage and battery passports.

The organization of this article is as follows. Section II describes EV battery chemistry, technologies, and modeling. Section III explains definitions of the second-life, preparation processes, degradation critiques, and applications. Section IV summarizes the recycling process, giving descriptions of significant steps. In Section V and VI, explain the barriers and the solution proposals can be applied to the cyclic battery chain respectively, and Section VII mentions the conclusions and inferences.

II. LITHIUM-ION BATTERY TECHNOLOGY

Reducing CO_2 using low-carbon electricity sources is the primary goal when producing a battery. For this purpose, the cathode mixed with binder, solvent, and additives is plated with aluminum, and the anode is covered with copper foil on the current collector. The cathode and anode electrodes are

TABLE 2. The review's motivation and originality.

Ref.	Subject matter and content	
[51]	• Explain the SLB reuse process, the technology implications and policies required.	• FB and SLB are compared from a technical and economic perspective.
	• EV battery storage projects in the market, standards, SLB models and formulations, the aging process, and the effect of degradation causes on the process are reviewed.	• At the same time, the SLB storage production process, potential market and future trends, business policies and strategies, and SLB's application areas are discussed.
[52]	• It evaluates the market trend for batteries, the process and management of reuse and recycling based on battery chemistries.	• Different battery chemistries, storage market volumes, demand forecasts, circular economy in the battery value chain, recycling, precious metals, and the market are addressed.
	• It also presents challenges and solutions for reuse and recycling. In addition, causal challenges and solutions are explained.	
[53]	• Expectations, challenges, and opportunities for the second life are presented.	• The discussed are the aging, experimental health prediction techniques, preparation for reuse, applications, recycling, precious metals and market, business models, and future.
	• In addition, battery degradation, experimental methods, cost analysis, and business models for SLBs are discussed.	
[54]	• Second-life studies are evaluated from technical, economic, and environmental perspectives, and the market price is investigated.	• The cost-benefit relationship in stationary storage applications and the market potential for their use areas were reviewed.
	• Industrial applications and R&D projects for SLBs are explained, and commercial products on the market are reported.	• The impact of SLBs on upfront cost reduction in the first life and initial conditions of use for moving to the second life are discussed.
[55]	• Key technological developments, economic analysis, challenges, and opportunities for SLBs are discussed.	• It emphasizes models of degradation that generalizable physical laws can explain.
	• It also presents degradation models, retirement processes and management procedures for the EV battery, and power electronics topologies for its performance.	• Cell-to-cell regrouping standards are evaluated. The economic evaluation criteria for preparation for a second life are detailed in the legal framework.
[56]	• The challenges of storage with SLB are discussed, and the process and barriers of preparing for reuse is presented.	• Transition to second life and preparation processes, the legal framework, and projections for rentability are explained.
[57]	• The applicability of SLB is investigated based on the application area and the technical and economic assessment procedure.	• A review of the identification, selection, and control of accuracy health indicators for state of health (SOH) estimation have been performed.
	• End-of-life extension methods and lifetime significance are also addressed.	• The impact of forecast accuracy on the revenue chain and future directions are also reviewed.
[58]	• The technical and economic feasibility of using SLBs in stationary storage application areas are systematically reviewed. The focus is on state-of-the-art modeling and experimental studies.	• It is emphasized that frequency regulation services face technical implementation challenges, while SLBs will not contribute to less demanding applications.
[59]	• The barriers, opportunities, uncertainties, and technological developments for SLBs are reviewed broadly.	• Feasibility performance analysis was performed for different chemicals in stationary storage application areas.
	• SLB projects and success stories, key industry players, and potential stationary storage application areas are also mentioned. Future direction and market potential are explained.	• The researchers discuss their five business models, three types of markets for SLB trade, and opportunities and barriers for each actor in the circular supply chain.
[60]	• Potential challenges and expectations for SLBs in a sustainable framework is presented. Policy gaps and legislative recommendations for critical players are presented.	• The risks of transport electrification and reuse in the industrial supply chains are evaluated, and cost-benefit relationship is highlighted.
	• Several issues are addressed, including the aging knee point for the second life, lifetime estimation, control of inconsistencies in reprocessing, and proposed solutions.	• Technical and economic performance analysis is performed for selected application areas, and a useful business model is identified. Future direction and market potential are explained.
[61]	• It emphasizes SLB applications in grid services, degradation mechanisms, interface architectures for power electronics, the SLB market, and BMS.	• Problems in BMS and mathematical modeling and experimental analysis of SLBs are reviewed from a technical perspective.
[62]	• Challenges and solutions are explored to maximize the potential use of SLB.	• It also explains the opportunities and expectations for the second-life.
[63]	• Existing standards and policies, different business strategies and circular economic assessment methods, SLB benefits before recycling, and SLB's potential are reviewed to identify possible application areas.	• The reuse preparation process, SOH estimation techniques, possible business strategies in reuse, second-life applications, the business model for the circular economy, and the recycling process is discussed.
This Study	• The cradle-to-grave circular battery supply chain and economics are discussed, and real projects support the current status. Potential challenges and solutions are defined.	• Three selected battery models commonly used in research are mathematically described and compared. The aging mechanism is also briefly explained.
	• Battery chemistries are compared using comprehensive terminology.	• End-of-life estimation methods are discussed, and the often-neglected SOF phenomenon is expressed mathematically.
	• The trade-offs and changeable behavior between FB and SLB performance in stationary energy storage applications are addressed by existing research.	• Standards and regulations, second-life application areas, the recycling process and the precious metal market are briefly explained.

dried after being rolled, and a separator is placed between them to form a battery cell. Battery cells compose modules and modules packages, and EV use is increasing by 3% yearly [7]. These batteries, which have been around for years, have a liquid or gel electrolyte [52], typically consisting of salt and solvent, a ceramic-coated microporous membrane separator made of polyethylene or polypropylene, and a natural graphite anode where exfoliations are processed to achieve a more homogeneous appearance. In addition, it is possible to see current collectors that contain different transition metal oxides, providing the cathode, which is the primary determinant of performance, and the junction. It is

also possible to frequently see cylindrical, prismatic, and pouch-shaped cell formats [53]. Lithium-ion battery type with dynamic and nonlinear behavior is advantageous [64] with low pollution, self-discharge, high energy density, specific energy, discharge current rate, coulomb performance, and no memory effect [65]. Cobalt, lithium, and nickel mineral utilization rates in the cathode have been changed daily, and their beneficial use in EVs has been improved. EVs constitute 47%, 24%, and 7% of lithium, cobalt, and nickel mineral demands, respectively [66]. In this way, widely used transition metal oxides have been developed, such as lithium cobalt oxide (LCO), lithium iron phosphate (LFP), lithium-titanium-oxide (LTO), nickel-cadmium manganese (NCM or NMC), nickel cobalt aluminum oxide (NCA). Continuous battery technology developments have become superior over other ESS, such as a flywheel, supercapacitor, hydroelectric pump, and fuel cell, more evident. Since compressed air and superconducting magnetic energy storage technologies are still innovating, the battery maintains its dominance.

A. COMPARISON OF TECHNOLOGIES

In LFP batteries, the use of modules is reduced with cell-to-pack technology (CTP) development, while the energy density is increased. It must also have a lower flame risk, cost, and longer cycle life. These batteries, which have better stable chemistry, have doubled EV use due to the high mineral price and incentive [66]. However, the fact that iron and phosphorus do not bring much financial profit after recycling has increased the interest in batteries with a high nickel content (almost seven times more than lithium) in the cathode (in NCM, especially NCM811, NCA). It accounts for 75% of the global cathode demand due to the related species' greater energy density, easy driving range, and fast charging [67]. Despite its advantages, the high extraction rate of pure and quality nickel in Russia (20%) and cobalt representing 5% of the battery's cost per kg are significant challenges. Especially the fact that Russia is at war and the violation of children's rights in Congo reduces the interest. Lithium-ion battery chemistries that will eliminate metal oxides and significantly increase the current energy density are still under development [52]. The authors in [68] focused on lithium-sulfur chemistry. Temperature and C-rate ($\frac{I_{chr}\ or\ I_{disch}}{C_{bat}^{rated}}$), the measurement of the charge and discharge current with respect to its nominal capacity, did not accelerate aging, and dramatic degradation did not accelerate even after reaching the aging knee or sudden death point. They also found no exponential loss of efficiency because cells do not suddenly cycle. Based on these determinations, it was reported that the Na-S battery should not be ignored. The frequently preferred battery chemistries, especially those used in EVs (LFP, NCM, NCA, lithium manganese oxide (LMO), LCO, and LTO), are compared in detail in Table 3. In EVs, depending on the trends in the cathode, batteries with NCM811 and NCA chemistry will become dominant, especially by 2028. Performance differences are evident between older (2012-2015) and newer (2018-2019) EV battery packs in terms of energy density and thermal management. New high-power density active liquid-cooled package designs have lower power density and efficiency than older technology and are expected to generate more heat [69].

B. BATTERY MODELS

To understand the degradation process well, it is necessary to explain the widely used models of the internal mechanism of the battery, which need to be addressed in reviews. At this point, three reputable battery mathematical models that researchers usually prefer before the degradation process are selected. Since it is known that thermal battery behavior causes the critical problem of runaway (spontaneous rise of temperature due to overheating) and that the optimum operating temperatures directly impact degradation, recently proposed mathematical thermal equations and obtained results are also discussed. In this context, the bucket model, which resembles a fuel tank and moves linearly with ampere-hour work volume, is simple and easy to implement [105] (see Figure 2 (a)). Also, ECM reflects internal dynamics by resistors and capacitors and external characteristics from the empirical (experimental) model [106], [107], [108] (see Figure 2 (b)). The single-particle type electrochemical partial or pseudo-two-dimensional differential model (P2D) uses nonlinear high-level partial differential equations (see Figure 2 (c)). Its use is widespread, with good handling of the transport process, kinetic and thermal stress, internal degradation dynamics, the solid electrolyte interface (SEI) thickness, ion conductivity, and porosity [109], [110]. These related models can be seen in Figure 2.

Physics-based degradation models provide sophisticated and near-accurate aging information based on internal degradation processes [111]. It also includes information on SEI growth and lithium plating. For example, linear degradation addresses SEI growth in the electrochemical-thermal physics-based model that incorporates SEI growth and lithium plating, while non-linear second-stage aging is due to lithium plating [112]. Another benefit is that by focusing on design optimization, internal reactions can be reduced and battery life extended. It is likely adaptable to other situations because the dominant role in the aging mechanism is similar. However, it is a complex process due to the sensitivity of the measurement and the difficulty of predicting electrochemical parameters [55]. The lack of historical data on usage makes it difficult to overcome the challenge of making predictions. Conversely, data-driven degradation models utilize historical data to train the model. Although predicting degradation can be done accurately when good quality data is available, the need to calibrate and train can lengthen the process. However, evaluating the extracted features may not guarantee a high prediction accuracy. Another data-driven approach is empirical modeling. Parameters such as C-rate, internal resistance, and discharge curve should be considered in

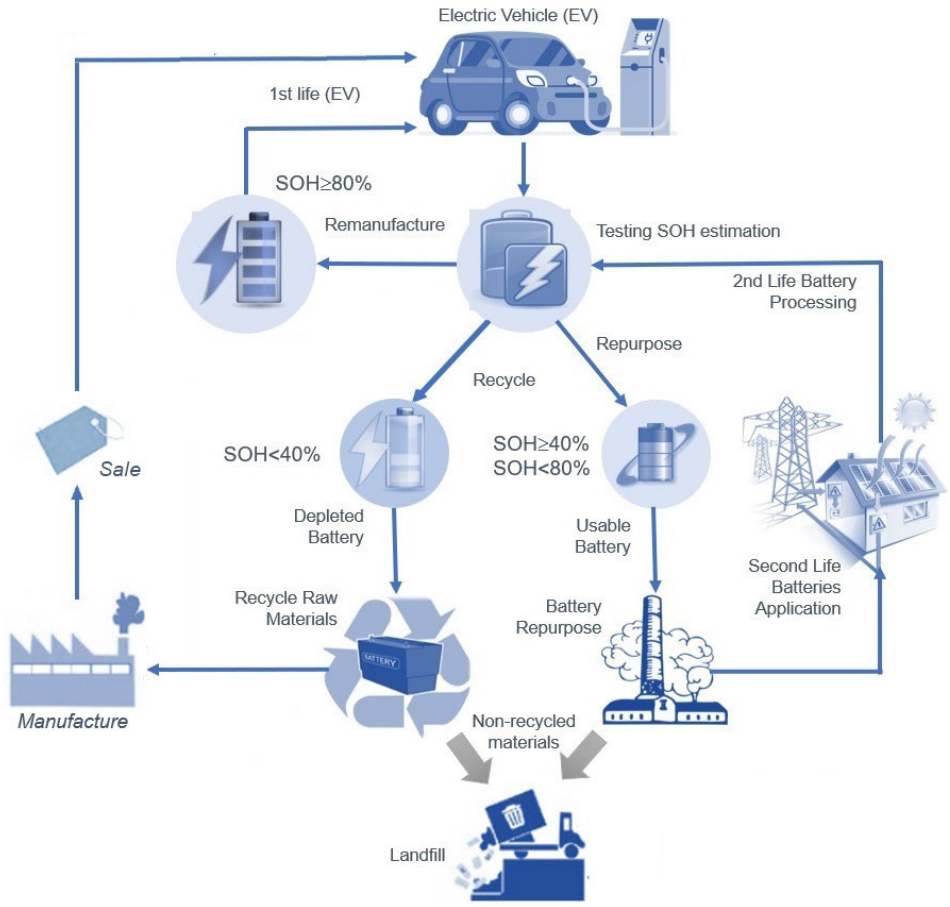

FIGURE 1. A comprehensive look at EV battery lifecycle or journey.

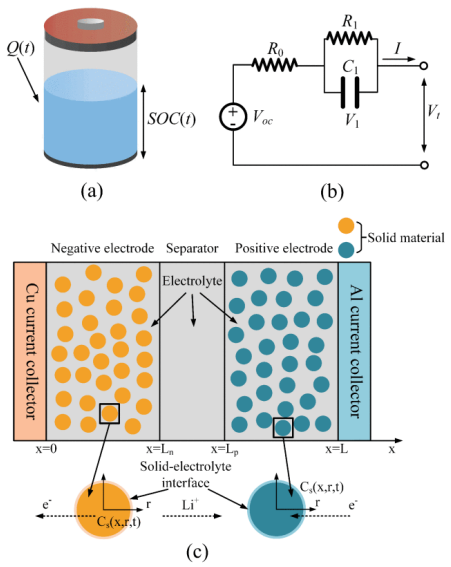

FIGURE 2. Battery models for energy storage: (a) Bucket model, (b) ECM, (c) P2D [109].

the degradation trend and analyzed in the regression model to characterize the battery. Although relatively simple, the experimental process makes it difficult to adapt to many situations, and the time and cost are relatively high. On the other hand, hybrid approaches that combine the strengths of individual battery life estimation models have recently been on the rise [113].

After introducing degradation models, the battery degradation process is discussed, and preliminary information for the second life is given to the reader (Section III). In this context, the battery efficiency, based on technical details, is related to the linear function of SOC and charge/discharge efficiency. Steady-state equivalent circuit models (ECMs) enable the relevant relationship to be obtained and the distortion tendency to be characterized [114]. Figure 3 shows the model consisting of three resistors representing open circuit voltage, ohmic losses (R_s), charge transfer (R_{ts}), and membrane diffusion (R_{tl}). Besides the steady-state ECM, Figure 4 shows the commonly used ECM stages. The 0^{th} equivalent circuit only considers the ohmic resistance of the battery. Therefore, it is useful for steady-state analysis as it does not respond to time-dynamic responses. The 1^{st} and 2^{nd} equivalent circuits should be used instead of the 0^{th} to improve accuracy, but this assumption is valid for short timesteps (<10 min. or 1/600 Hz) [115]. Parallel R-C is used

TABLE 3. Comparison of EV battery chemistries.

Specifications	Lead-acid	NiCd	NiMH	LCO	LMO	LFP	NCM	NCA	LTO
Specific energy density [Wh/kg] [70–73]	30-50	45-80	60-120	150-190	100-135	90-120	200-300	200-300	50-80
Internal resistance [mΩ] [74–77]	100	100-300	200-300	150-300	25-75	25-50	75	79	150
Cycle life [80% disch.] [78–81]	500-1000	1000-2500	500-3000	500-1000	500-1000	2750-12000	2000-8000	1000-10000	3000-7000
Fast charge time [78–80]	8-16 h	1 h	2-4 h	2-4 h	1 h	1 h	1 h	1 h	1 h
Overcharge tolerance [82, 83]	High	Moderate	Low	Low	Moderate	Moderate	High	Moderate	Moderate
Self-discharge/month [84, 85]	5%	20%	30%	10%	Very low	Very low	Very low	Very low	5%
Nominal cell voltage [70, 86]	2	1.2	1.2	3.6	3.8	3.3	3.6	3.6	2.4
Best charge-discharge rate [86, 87]	0.2 C	1 C	0.5 C	1 C	10 C	10 C	0.1 C	0.1 C	1 C
Charge temperature [°C][88–91]	(-20, 50)	(0, 45)	(0, 40)	(0, 45)	(0, 50)	(0, 55)	(0, 55)	(0, 45)	(-40, 50)
Discharge temperature [°C] [89–92]	(-20, 50)	(-20, 65)	(-20,70)	(-20, 60)	(-20, 60)	(-20, 60)	(-20, 55)	(-20, 60)	(-50, 65)
Maintenance [86, 87, 93, 94]	3-6 months	30-60 day	60-90 day	Not req.	Not req.	Not req.	Not req.	Not req.	Not req.
Toxicity [95–98]	Very high	Very high	Low	Low	Low	Low	Low	Low	Low
Cost [$/kWh] [99–104]	100-600	400-2400	170-2280	400-600	490-750	580	420	350	400-1005
In use since [86, 104]	1881	1960	1990	1991	1999	1996	2008	1999	2003

for different chemical reaction dynamics. For instance, R_1 and C_1 represent ion diffusion (Warburg impedance), R_2 and C_2 represent anode-cathode capacitance or constant phase element [116]. The Warburg's time constant is much larger than the constant phase element. Impedance parameters vary with current, SOC, SOH, temperature, and sensitivities. Therefore, Equation (1) represents the 2^{nd} order equivalent circuit.

$$\begin{aligned} i_{bat} &= i_{bat}^{+} + i_{bat}^{-} \\ \frac{\partial v_1}{\partial t} &= \frac{-1}{R_1 C_1} v_1 + \frac{1}{C_1} i_{bat} \\ \frac{\partial v_2}{\partial t} &= \frac{-1}{R_2 C_2} v_2 + \frac{1}{C_2} i_{bat} \\ v_{oc} + R_0 i_{bat} + v_1 + v_2 &= v_{bat} \end{aligned} \tag{1}$$

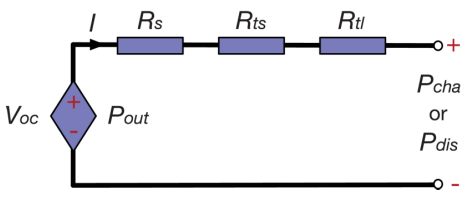

FIGURE 3. Steady state battery equivalent circuit [114].

The steps associated with Equation (1) provide the non-linear function and its solution [117]. In addition to efficiency,

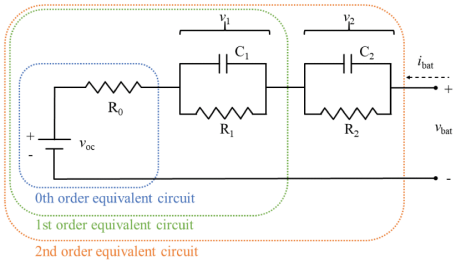

FIGURE 4. Equivalent circuit models [117].

ECMs are often used to determine the relationships between voltage, current, DC power, and AC power, depending on the order number. The precise relationship between the parameters is defined by Equation (2) and (3) [114].

$$\eta_{chr} = \frac{V_{oc}}{V_{oc} - R_{tot} \frac{V_{oc} - \sqrt{V_{oc}^2 - 4.\, R_{tot} P_e}}{2.R_{tot}}} \tag{2}$$

$$\eta_{disch} = \frac{V_{oc} - R_{tot} \frac{V_{oc} - \sqrt{V_{oc}^2 - 4.\, R_{tot} P_e}}{2.R_{tot}}}{V_{oc}} \tag{3}$$

Experimental analysis, electrochemical impedance spectroscopy (EIS), and parameter estimation based on analytical data are prominent for parameter identification using Rint (0^{th} order), Theven's (1^{st} order), and double polarization (2^{nd} order) ECMs.

In experimental analysis, charge/discharge tests using constant or pulsed currents. Transient voltage responses are evaluated to determine the internal resistance, RC-based time constants, or the relationship between SOC and open-circuit voltage (OCV). Such procedures are performed by charging or discharging with minimal current or intermittent application of a normal current level. Although easy to implement, OCV-SOC calibration takes a long time, and testing large-scale cells is more complex. While accelerated charge/discharge protocols are available, time is compromised. However, the increasing trend of SOC with OCV in ECM-based SOC estimation strongly favors OCV iterative methods. These methods, such as iterative least squares and Kalman filter, have proven highly efficient and reliable. On the other hand, using a real-time test system equipped with multi-channel digital-to-analog and analog-to-digital converters operating at sampling frequencies up to 50 kHz, with currents between 0.5-200 A, ECM component values can be calculated by evaluating the transient voltage response of the cell versus current for different load cycles [118]. After the charge and discharge protocol in the experimental analysis, two methods were proposed to determine the model parameters: one is based solely on measured data, and the other uses exponential curve fitting and extrapolation [119]. The curves corresponding to OCV and SOC are initially plotted for comparison. It is expected that if the rests between charge/discharge are not long, the curves will not overlap and will represent the OCV. If they do not match, the cells have not reached a steady state, and the area of the resting zone determines the OCV. Suppose the best-fitting exponential curve is extrapolated away from the trade-off between the curve fit and the actual measurement data. In that case, the best average OCV steady state value is obtained and constitutes the second method. The curves of the two methods are almost identical under different test conditions and currents, thanks to the parameterization. From another point of view, rest periods are ideal for characterization-dependent calculations of R and C parallel component values since SOC is constant. The relaxation characteristics of the voltage are planned according to SOC, temperature, and velocity, considering short and long constant time branches between separate time windows divided into rest periods of the pulsed charge and discharge characterization tests. In this way, an analytical time domain-based approach for parameter identification is realized [120].

EIS is another approach. Impedance properties are extracted by observing electrochemical processes, and EIS data are collected to determine ECM parameters. In such procedures focusing on impedance characterization, other aspects of cell dynamics are left out of the evaluation phase. EIS measures frequency response by varying voltage or current. It involves perturbation and measurement of voltage and current in the selected frequency range. There are online and offline applications according to the perturbation process. The offline method used for frequency response is often preferred because the DC offset current is low. In the online method, measurement with the charge function is valid, and the offset current is high. Although limited to high-precision measurements in a laboratory environment, EIS must be performed under high levels of measurement noise and approximation's effect and using low-cost sensors. Accordingly, the ECM parametric response of the cell to voltage and current excitation signals over a broad frequency spectrum can be analyzed. Fast Fourier transform feature extraction, curve fitting, and least squares estimation can serve this goal [121]. The Warburg impedance decreases at rising frequencies, and the impedance spectrum is evaluated according to this frequency response. In addition, the cell response (current and voltage) is measured by applying an AC perturbation signal (voltage and current based). This data in the time domain is then transformed into the frequency domain using a discrete Fourier transform. The impact of the DC component is obtained by subtracting the average before the transform. The branches related to the electrochemical process in the qualitative impedance graph are evaluated using the least squares method. Also, parameter extraction is performed by utilizing the geometric properties of the Nyquist spectrum. Another algorithmic analysis process based on the impedance spectrum of the cell was performed in [122]. Like before, the impedance spectrum is determined from voltage and current measurements after perturbation, and the frequency domain transformation is performed. The complex impedance is calculated for the frequencies corresponding to the frequency domains of interest, and the impedances are decomposed into real and imaginary to obtain the impedance plot according to Nyquist (real and imaginary impedance plot) and Bode (frequency-phase and amplitude plot) theory. The electrochemical behavior of the cell is determined by evaluating the minimum real and maximum imaginary impedance regions, resonance moments, and constant slope obtained from these graphs. On the other hand, given that the terminal voltage can be divided into electrolyte potential, OCV, electrode overpotential, and internal resistance drop, the electrolyte potential can be linearly simplified. Therefore, pseudo-two-dimensional models based on partial differential equations can be developed for parameter estimation. The differential equations can be simplified by applying the inverse Laplace transform and the Pade approximation while reducing the model order. In this way, the cell voltage and current relationship can be reduced to a second-order unified transfer function. Thus, the relationship between electrical and electrochemical parameters can be obtained [123].

Analytical data-driven parameter estimation focuses on system identification using current/voltage measurement data and unknown ECM parameters. In particular, in these procedures, pulse current charge/discharge experiments are performed, and parameters are determined by fitting the model to the pulse phase voltage, relaxation phase voltage, or both. Apart from these, optimization-based algorithms

can also be used for parameter estimation. Especially in Thevenin-based ECM models with multiple RC branches, since offline estimation parameterization methods are not available, systematic, iterative numerical optimization algorithms that do not require impedance measurement can come to the forefront for parameterization and transient analysis of the model. Especially if the system theory approach is elaborated, the resistance and capacitance values for first-order linear time-invariant RC branches can be parameterized using the relevant theory and experimentally verified by controlled pulse discharge tests in the LabView set [124]. The discharge experiment initially determines the voltage drop across the series resistor at the beginning or end of the current pulse. The periods of the different transients are set (for example, after the first RC branch, the periods can be increased by a factor of 5 compared to the short transient current to reduce the transient voltage effects of specific branches). Since the transient voltage cannot be measured directly in characterization tests, the time constant for the RC branches is determined from pulse discharge experiments. The final parameterization is obtained by correlating the steady state and transient response. Changes in model parameters under environmental conditions, such as operating temperature, increase prediction errors such as SOC and SOH. In addition to the similar steps in [125], a new parameter extraction step is included in the method to compensate for temperature effects. Following pulsed charge/discharge tests at different temperature conditions, the coefficients determined for the relationship of parallel R and C components with SOC based on a polynomial regression model were specified as a function of SOC and temperature. An empirical model to determine the effects of SOH on ECM parameters other than SOC, OCV, and temperature was proposed in [126]. A high power pulsed charging (HPPC) test (initiated by a 10-second discharge at 1°C at 90% SOC, a 40-second rest, and a 10-second charge at 0.75°C) was used to determine the ECM parameters at different temperatures and SOC levels. An Urban Dynamic Driving Schedule profile and a non-dynamic constant charge/discharge cycle current profile were used to test the proposed empirical model performance. The model calculated ECM parameters based on cell SOH, SOC, and temperature; voltage was estimated by comparing them with experimental measurements. Another perspective is using a weighted average of the vectors to optimize the ECM parameters. An AI-based parameterization approach, which has been comparatively validated with innovative meta-heuristics, can serve the purpose [127]. The mismatch between the predicted and measured battery voltage is reduced by the developed algorithm. At the same time, the average information forms a single vector, considering the relative significance of the various vectors. The differential equations in continuous time are converted to discrete time for easy handling. A sixth-order polynomial exponential function relationship is established between OCV and SOC, while battery dynamics during charging and discharging are included in the mathematical model. The method overcomes the demanding requirements of controlled charge/discharge static tests, as current profiles and rest intervals must be compatible for accurate OCV measurements according to SOC. Finally, related methods for extracting ECM parameters have a challenging and time-consuming methodological framework. Parameter identifiability analysis and two identification approaches (to eliminate redundant estimates of the non-convex problem) for extracting all parameters from offline current/voltage data were proposed in [128]. Starting with the parameter identifiability analysis and continuing with the parameter identification problem, the procedure is guided by the objective of estimation-error minimization. The first one of the two identification approaches constrains the parameter search space to determine parameter boundaries. The other one concerns adjusting the cost function according to the estimates.

Determination of ECM parameters is typically performed using HPPC tests, one of the test methods recommended in the battery test guide for next-generation vehicles (PNGV) [129]. HPPC testing can be performed using three methods: constant current constant voltage (CCCV), constant power, and constant current constant time (CCCT). The procedure of the CCCV method is to charge the cell with a constant current until it reaches a specific voltage (usually the upper cut-off voltage), and when the charge is complete, discharge the cell with a constant current until it reaches a specific voltage (usually the lower cut-off voltage). In the constant power method, which is more suitable for testing cells of different capacities, the cell is charged with a constant power until a specific voltage level (usually the upper cut-off voltage). After charging, the cell is discharged at a constant power up to the lower cut-off voltage. The CCCT method, in which the cell is first charged and then discharged at specific times and current levels, is more suitable for cell performance tests of the same capacity. While there are other methods, such as constant power, constant time, constant voltage, etc., it is necessary to determine the appropriate charge/discharge protocol based on the specific requirements under actual operating conditions.

The close link between model parameters under complex operating conditions allows a precise characterization of the cell's internal properties via HPPC tests [130]. In related tests that monitor current and voltage responses or cell voltage response to a rectangular current pulse, the exposure of the cell to a high current pulse of varying length and amplitude and the subsequent data determine the cell model under different operating conditions. Very exponential waveforms must be specified when defining the time constants according to the cell response of interest. It is recommended that the voltage responses be several times longer than the expected time constant length to determine the time constants [131]. The HPPC pulse should be as short as possible if the cell SOC is not to change [132]. There is a trade-off for preferred HPPC pulse lengths in applications for the mentioned reasons

and requirements. An even number is usually preferred for HPPC profiles with different pulses when one discharge and one charge pulse are desired to be generated and to keep the cell SOC unchanged [126]. The current values in each pair used more than once may be different. High-current pulses are thought to cause a significant change in cell voltage and SOC and, therefore, are easier to record [132]. Also, the pulse sequences in the pair need to be correctly determined. Starting with a charge pulse at high SOCs increases the voltage across the charge and can cause pulse interruption in the transition from CC to CV mode. The rest time between pulses is another consideration. The time constants must be longer than expected to allow enough time for the cell voltage to stabilize before the next pulse. On the other hand, HPPC test data can be easily determined in the time domain, which favors the DC pulse compared to the EIS method, which uses the AC excitation signal as input. HPPC tests evaluate the cell charging and discharging process with high current in repeated cycles and, thus, the cell's performance. The relevant time domain test based on DC pulses consists of a discharge pulse, a relaxation, a charge pulse, and another relaxation, each with a defined pulse current amplitude. To properly obtain the time constants, the ohmic and polarization resistance must be derived from the terminal voltage curves as a function of SOC. Therefore, models using resistance measurements should be preferred for a dynamic analysis. It should also be noted that input features extracted from HPPC test data into a least squares-based function fit as time series voltage with different sample intervals directly impacts ECM parameter identification [133]. On the other hand, ECM can be determined for cells based on the voltage response from the tests, which will determine the lifetime performance. However, HPPC tests determine the cell's dynamic pulse power capability, including discharge pulse and regeneration pulse power capability, where the correlation between each parameter and model accuracy should be carefully evaluated. Parameter optimization, including fast charge/discharge voltage and heat generation, is also required, and advanced cooling systems or thermally controlled chambers are recommended [134]. Also, charge/discharge rates may need to be checked by the BMS [135]. Other suggestions for the problem include setting the pulse feature, continual monitoring and modeling, and pre-test simulations. Besides issues to overcome, HPPC has benefits. For example, since achieving the pulse power capability is time-based, the test duration can follow the guidelines set by manufacturers, and tests can be performed at various DOD levels.

The HPPC test data is used as input for ECM parameterization and offline parameterization. However, the relevant test procedure was developed much earlier to determine the cell's dynamic power capability due to discharge and regen pulses. Therefore, adapting the profile to the parameterization is essential. Accordingly, it is recognized that HPPC profiles with varying current, pulse width, and rest time directly impact the identification accuracy [131]. A possible increase for either of these improves accuracy under conditions where the pulse width and rest time are sufficiently low, while in the opposite condition, there is no improvement. The researchers in [136] think that the correlation effect in parameter identification for the 2RC model will decrease with increasing pulse length and rest time. On the contrary, it was argued in the 1RC model in [137] that changes in the current signal do not affect the precise parameter identification. For this purpose, researchers in [138] used the Taguchi method to investigate the effects of varying HPPC profiles of positive and negative pulse height, pulse, and relaxation length on ECM parameter selection under operating conditions, including dynamic, non-dynamic, and quasi-static tests. Due to the complete factorial approach for the space of parameters whose effects are to be investigated, the measurement times become more extended. Therefore, the Taguchi orthogonal array was used for the optimum parameter levels [139]. Finally, it is recommended to consider lower positive impact heights, higher negative impact heights, shorter impact lengths, and longer relaxation lengths under unpredictable operational conditions. On the other hand, the measured pulse power capability is closely related to sensitivities such as temperature, current, lifetime, and sensor accuracy. To guarantee the accuracy of HPPC parameterization in practical applications, single-factor experimental methodology for DOD, SOH, temperature, and current should be emphasized. Accordingly, a finite difference algorithm must first be developed to calculate the partial derivative of the nonlinear function to perform the 2RC ECM parameterization process and SOC estimation via HPPC tests. The ultimate goal can be achieved by reducing the linearization error in this way, with extended Kalman filters that keep up with the ambient conditions and can analyze real situations even under other data and noise conditions [140]. [134] considers a similar approach (2RC, extended Kalman filter) but an HPPC test-based methodology designed on a multi-station co-motion system for ternary lithium cells. Here, OCV is used to determine cell parameters. Also, this methodology simultaneously solves linear or nonlinear problems to obtain optimal parameter results and SOC level.

Besides comprehensive ECM methodology, electrochemical models consider chemical, thermodynamic, and physical properties [141]. Equation (4) provides the determination of SOC for a constant discharge rate based on the calculations of Peukert's law [142]. Based on the same law, Equation (5) calculates the battery capacity in Ah for certain discharge rates [142]. Thus, SOC is determined by Equation (6) from the capacity relationship [142]. The SOC is controlled according to Equation (7) [142], especially for non-constant discharge rates.

$$I_n^* T_i = K \tag{4}$$

$$C_i = C_n (I_n / I_i)^{n-1} \tag{5}$$

$$SOC = 1 - \frac{I_i t}{C_i} \tag{6}$$

$$SOC_k = SOC_{k-1} - \frac{I_i \Delta t}{3600.C_n}\left(\frac{I_i}{I_n}\right)^{n-1} \tag{7}$$

The single particle model was created in [143] for a lithium-ion battery with two porous electrodes and a separator containing the electrolyte in three regions. To capture the dynamic behavior of the porous electrode, the relevant model performance is high [144]. While metal oxide is stored in the cathode of the discharged battery, electrode diffusion of lithium must first be ensured for the charging process. As a result of deintercalation from the cathode, lithium is transported to the anode surface by following the electrolyte path and is stored in the anode until the discharge process begins. Based on Fick's 2^{nd} law, the diffusion is governed by Equation (8) [145]. Intercalation and deintercalation reactions are based on Butler-Volmer kinetics and are calculated using Equation (9) [146]. As it is more chemically based, its details can be examined in [143].

$$\frac{\partial c_i^s}{\partial t} = D_{s,i}\left(\frac{\partial^2 c_i^s}{\partial r^2} + \frac{2}{r}\frac{\partial c_i^s}{\partial r}\right) \quad i = n, p \tag{8}$$

$$j_i = 2k_i\left(c^s_{max,i} - c^s_i\right)^{0.5} c_i^{s.0.5} c^{0.5} .\sinh\left[\frac{0.5\,.\,F}{RT}\left(\Phi_1 - \Phi_2 - U_i\right)\right] \quad i = n, p \tag{9}$$

The bucket model, known for its similarity to the fuel tank, is created in [147] as a space model with a control variable, a power flow for charging and discharging the battery, a single state variable, and a SOC-dependent space model. Calculations of the relevant model and aging technique are suggested by Equation (10), where the battery life is assumed to be 8000 full cycles when 20% of the capacity is lost [147].

$$\begin{aligned} \frac{dz}{dt} &= \frac{P(t)}{E_{Wh}} \\ 0 \le z(t) &\le 1 \\ R(u(t)\ \ x(t)) &= P(t).\lambda(t).N \\ E_{lost,Wh} &= 2.15\,.\,10^{-4} max\,|P(t)| \\ &\quad + 1.25\,.\,10^{-5}.\int_0^{T_{end}} |P(t)|\,dt \\ C(u(t)\ \ x(t)) &= E_{lost,Wh}\lambda_{degrad,Wh}N \end{aligned} \tag{10}$$

The construction of the space function based on control variables has been implemented in a similar way in ECM [147]. While the charge state and the current flowing through the parallel resistor are considered as state variables, the state space model consists of two equations and the solutions are performed depending on the steps in Equation (11) [147].

$$\begin{cases} \dfrac{dz}{dt} = \dfrac{I(t)}{E_{Ah}} \\ \dfrac{dI_r(t)}{dt} = \dfrac{1}{R_p C_p} I(t) - \dfrac{1}{R_p C_p} I_r(t) \\ V(t) = OCV(z(t)) - R_p I_r(t) - R_s I(t) \\ 2.7 \le V(t) \le 4.2 \\ 0 \le z(t) \le 1 \\ R(u(t)\ \ x(t)) = I(t).V(t).\lambda(t).N \\ E_{lost,Wh} = \Big(\alpha\left(V_{mean}\,T(t)\right) T_{end}^{0.75} \\ \quad +\beta\left(V(t)\ z(t)\right)\sqrt{\int (|I(t)|\,.dt)E_{Ah}}\Big) \\ C(u(t)\ \ x(t)) = E_{lost,Wh}\lambda_{degrad,Ah}N \end{cases} \tag{11}$$

One of the control-oriented electrochemical modeling is P2D. The physical size of the cell's longitudinal axis and the pseudo-size of the radius of the active particles are represented in [148]. The binary intercalation process is defined, and the finite difference method (FDM) is used for spatial discretization. Each electrode forms a correlation of active particles equal to the ratio between the electrode volume and the sphere volume. Chemical calculations for the cell performance equation, SOC, and thermal model were carried out according to Equation (12) [148]. As this is more of a chemical and design proposal, its details can be found in [148].

$$\begin{cases} v_n = \dfrac{\delta_n.A.\varepsilon_{s;n}}{\frac{4}{3}\pi R_s^3} \\ v_p = \dfrac{\delta_p.A.\varepsilon_{s;p}}{\frac{4}{3}\pi R_s^3} \\ v_n^{\Delta x} = \dfrac{v_n}{N_n} \\ v_p^{\Delta x} = \dfrac{v_p}{N_p} \\ j_m^{Li} = \alpha_s j_0\left[exp\left(\dfrac{\alpha_a F}{RT}\eta_m\right) - exp\left(-\dfrac{\alpha_c F}{RT}\eta_m\right)\right] \\ \eta_m = \phi_{s,m} - \phi_{e,m} - U\left(c_{s,(m,N_r)}\right) \\ i_{s,m} - i_{s,m-1} = -\Delta x_m j_m^{Li} \\ i_{e,m} - i_{e,m-1} = \Delta x_m j_m^{Li} \\ V = \phi_{s,N_n+N_s+N_p} - \phi_{s,1} - \dfrac{R_f}{A} I \\ SOC = \dfrac{1}{N_n R_s^3}\sum_{m=1}^{N_n}. \\ \sum_{p=1}^{N_r} c_{s,(m,N_r)}\left(r_p^3 - r_{p-1}^3\right) \\ \Psi(T) = \Psi_{act} exp\left[\dfrac{E_{act}^{\Psi}}{R}\left(\dfrac{1}{T_{act}} - \dfrac{1}{T}\right)\right] \end{cases} \tag{12}$$

As a result, by accepting battery charge and discharge power as a control input, the bucket model in which monitoring SOH and energy status cannot appropriately reflect the nonlinear degradation process in different operating

conditions. Therefore, the prediction accuracy could be better. ECMs, in which stress parameters such as DOD, temperature, and C-rate taken from the experiments are fitted, and charge and discharge currents are used as control inputs, are more accurate than the buck model and have lower complexity than P2D. It also provides moderate accuracy in online use. In both models, it only considers the initial life of the battery, i.e., the EV operating period. Although physics based P2Ds, which consider the second lifetime, seem superior, using ECM is more common due to the difficulty of solving high-level differential equations.

The optimum temperature should not be exceeded in EV batteries. Thermal management plans and battery energy management systems should be followed to achieve this goal [149]. In [150], a configuration consisting of fins, metal foam, and phase change material (PCM) is proposed, and a parametric method combining computational fluid dynamics and artificial neural network (ANN) is recommended to serve the relevant goal under extreme operating conditions such as high discharge currents. In particular, ANN is preferred over fluid dynamics for the prediction of the liquid part of the PCM and the battery temperature. A non-equilibrium thermal pathway was followed for the metal foam model. The enthalpy-porosity method was used to model the PCM around the LIB and easily incorporate the phase change into the one-step flow configuration. The thermal functions generated for the lithium-ion battery (LIB), including pure PCM, fin, and enclosure, are shown in Equations (13)-(16) [150]. The effects of sensitive parameters such as the number of fins, height, and length on thermal energy management are evaluated material-wise and under different ambient conditions. The hybrid approach, which consists of PCM, metal foam, and fins, guarantees the lowest temperatures compared to pure PCM. Applying copper metal foam and fins, increasing the fin length, and adding more fins are also suggested for minimum temperatures. On the other hand, the safety regime response of the LIB varies for different cathodic chemistries. Since it is essential to maintain the optimum operating temperature and thus minimize thermal runaway in different cathodic chemistries and comply with the respected government norm GB 38031/32 for thermal packaging, a four-equation thermal abuse use battery model is proposed in [151]. Also, it is suggested that the thermal behavior of organic-based, graphene-reinforced composite PCMs (CPCMs) be monitored. The relevant regulation specifically mandates that thermal runaway propagation in heavy commercial EVs must be delayed by at least 5 minutes. The choice of CPCM is motivated by the instability in delaying the thermal runaway trigger point due to the low thermal conductivity of conventional PCMs. The formulations of the corresponding thermal battery model belong to the four stages (SEI, the negative and positive electrolyte reaction, and the decomposition of the electrolyte and the remaining binders). The corresponding mathematical modeling can be found in Equations (17)-(20) [151]. Especially when monitoring thermal runaway in common cathode materials ($LiNiMnCoO_2$, $LiFePO_4$), a large format prismatic cell profile is preferred. It is emphasized that by choosing CPCM, the onset of thermal runaway can be delayed by 20 minutes, and peak temperatures in the battery module can be reduced up to 113.2 minutes with even the most minor addition of expanded graphene. On the other hand, heated wall configurations (square, rectangular, trapezoidal, and curved) can be considered thermal storage capacity and serve thermal safety limits [152]. The enthalpy porosity method calculates the melting time, energy storage, and the PCM-filled liquid fraction. Local closed zone-based heat sources at the heating boundary, especially curved wall profiles, increase the melting time to 57.6%. These wall profiles have a smooth and continuous surface, facilitate free convection, minimize flow separation, and promote proper fluid flow. Latent heat is reduced while thermal conductivity increases in thermal energy management schemes involving RT-47-based PCM beyond CPCM or pure PCMs [153]. For optimizing the thermal mechanism inside the battery, the coolant flow, and the heat transfer dynamics in the relevant schemes, the system management using a cold plate with serpentine channels can be resorted. Also, the synergy principle for the innovative variable cross-section couple can be applied [154].

$$\rho_{PCM}\frac{\partial\left(h_{ref}+\int_{T_{ref}}^{T}C_{p,PCM}dT+\beta L_{PCM}\right)}{\partial t}+\rho_{PCM}C_{p,PCM}\left(v_r\frac{\partial T}{\partial r}+v_z\frac{\partial T}{\partial z}\right)=k_{PCM}\left[\frac{1}{r}\frac{\partial}{\partial r}\left(r\frac{\partial T}{\partial r}+\frac{\partial^2 T}{\partial z^2}\right)\right] \tag{13}$$

$$(\rho C_p)_{LIB}\frac{\partial T}{\partial t}=k_{LIB}\left[\frac{1}{r}\frac{\partial}{\partial r}\left(r\frac{\partial T}{\partial r}\right)+\frac{\partial^2 T}{\partial z^2}\right]+94023.8 \tag{14}$$

$$(\rho C_p)_{FIN}\frac{\partial T}{\partial t}=k_{FIN}\left[\frac{1}{r}\frac{\partial}{\partial r}\left(r\frac{\partial T}{\partial r}\right)+\frac{\partial^2 T}{\partial z^2}\right] \tag{15}$$

$$(\rho C_p)_{ENC}\frac{\partial T}{\partial t}=k_{ENC}\left[\frac{1}{r}\frac{\partial}{\partial r}\left(r\frac{\partial T}{\partial r}\right)+\frac{\partial^2 T}{\partial z^2}\right] \tag{16}$$

Here, C_p, ρ, k and T represent specific heat, density, thermal conductivity, and temperature, while r and z represent directions. Also, β means liquid fraction, and h_{ref} refers to sensible enthalpy. L, v_r and v_z represent the latent heat of fusion, the velocity in the r-direction, and the velocity in the z-direction.

$$C_{SEI}=-A_{SEI}C_{SEI}.exp\left(-\frac{E_{SEI}}{RT}\right)C_{SEI}^{m_{SEI}} \tag{17}$$

$$C_{ne}=-A_{ne}.exp\left(-\frac{t_{SEI}}{t_{SEI,ref}}\right).exp\left[-\frac{E_{ne}}{RT}\right]C_{ne}^{m_{ne}} \tag{18}$$

$$C_{pe}=A_{pe}.exp\left[-\frac{E_{pe}}{RT}\right]\alpha^{m_{pe,1}}(1-\alpha)^{m_{pe,2}} \tag{19}$$

$$C_e=-A_e.exp\left[-\frac{E_e}{RT}\right]C_e^{m_e} \tag{20}$$

TABLE 4. The technical specification of battery cell for the models.

Ref.	Battery Chemistry/Model	Anode material	Cathode material	Electrolyte material	Nominal voltage (V)	Nominal capacity (Ah/kWh)	C-rate
[107]	TS-LFP40AHA	A graphite carbon electrode with a metallic backing	Lithium iron phosphate	A lithium salt dissolved in a solvent	2.8-4	26 and 32 Ah	0.05 and 1C
[108]	$LiFePO_4$	A graphite carbon electrode with a metallic backing	Lithium iron phosphate	A lithium salt dissolved in a solvent	3.2	20-30 Ah	-
[110]	LCO and NCO (Kokam 740 mAh pouch cells)	A graphite carbon	A cobalt oxide and nickel cobalt oxide	-	2.7-4.2	2.236 mAh	C/2 and C/25
[111]	NMC622	A graphite carbon	Nickel, manganese and cobalt	1 M of $LiPF_6$	2.8-4.2	12.4 Ah	C/10, 1C, and 2C
[115]	TCL PL-383562 polymer Li-ion	Graphite, coated on copper foil	Lithium iron phosphate	Polyethylene glycol (PEG), polyacrylonitrile (PAN), polymethyl methacrylate (PMMA) or polyvinylidene fluoride (PVdF)	3-4.1	850 mAh	0.01 and 0.4C
[141]	Li-ion GP1865L180	A graphite carbon	Lithium iron phosphate	A lithium salt dissolved in a solvent	3.7	1800 mAh	0.05, 0.2, 0.5, 0.6, 1, and 1.5C
[144]	$LiPO_8$-$LiCF_3SO_3$-TiS_2	A lithium	Composite insertion	Solid-polymer and lithium salts	1.7-3.2	Changeable	0.01, 0.5, and 0.8C
[145]	Li_xCoO_2 positive electrode and mesocarbon microbead negative electrode.	A graphite carbon	A cobalt oxide and nickel cobalt oxide	-	3-4.2	2.187 Ah	C/20
[147]	A Kokam 16Ah NMC cell	A graphite carbon	Nickel, manganese and cobalt	-	3.64	2.7 Ah	1, 2, and 3C
[155]	$LiPF_6$	A graphite copper carbon	Ethylene and propylene carbonate	High-purity LiPF6 salt, distilled organic carbonate solvents, and some additives	2.5-3.9	1.18-1.79 mAh	0.4 and 0.5C
[156]	NMC111 and LMO, NMC811 (18650 cells)	A graphite carbon	A blend of NMC and LMO, nickel-rich.	-	3-4.2	2.1 and 3.5 Ah	C/10, C/2, 1C, and 2C
[157]	NMC and LMO (18650 cells)	A graphite carbon	NMC + LMO	-	2.8-4.2	2.1 Ah	C/10, C/2, 1C/-1C, -2C

TABLE 5. Methodological framework for battery models.

Ref.	Method	Equipment / Software	Model Input	Model Output
[107]	The cells are grouped based on their remaining capacity, and a configuration is found to reduce the total capacity difference between parallel rows of cells. Passive balancing is applied.	Arbin BT2000 and Lithium Lithiumate Pro BMS	The function of the SOC consists of a voltage source, an equivalent RC circuit, and a resistor for transient response.	Battery cycling power and SOC during charge or DOD during discharge.
[108]	The developed BMS algorithm is implemented in a PV-based charging station with Zigbee data communication using passive balancing. SOC and SOH are estimated using an equivalent circuit-based extended Kalman filter for the estimator.	BMS, current sensor, passive balancing cards, a data acquisition system, Tigo®, WirelessGlue™, and ClipperCreek® vehicle charger.	Cell characteristics, battery current, voltage, charge and discharge power, and temperature.	SOC and SOH
[110]	A diagnostic algorithm is developed to identify and quantify the nature and extent of each degradation mode in Li-ion cells.	BioLogic potentiostats of type MPG-205, SP-150, and thermal chambers.	Cell characteristics, charge and discharge current, measurable capacity, OCV, and charge and discharge end.	SOC, SOH, expected capacity, LLI, LAMNE, and LAMPE degradation
[111]	CCCV testing and a physics-based lithium-ion battery (LIB) aging model accounting for both lithium plating and SEI growth are presented.	Arbin BT-2000 and an environmental chamber (Tenney T10c, Thermal Product Solutions)	Cell characteristics, voltage, current, ambient temperature, voltage loss, and number of cycles.	SEI growth, increase in lithium plating rate, local electrolyte potential gradient at the anode, dimensionless anode thickness, local anode porosity, lithium storage potential, and coulombic efficiency.
[115]	An accurate, intuitive, and comprehensive electrical battery model is proposed and implemented in a Cadence environment (runtime-based models). CCCV testing is also performed.	The battery test system, implemented on a PCB prototype, includes a charge and discharge circuit and a computer program.	Cell characteristics, current, voltage, temperature, number of cycles, storage time, and self-discharge.	Stable and transient response, runtime, available capacity, and nonlinear OCV.
[141]	Levenberg-Marquardt method, empirical model in Mathcad (using logfit and pwrfit function), and CC and CV testing. Five methods for modeling cells (stochastic, electrochemical, fractional discharge, and ECM) were examined, and an experimental model was developed.	MTX3283 Multimeter and empirical model in Mathcad.	Cell characteristics, charging time, voltage, charging current, and temperature.	Remaining capacity, OCV, and SOH.
[144]	Concentrated solution theory models the galvanostatic charge and discharge of a lithium anode, solid polymer separator, and insertion cathode cell.	VAX 6510 CPU timer.	Diffusion coefficient, conductivity, transfer coefficients, concentration, reaction rate constant, and exchange current density	Cell potential, utilization, pore wall flux, current, and power.
[147]	Multiple degradation experiments were performed in the Mat4Bat project, and the Bucket, ECM, and SPM models were compared with the experimental data.	Instead of experimental tests, degradation models are included in the optimization that has been developed.	Power, current, charge/discharge time, charge capacity, throughput, voltage, temperature, SOC, lithium concentration, battery temperature, number of cells, thickness of the SEI layer, and amount of ions consumed.	Residual capacity, full equivalent cycle, SOH, SOC, and revenue.
[156]	Cell characterization involves control testing. Arbin and Maccor multi-channel battery test systems are used for cycles and checks.	Arbin and Maccor multi-channel battery test systems, 18.19 BioLogic®'s modular multichannel potentiostat/galvanostat/EIS VMP3, and Zeiss® LEO1530 electrodes.	Cell characteristics, maximum charge rate, discharge current, temperature, and cell skin temperature range.	The number of cycles, SOH, internal resistance and impedance, and LLI (%) depend on the current collector's mass load, deposit density, thickness, and weight.
[157]	R-2RC model parameterization is performed for the Li-ion cell for the second life. Coulomb Counting is used for SOC estimation to determine the instantaneous capacity by measuring the current, and EIS is used for parameterization.	Arbin Bt2000, Maccor Series 4000 battery test systems, and the climate chamber.	The current and voltage of the Li-ion cells, ambient temperature, SOC, SOH, charge and discharge cycles, and discharge current.	An internal resistance and two RC branches.

Here, A represents the chemical function at the anode. A_{SEI} actually refers to the SEI decomposition reaction at the anode. Similarly, A_{ne}, A_{pe}, and A_e represent the negative electrode-electrolyte solvent reaction, positive solvent reaction, and electrolyte decomposition reaction at the anode. C_{SEI} and C_e represent the SEI and electrolyte decomposition reaction at the cathode. E_{SEI}, E_{ne}, E_{pe} and E_e indicate the SEI decomposition reaction at the electrode, the negative and positive electrode-solvent reaction, and the electrolyte decomposition reaction. C is the specific heat for each stage.

Finally, Table 4 summarizes the cell-specific definitions for the models and the electrical inputs of the test for the studies on battery models, and Table 5 presents the methodological comprehensive framework for the model.

C. DEGRADATION PROCESS

The protective barriers, which have a lower operating voltage than the electrolytes, alleviate the reaction effects between the electrode and the electrolyte, and concern the material combination, are described as SEI [109]. This barrier, formed

in many steps, begins to decompose through a series of reduction reactions in which insoluble compounds such as electrolytes, lithium dioxide, and lithium fluoride are formed. Currently, the high impedance SEI does not affect the grinding at the cathode (> 0.25V). After lithium is added to the anode at lower voltages, the SEI forms a tightly knit, highly conductive layer. The SEI structure, which can grow or degrade depending on the usage profile, shows improved thermal stability if exposed to higher temperatures over time than lower ones. However, SEI can dissolve and even create salts inhibiting lithium-carbon ion transition [158]. In contrast to high temperatures, at shallow temperatures, the metallic lithium plating in the SEI (especially during fast charging) becomes quite severe, and dendrite formation is observed. Such parasitic reactions cause the lithium-ion between the cathode and anode electrodes to be absent from the cyclic process. The growth of the surface films creates the perception of power fading. As a result of the continuity of the relevant operating condition, a catastrophic thermal failure occurs between the electrodes [159]. As a result of the decomposition experienced, active material loss at the anode and cathode, binder separation, formation of a surface resistive layer between the active electrodes, and electrode particle cracking occurs. In addition, many internal defects develop adversely, such as exfoliation and the interaction of solvents released from the SEI with the electrode with graphite material. The gas to be formed is harmful to SEI [51]. Besides the electrode-to-electrode relationship, current collectors and electrolytes are highly susceptible to degradation. Apart from the increase in active lithium loss, which represents the loss of anode and cathode active mass, high impedance and corrosion are observed in the electrode due to the degradation of the binder composition over time and electrolyte decomposition.

In addition to cyclic aging, influenced by the number of charges and discharges, calendar aging caused by electrolyte decomposition over time is another critical issue. Parameters such as storage temperature, time, and SOC (a high value creates a significant imbalance in the lithium-ion distribution) on the charge/discharge profile significantly impact the increase in degradation. It is indisputable that the two most important consequences of battery degradation are capacity loss and resistance growth. The loss of lithium-ion inventory (LLI) and anode/cathode active materials (LAM) mainly causes these two events [64], [160]. LLI loss is affected by the number of recyclable lithium ions and active electrode materials (lithium plating effect due to the charge profile) surviving in the intercalation and deintercalation process between the active materials in the anode and cathode [109]. Apart from this structure, where dendrite formation is typical, LAM loss can be affected by exfoliation, metal dissolution, and particle cracks [110], [160], [161]. With differential voltage analysis, the effect of thick lithium plating on cells started at 0°C and below. In contrast, with the adoption of post-mortem analysis, LAM loss was observed at 25°C after 900 and above cycles [156]. The effective aging procedure was developed while integrating the relationship between the two relevant criteria, using open data and ECM, while complying with SOH, SOC, current, and temperature limits [157]. Most studies show the main cause of degradation as time, temperature, cell voltage, mechanical stress, stoichiometry, and battery usage profile. However, the researchers in [162] proved that the profile due to high charging demand is the main factor in battery degradation. For whatever reason, batteries with a near-linear degradation profile in the first stage evolve into a nonlinear process that causes rapid capacity reduction and resistance increase after the knee point. Although manufacturers commit to life points in the shared profile, the variation of operations under operating conditions such as temperature, C-rate, and SOC ranges remain SOH estimation uncertainty.

D. MARKET

Since the discovery and development of lithium-ion technology in the 1990s, batteries in consumer electronics, stationary energy storage applications, and EVs have become indispensable elements of the circular economy. Almost every research company, academician, manufacturer, and international commission has examined the battery popularity according to capacity, quantity, and cost for the future, as in Table 6. Specifically, lithium mining efforts are expected to increase as demand for batteries is expected to increase 14-fold compared to 2018 [162], or exceed 275 GWh capacity [163], and market share is expected to reach 53.6 billion $ [164] with 500 kilotons of lithium to be mined [165].

III. SECOND-LIFE BATTERY

A. DEFINING AND DESCRIBING

There are distinct differences between reuse, remanufacturing, repair, reconditioning or refurbishment, remodeling, and reuse. The procedure in which the product is used directly again without making any changes to its original intended function is known as reuse [172], [173], while remanufacturing refers to the aesthetic improvement of the product with limited functionality improvements [174]. Remanufacturing aims to return components to at least initial production performance. The components should comply with the original factory specifications and design. Since the rules determined by international standards organizations must be followed, action is taken in a safe and high-quality manner. Repair refers to modifying battery components to correct faults and restore operational capability [175]. Reconditioning also involves disassembling, cleaning, replacing, and reassembling components. It does not assure customers as there is no indicator by which performance can be evaluated when compared to original equipment manufacturer (OEM) specifications. Remodeling involves only changing the aesthetic appearance rather than improving the product's technical features. Due to high cost, time, and energy consumption, it is preferred to define reuse or second-life

TABLE 6. Global interest and market in battery technologies.

Global Projection	Source
To reach 53.6 billion $ by 2027.	[164]
EV battery capacity will exceed 275 GWh per year by 2030.	[163]
It will grow by 25% annually to reach 2,600 GWh in 2030.	[166]
Lithium extraction will increase to 500 kilotonnes due to growing demand for EV batteries.	[165]
The stationary installed battery capacity will be 421 GWh in 2030.	[167, 168]
Global EV sales will reach 26 million, and lithium-ion battery capacity will reach 2,000 GWh by 2030, accounting for 50% of EV cost (from 40%).	[169, 170]
Compared to 2018, the demand for batteries will increase 14 times by 2030.	[162]
Up to 250 new EV models, powered by 15 different battery manufacturers, will be on the market by 2025.	[171]

instead of the relevant expressions. Battery packs, which age and degradation over time depending on the production process, driving profile, and operating conditions of EV owners, come to life again in lower-capacity applications. The US Advanced Battery Consortium proposed this idea in 1996 [176], [177]. Second-life, defined by the organization as a 20% reduction of rated cell capacity or power density at 80% DOD, has varied for many researchers. First use: with over 1000 incomplete charge/discharge cycles over a 5-10 year period [60]; at a travel distance of 160,000 km, with a period of 5-8 years [178]; 7-10 years [179], [180], [181], [182]; when the knee point of accelerated degradation tendency is reached [67]; terminate at 5% self-discharge and 80% remaining capacity [171] has been reported. In addition, 1-3% of battery defects, such as EV accidents or manufacturing defects, thermal stress, mischarging, and electrolyte and separator damage, are observed. Industry representatives predicted that the second-life would fall below eight years in this context [177]. A lifetime schedule that reflects an EV battery's first and second-life and end-of-life (EOL) can be created, as in Figure 5.

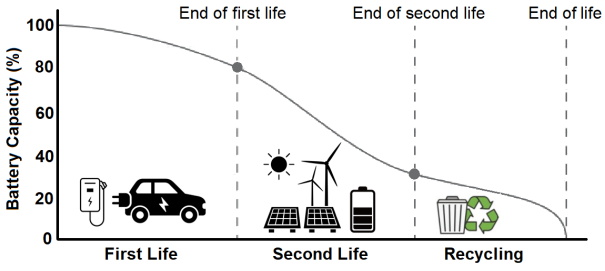

FIGURE 5. Shifting points of EV battery.

As for other approaches to end-use: in [183], second-life was estimated at various DODs at the specified EOL limits of 70% and 60% capacity. Under 70% and 60% EOL limits, the second life could be extended by 4 to 8 years by reducing the DOD to 30% (50-80% SOC). However, the DOD range, which has critical importance on life, must be selected appropriately. For example, in critical second-life applications, even if the lifetime is increased, a lower DOD will not fully meet the supply-demand balance and will increase grid dependency and cost. Such low DOD values can be helpful in smaller-scale applications. On the other hand, it has been reported that the initial battery life can be increased by six years in ancillary services, 15 years in transmission and distribution network and EV charging support, 5.9 years in self-consumption, 4.7 years in area regulation, and seven years in energy management [184], [185].

There are three main reasons for reaching EOL. An EOL condition may occur as the vehicle reaches end-of-use, and depending on the physical condition and health of the battery, the pack may be used directly and separated into modules or cells at later steps in the life cycle. Due to increased internal resistance and decreasing capacity, batteries may not be able to meet driver needs and may reach EOL. For warranty reasons, the vehicle and battery may require age or mileage procedures, and EOL may be reached beyond the driver's control, as it limits usage [186]. Regardless of specific application requirements, a universal acceptance for all battery capacities is that 70-80% of EOL will be achieved. A common misconception is that the transition to secondary use will occur at 70-80% capacity. The main cause of EOL is due to capacity constraints. Then come the power constraints. While EV battery capacities above 40 kWh reach EOL due to capacity constraints, power constraints are the leading cause of EOL for batteries below the relevant capacity [187]. High EV battery capacity may cause the batteries to be used less than necessary. A fixed threshold was introduced so EV drivers would not notice reduced performance. Prognostic approaches take advantage of the number of charge/discharge cycles, capacity, and internal resistance results while keeping track of SOH properties. While the cell's internal resistance is high, it may not have sufficient capacity, and the accuracy of SOH estimation will be affected. Additionally, regarding remaining useful life (RUL) estimates, a fixed threshold causes simplification and increases the margin of error. In this regard, SOF estimation is required in addition to RUL, SOH, and EOL algorithms. SOF indicates how far the battery is from its EOL limit or relates the current state of the battery to its EOL limit. It uses the weight of the SOC range, charge/discharge rate, environmental temperature, and other factors when evaluating functionality [188].

SOF measures the extent to which the actual power demand is met, but even when a certain amount of power is supplied to a load, not all of the stored energy is used due to several obstacles [189]. Although discharging the battery at a low current reduces the voltage drop in cells with high internal resistance, increasing the discharge rate raises the amount of usable energy, the internal resistance, and the voltage drop. Given the high internal resistance at low temperatures, battery functionality will decrease at lower temperatures. As demanding too much power from the pack will reduce the SOF and bring it closer to the limit, requiring more power from the battery is not allowed and is limited. The currents used for level 1 and 2 EV charging, particularly in the Society of Automotive Engineers (SAE) J1772 standard, are generally between 0.5 and 2C, depending on the battery capacity. Considering that the charging process is sensitive to SOF, a low charge rate is better to control the balance between the cells. On the contrary, high charge rates increase the voltage difference between low and high internal resistance. If the charge rate increases, the SOF will decrease faster than the discharge rate at constant ambient temperature [190], [191], [192]. Figure 6 illustrates the sensitivities affecting SOF [193], [194]. At the beginning of life, SOF has a value of one, while at EOL, it is assumed to be zero, and SOF estimation can be realized using Equations (21)-(23) [195]. However, SOF is subject to three limitations. These are terminal voltage, SOC, maximum discharge, and minimum charge current, which are concerned with design limits. Equation (24) is considered by including the relevant constraints [196].

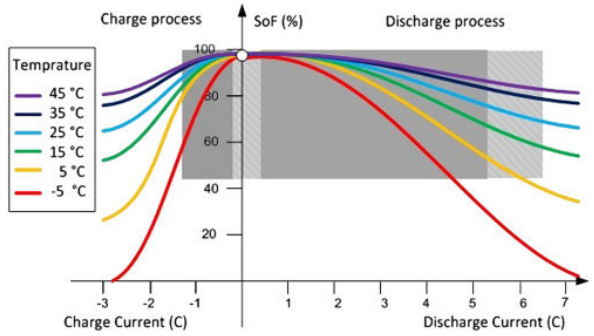

FIGURE 6. SOF changes vs. charge/discharge rates and environment temperature [193], [194], [195], [196].

Another approach is the open circuit voltage (OCV)-based Equations (25)-(29) [196], which limits the terminal voltage and current within a specific range and limits the maximum available power [197]. In addition, the upper/lower limits for voltage, charge/discharge current, and operating temperature specified by the battery manufacturer provide a safe working region. Considering this range, the determination of the maximum instantaneous output capacity as an indicator of the battery condition is achieved by Equations (30)-(33) [198], [199]. Thus, SOC, SOH, and SOF can be estimated within a common framework. However, to define driving requirements, historical driving profiles and data from the battery energy management system (BMS) need to be analyzed and compared with the level of impairment [200]. When considering SOF, it is emphasized that the minimum battery capacity should be 40 kWh throughout the lifetime of the EV to ensure that the capacity is not under-utilized [201]. Contrary to popular belief, vehicle-to-grid technology does not cause early battery retirement for high-capacity batteries, prevents under-utilization of capacity, and provides more economic benefits than SLB.

$$SOF_{capacity} = \frac{C - C_{EOL}}{C_{BOL} - C_{EOL}} \tag{21}$$

$$SOF_{capacity} = \frac{C - C_{EOL}}{C_{BOL} - C_{EOL}} \tag{22}$$

$$SOF_{Ri} = \frac{Ri_{EOL} - Ri}{Ri_{EOL} - Ri_{BOL}} \tag{23}$$

$$SOF_{safety} = \min_{i=1,2,\cdots,n} \left(\frac{X_i - X_{i,\,EOL}}{X_{i,\,BOL} - X_{i,\,EOL}} \right) \tag{24}$$

$$P_{min}^{chr} = max\left(P_{min}, U_{t,k+L} I_{min}^{chr}\right)$$

$$P_{max}^{disch} = min\left(P_{max}, U_{t,k+L} I_{max}^{disch}\right) \tag{25}$$

$$I_{max,vol}^{chr} = \frac{U_{max} - OCV}{R_0} \tag{26}$$

$$I_{max,vol}^{disch} = \frac{OCV - U_{min}}{R_0} \tag{27}$$

$$I_{max}^{chr} = min\left(I_{max,vol}^{chr}, I_{max,cur}^{chr}\right) \tag{28}$$

$$I_{max}^{disch} = min\left(I_{max,vol}^{disch}, I_{max,cur}^{disch}\right) \tag{29}$$

$$P_{max}^{chr} = I_{max}^{chr} \,.\, \left(OCV + I_{max}^{chr} R_0\right) \tag{30}$$

$$P_{max}^{disch} = I_{max}^{disch} \,.\, \left(OCV - I_{max}^{disch} R_0\right) \tag{31}$$

$$P\,(t) = P_{max} \,.\, SOC\,(t) \,.SOH\,(t) \tag{32}$$

$$SOF\,(t) = \frac{P\,(t) - P_d\,(t)}{P_{max} - P_d\,(t)} \tag{33}$$

B. REMANUFACTURING

Degraded EV battery packs are first examined and separated from their protection. Then, the electrical test equipment is connected, and the characterization process is managed according to voltage. The test equipment connections are left, and the individual packages are checked for the last time and separated from their upper parts. After the junction box and busbar connect the battery, the cell management controller, battery management system, and charge circuit are disconnected [162]. The electrical and mechanical connections between the cells are removed when the individual packages are made into modules. However, the separator between the anode and cathode electrodes, which is covered with a cylindrical metal case, is made from a single plate, making it very difficult to separate the cylindrical cell form. Another area for improvement is that the battery module is not detachable. The use of welding in cell junctions and the most fragile nature of the joints in the outer shell complicate

the process [202]. The other electronic parts (control and connection circuit, etc.) are removed and taken to a different place in the following procedure. This activity can take between 8 and 16 hours, depending on the worker and the difficulty of disassembly [53]. Battery manufacturers have adopted module standardization that will facilitate recycling and reuse. Replacing battery components is carried out in three different ways. The first is relocating the components to be replaced into the module, providing a warranty equal to the remaining lifespan specified in the warranty. If the size of the fault is serious, replacing the components with a warranty and reinstalling them in the EV is the second method. The third method involves procuring the component from two or more battery components to obtain the battery to be reinserted into the EV [203].

Cells dismantled in mechanical, safety, and electrochemical scope are then characterized. An OCV test to measure the SOC is performed in the second commissioning phase. An overall OCV is measured, and the status of the removed modules and cells is queried before the pack is disassembled. Note that if the module contains internal cells, the OCV of the cells is measured. The total combined OCV of the cells shall equal the OCV in the module. A similar relationship must also meet the required harmony at the module and pack level. In the event of a discrepancy, faulty cells must be identified and, after disassembly and detailed analysis, sent for recycling if they do not meet the manufacturer's requirements. The isolation of the terminals inside the battery from other external parts that may conduct electricity is carried out by an incoming high-voltage insulation test. The relevant insulation criterion must be met in advance to prevent accidents related to occupational safety (fire, electric shock, etc.). The insulation resistance measured between the positive and negative terminals and metal components for at least 60 seconds at a voltage of 500 V_{DC} must be at least 100 Ω/V for DC circuits and 500 Ω/V (or 50,000 Ω) for AC or combined circuits [204]. Another test concerns capacity. The battery, fully charged at room temperature (0.2 C), is left to rest for the required time (1-2 hours) in a fully charged state. Following the rest period, the loss of capacity due to a complete discharge at the same C-rate is calculated using existing measuring instruments (Chroma, Arbin, etc.) based on the current and time data recorded. Compared to the original capacity data, cells found to be healthy are grouped according to their current capacity. However, when carrying out the capacity test, it is essential to comply with the maximum and minimum voltage limits promised in the manufacturer's catalogs during the charge and discharge process so that full charge and discharge are carried out within the relevant maximum and minimum voltage limits. The primary purpose of the charge/discharge cycle test is to monitor the temperature, voltage, and current of cells and modules after at least one charge/discharge cycle at room temperature and to monitor any irregularities that may occur. The internal resistance test uses methods such as EIS, which is used in the literature, including package, module, and individual cells. However, the most common method of determining internal resistance is to monitor the voltage drop caused by current pulses. In particular, the current-off technique measures the change in voltage concerning the current between charge and discharge transitions [205].

The other method, the current switching method, analyses the current-dependent voltage shift from the maximum discharge point to the charge point [206]. While International Electrotechnical Commission (IEC) 61960-2003 standards mainly carry out internal resistance measurements, test devices such as Chroma are used. Another second preparation test is to examine spontaneous discharge. If the entire package is to be used or fully charged to the maximum voltage at the cell and module level, they are stored at room temperature of 20 ±5°C for not less than one day. Whether the promised self-discharge rates align with the manufacturers' instructions is evaluated by OCV measurements recorded at specified time intervals. The relevant time interval can vary from 5-10 minutes, 1-2 hours, or 24 hours.

Since the open circuit voltage includes essential information, the voltage check must be repeated several times at the cell and module levels. Internal resistance and capacity examinations require more time and money due to additional tests. The SOH determination is made by capacitance reduction matching based on changes in current-voltage relationships. Non-destructive acoustic testing, which examines corrosion, cracking, and fatigue in structures such as concrete and steel, and listens for metal defects, has just begun to be used. The sensor-based acoustic system integrating electrochemical processes with voltage curves can capture battery data [202]. EIS, which evaluates operating conditions by examining the increasing number of cycles and impedance change, is frequently used with its non-destructive, low-cost, simple, and fast programming structure and online opportunity.

Another sensitive issue in the characterization phase is using stability agents to reduce cell heterogeneity. The performance of stabilizers to reduce heterogeneity between cells to be re-used is essential to minimize preparation costs, thereby increasing the economics of SLB. Passive stabilizers based on heat in shunt resistors do not serve this purpose as their efficiency is 0%, and load balancing is performed according to the weak cell. In addition, significant differences in capacity reduction and self-discharge between cells indicate that the heterogeneity problem cannot be solved. Active balancers, where the load is balanced and no energy is wasted when operating cell to cell, cell to module, or vice versa, are relatively more efficient [207]. The balancing techniques can be classified as a capacitor, inductor/transformer, and converter-based. In inductor-based load balancing methods, short transient times, high currents, and high switching speeds are desired, so groups of capacitors are used to filter high frequencies. Active load balancing, including centralized, distributed, and modular, can be performed at the

converter base and uses conceivable types (cuk, boost, buck-boost). Although efficient, the design and implementation phase is complex and costly. Capacitor-based systems, on the other hand, use external energy storage to equalize the energy balance between weak and vital cells. Although current fluctuations are the main problem, they vary depending on the number of switches and layers. Although their design is simple, they take a long time to synchronize. Two-stage balancers are obtained by combining passive and active balancers to compensate for the loss of cell capacity due to self and discharge voltages. While reducing the performance deficiencies, the cases where inductive drivers are used have the advantage of being simple, cheap, and space-saving. In most cases, however, transformer-based DC-DC converters are used, resulting in high space requirements and costs [208]. A comparison of dynamic active balancers that transfer the load from a stronger cell to a weaker one in adjacent cell-to-cell, direct cell-to-cell, cell-to-packet, and packet-to-cell conditions is an element that increases performance. In this direction, the best performance is achieved in direct cell-to-cell architectures, while there is a good trade-off between performance and complexity in adjacent cell-to-cell and packet-to-cell architectures [209]. By balancing the SOC in both charge and discharge phases, the usable battery capacity is increased by 16% compared to DC/DC converter types with only 70% power efficiency. It also increases the capacity from 14.5% to 17.4% compared to conditions without dynamic equalization [210]. Determining the capacity of each cell in the control target map according to the SOC operating window of other cells and obtaining differential currents along the cell can provide other gains. For example, committing to a final capacity imbalance of 0.1% and an overall capacity loss of 0.005% can achieve a low renewal time of 1.3 months. In addition, the capacity imbalance of the cells can be reduced by 7.25% in 78 days [211].

Characterization methods are constantly being developed for various problems encountered in the second-life stage. The cell spread problem was eliminated by the statistical approach using spatial and temporal, three-parameter gamma processing [212]. With the new two-level equalizer method, which considers the weakest cell and acts from the average discharge capacity of the cells, problems such as capacity loss due to imbalance, current rating, and heat dissipation have been overcome [213]. With the lite-sparse hierarchical partial power handling (LS-HiPPP) method, which reduces heterogeneity in voltage and capacity, energy use and resistance to usage uncertainty were increased to 94% and 80%, respectively, while derating was reduced to 84.3% [214]. It was stated that EIS is more economical than capacitance and current breaking (CI), with minor differences, but the measurement error is higher than CI. With the emphasis on sensitive quantities, EIS is more costly and slower [215]. However, in health status predictions, the new methodology based on neural networks can reduce the number of frequencies and dimensionalities to be measured in EIS. The measurement time can be reduced to 19.1% of the original value, and the number of entities in the measurements can be reduced from 81 to 4 [216]. Even in the most pessimistic scenario, the mean absolute percent error (MAPE) was reduced below 4.2% with the method that does not require special equipment, shortens the time compared to the traditional, and measures the AC/DC resistance in various SOCs for the package/module/cell [217]. In constant current-voltage charging, characterization with incremental capacity analysis (ICA) and constant voltage phase is difficult and impossible. Similarly, the SOH prediction strategy may fail due to the heterogeneous form and unknown initial lifetime. Therefore, with a new generic rapid characterization test based on a partial coulometric counter using offline experimental data, the maximum error at the package/module level was reduced to 5.1% [218]. While the degradation profile was created with the exponential triple smoothing algorithm, the measurement error of internal resistance, capacitance, current, SOC, and SOH was eliminated by quadratic ECM [219]. Adopting the incremental constant current charge-discharge cycle and EIS reduces the capacity loss to less than 5% in both NMC and LFP cells [220]. DC internal resistance and power capacity were determined effectively using the constant current-voltage method in capacitance analysis and the constant current-open voltage method in the SOC test [221].

After this type of cell characterization, the grouping stage is started. Battery management tests such as voltage equalization, safety check, and fault diagnosis are re-executed and connected to integrated and adaptive electronic components. Cell, module, and package assembly technologies are essential in manufacturing and disassembly processes. Uncertainties in these processes make the total cost of ownership uncertain. The main sources of uncertainty are the creation of electrical and structural interconnects, the combination of conductive/reflective materials due to the wide range of thicknesses, and the difficulty of bond durability. Many joining technologies are available, including ultrasonic welding, resistance spot welding, micro tungsten inert gas (TIG)/pulsed arc welding, ultrasonic wedge bonding, brazing, laser welding, magnetic pulse welding, and mechanical assembly [222]. Although ultrasonic welding is valuable with its advantages, such as high durability, speed of process, and low energy consumption, it can only be applied to pouch cells and causes high heat production that can damage the battery. Similar advantages and disadvantages can be seen in Table 7.

It is made ready for the customer for sale. At the end of this whole process, voltages between 800 and 1000 V are generally reached in the application areas [180]. All this second preparation process can be summarized in Figure 7.

Looking at the total financial breakdown of this entire repurpose process, the purchase price of the battery is 52%, labor is 32%, warranty is 5%, insurance is 3%, and others are 8% [234], [235]. In International Renewable Energy

TABLE 7. Joining technologies for the second-life EV batteries.

Joining Technology	Advantages	Disadvantages
Ultrasonic welding [222]	• Fast process • High strength and low resistance • Able to join dissimilar materials • Low energy consumption • Self-tooling • Excellent for highly conductive materials	• Only suitable for pouch cells • Needs two-sided access • High heat generation can damage batteries • Expensive consumables • Limited joint thickness • Challenging on high strength and hard materials • Sensitive to surface conditions
Resistance spot welding (RSW) [223]	• Fast process • Low cost • Well quality control • Easy automation • Self-tooling	• Difficult for highly conductive and dissimilar materials • Difficult to produce large joints or joining of more than two layers • Risk of expulsion
Micro-TIG / pulsed arc welding [224–226]	• Low cost • High joint strength and low resistance • Able to join dissimilar materials • Easy automation	• High thermal input and heat affected zone • Porosity • Difficult to join more than two layers
Ultrasonic wedge bonding [227, 228]	• Fast process • Acting as fuses • Able to join dissimilar materials • Low energy consumption • Easy automation	• Only suitable for small wires • Low wire and joint strength • Complex manufacturing
Soldering [229, 230]	• Joining dissimilar materials • Widespread in electronics industry	• High heat • Labour intensive • Need for solder material • Low joint strength
Laser welding [51]	• High speed • Less thermal input • Non-contact process • Easy automation • High precision	• High initial cost • Need of shielding gas system • Quality control is difficult • Needs well joint alignment • Process monitoring is difficult • Challenges in dissimilar joining
Magnetic pulse welding (MPW) [231, 232]	• Solid state process • Able to join dissimilar materials • High joint strength	• Potential large distortion • Rigid support required • Possibility of Eddy current passing through the cells
Mechanical assembly [233]	• Easy dismounting and recycling • Easy repair • Cold process	• Additional weight • High connection resistance • Expensive (not if TCO) • Additional weight

Agency (IRENA), on the other hand, the purchase price is attributed to 56%, labor and administration 26%, packaging 7%, and others 11%. Today, the breakdown of FB and total SLB cost is as in Figure 8. Typically, the purchase price of a battery in the N^{th} year can be calculated by Equation (34) [53].

$$(Cost_{SLB-re})_N = \left(\left[Cost_{cap}\right]_{FB}\right)_N .SOH .(\,1 - Per_{re}) \quad (34)$$

C. STANDARDS AND REGULATIONS

Although no adequate standard or regulation can be used at the international level and covers the whole process today, it is promising to see new ideas and initiatives. A short 35-page document was published in 2018 by the Underwriters Laboratory (UL), which became operational in 1974. While the safety procedures and performance tests for battery packs, modules, and cells are described, production and repurposing could be more detailed. As the first document approved by 4R Energy Corporation, this directive is applicable as a first step. Following the proposal on batteries and their waste on 10 December 2020, the European Commission requested information about their systems from battery system manufacturers larger than 2 kWh. This way, battery composition, production, technical performance, and sustainability parameters were made available to the public or accredited companies. In addition, it was emphasized that a database called "battery passport" should be established for each battery/cell/module/package manufacturer operated by the operators. Thus, the cyclical supply and economy of the purchasing-production-waste chain would enable ways such as blockchain. The United Nations (UN) emphasized in a regulation published in March 2022 that reducing EV battery capacity by 20% should take at least five years or cover 100,000 km. Likewise, a capacity reduction of 30% was requested for eight years or 160,000 km, respectively. It is thought that the benefit can be increased with more durable battery technologies developed in this way. Some international organizations believe that existing standards,

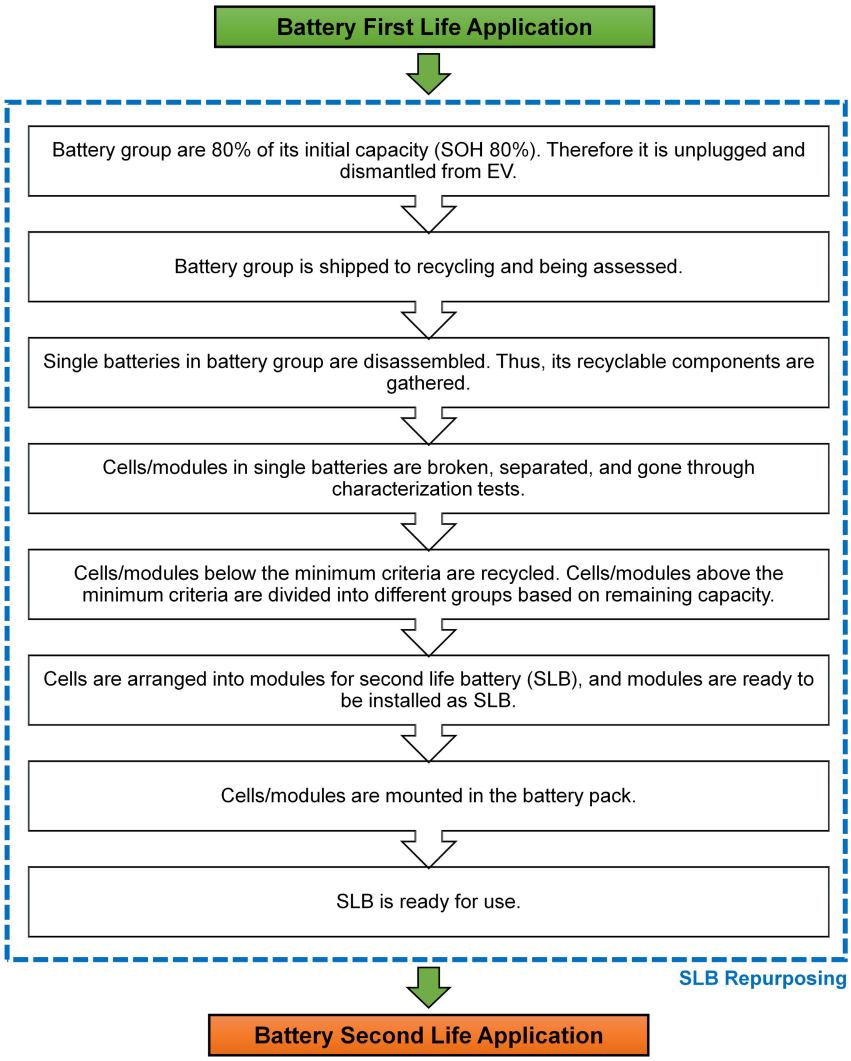

FIGURE 7. Evaluation procedure of retired lithium-ion batteries.

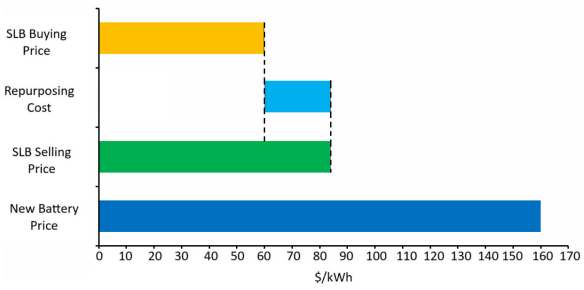

FIGURE 8. Comparison of FB and SLB financial breakdown.

such as International Organization for Standardization (ISO) 12405-2:2012 and IEC 62660-2, can be developed. In this context, SAE has addressed SOH, labeling, and processing for safety procedures with the J2997 coded directive, and the development and determination phase is still ongoing.

D. ESTIMATION METHODS

In a simple framework, SOH, which relates the change in energy to the internal resistance and power reduction, is frequently used in estimating the remaining life. Apart from SOH, the Coulomb counting procedure, in which the current is continuously measured, is another method. Standard prognostic methods are also available to characterize the degradation in the complete sense, not simply. Post-mortem analysis using conventional disassembly techniques and differential voltage and charge-discharge curve-based methods, with ICA being the most common, are some of these. Also, the methodology (model-based, data-driven, hybrid variants) is the most important one combining EIS and ECM, which relates the measured electrical response to internal chemical and physical changes [202]. K-nearest neighbor regression and differential optimization strategies are available, which use the estimated data for all cells connected internally to the battery pack. Considering SOH,

time convolution mesh and enhanced unscented Kalman filtering, F-distributed particle filtering, kernel smoother, and long short-term memory model are also mentioned. In addition, combined multiple linear regression (MMLR) and recurrent neural networks can be listed as other methods. The support vector machine (SVM) algorithm performs the online RUL estimation by analogy with the measured battery charge curve segment. Both SVM and dual polarization methods can be seen in the market, albeit slightly [65].

Moving forward in model scope, ECM, electrochemical, empirical, physical, data-driven (artificial intelligence, statistical, signal processing), and hybrid models are common [64], [109]. ECM, which reflects battery performance, includes electrical element combination, and is solved by techniques such as circuit analysis, is the simplest method. But, the prediction accuracy is relatively low, far from real data [161]. Although electrochemical models and internal parameters are represented mathematically, their popularity has declined due to increased computational complexity of the process. In empirical models that include experimental test methods and evaluate the correlation between large volumes of data, support elements such as semi-empirical and curve fitting can be added to the system. In this way, the relationship between SOH and internal resistance can be captured, and SOC, state of power (SOP), and state of energy (SOE) estimation can be benefited from the added semi-empirical support. Taking temperature, SOC, speed, and cycle number as independent variables, this model has poor generalization ability for different battery chemistries and operating conditions [236]. In a physical or regression model, which processes internal battery mechanisms and reaction kinetics such as SEI growth, lithium plating, active material cracking, and electrolyte decomposition, in partial differential equations, an intensive processing capability and accurate definition of parameters are required. A data-driven model is a procedure that maps parameters and SOH from test data, where the operating mechanism is use-specific; that is, there is no standard. It also uses machine learning algorithms where no complex mathematical model is created. The last representative of artificial intelligence is deep learning algorithms, which are tightly dependent on data quality and quantity, flexible and applicable, capable of nonlinear fitting, and the relationship between health indicators (HI) [237]. Although hybrid techniques combine more than one method, it is always challenging to achieve complete harmony. When all such disadvantages are examined, it has been reported that high-precision SOH estimation is most applicable to the physical model using simplified mathematical techniques and computing power [109].

Observing the battery temperature distribution is another area of estimation. The state of temperature (SOT) is not widely used and is not yet a well-understood phenomenon. Electrochemical and thermal models based on heat production equations can handle gases and fires above 100°C with SOT prediction [238], [239]. The research trend on SOT in recent years is to prevent failure by estimating the temperature in the battery core, estimating the temperature in large battery packs, and evaluating the relationship between transient events in batteries (overcharge, internal/external short circuit, etc.) and thermal states [197]. To assess the detrimental effects of thermal runaway, particularly in Li-ion batteries, it is necessary to measure temperature, mass loss, cell/module voltage, and qualitative vent gas composition [240].

Also, system stability can be achieved using thermal models that imitate heat generation and dissipation. According to the size of the thermal distribution, it can be divided into subclasses such as lumped, one-dimensional, and two-dimensional thermal models. The prediction accuracy of lumped thermal models is limited. Other thermal models that present the temperature distribution as 1-D and 2-D have partial differential equations available for online use and face heavy computational load. This situation can be solved with advanced computer requirements. While fans are generally used in air-based active thermal management, it stands out with their low cost and simple structure. Liquid-based active thermal management has a higher heat dissipation rate and efficiency. It also reduces interference and noise by 40%. Heat is absorbed or released within the allowable temperature range in the phase change material-based passive method. It also saves parasitic power. Apart from the low cooling performance of the air-based active method, the low complexity, high cost, and leakage risk of the liquid-based active method make the phase-change method reasonable [99]. It is possible to see all these parametric estimation processes in Figure 9.

Many researchers have improved the accuracy of second-life and EOL prediction by developing new SOH, RUL, and SOC strategies. For example, RUL prediction under coupling stress was performed in [251] based on support vector regression and experimental data of 6 sets of coupling stresses. In [252], where short-term and long-term online SOH prediction are combined, the predictive power is increased by using the Kalman filter. In [253], a method applicable to specific SOC profiles has been proposed by acting in an open data manner, considering the cycle depth, average SOC and current value parameters, and the uncertainty of the initial SOC and aging rate. In [254], ICA and infrared techniques were combined for battery packs disassembled according to aging cycle procedures accelerated at different rates, and the actual EOL could be obtained with high accuracy. In [255], where online and offline methods were used to estimate SOH, rarely analysed in SLB operations, HIs were obtained using experimental data from partial charge, cycle and calendar ageing tests, and the prediction error was reduced to 1.3%. Incremental capacity (IC), stress, and probability density function analyses were evaluated for SOH prediction models with and without multicollinearity in [256]. While the peak features in the curves of the relevant analyses demonstrate the excellent correlation between SOH and HIs, multicollinearity

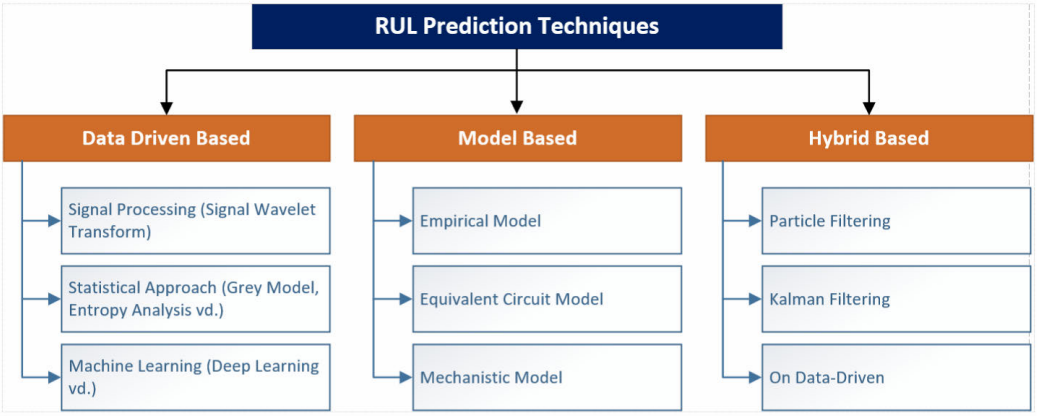

FIGURE 9. RUL estimation methods for lithium-ion batteries (Signal processing [241], grey model [242], entropy analysis [64], deep learning [243], empirical model [244], ECM [245], [246], mechanistic model [247], particle filtering [248], Kalman filtering [249], on-data driven [250]).

was reduced by principal component analysis, which was then used to minimize the prediction error to 1.06%. Applicable HIs were selected to estimate SOH between 24% and 71% over long-term obsolescence periods [257]. It is emphasised that the best indicator is obtained by ICA with low prediction error, while partial charging is the most durable method for second-life aging. Linear regression, on the other hand, promises to reduce the prediction error of the proposed indicators to below 2% with low computation times. In [258], which uses three machine learning models, the input parameters are selected from the batteries' charge and discharge profiles, while the models' training is tested on eight different inputs with and without K-fold (K = 10) cross-validation. Using the K-fold cross-validation method, the mean square error was found to be 0.009147. In [259], using regular logistic regression classification, multivariate linear regression and multilayer perceptron regression, the number of RUL cycles was determined to have a prediction error of 0.041 by simple charge and discharge tests and voltage waveform analysis. In [260], where three types of regression (least squares, ridge, etc.) were proposed for RUL estimation, IC curves were transferred to the regression inputs, and the estimation error was limited to 2%. In [261], three different RUL estimation methods are proposed. The first uses battery history data and IC curve characteristics similar to the regression input. However, a filter-based feature selection procedure is performed to eliminate multicollinearity. The second is the dynamic time-bending algorithm, in which past data cannot be used. The corresponding algorithm obtains the contraction coefficients by ensuring curve matching between the reference and target cells. The third is the degradation mechanism-based method, where only part of the battery curve can be used and is based on the charge voltage segment. Similar techniques can reduce the prediction error to 1.5%. In [262], which uses the cell difference model and the adaptive damping unscented Kalman filter algorithm, second-order resistor/capacitor ECMs, namely the Rint model, are used, and the prediction error is guaranteed to be ±2%. Since the correlation between internal impedance and SLB storage capability is known in accelerated SOH estimation [263], Bayesian optimization based on Gaussian process regression can be used to hyper-parameter such procedures [264]. The correlation storage between cell impedance, SOC, temperature, and SOH is generated by the machine learning model using all EIS data or selected features, while the prediction error is 1.1%. In [265], which uses the indicator referred to as the optimum retirement score, the compromise between the first and second-life is targeted. Multi-objective optimization problems based on Pareto fronts, which include the total cost and energy storage cost, are evaluated with the ε-constraint method to determine the SOH range (71.5-86.4%) accurately. In [266], which focuses on fast charging protocols, charge-based features are first selected from charging data thanks to an extended convolutional network for early and accurate prediction. The features taken from the discharge curve are developed with deep neural networks. Charge and discharge-based features are combined and used in random forest regression to predict cycle life. By optimizing the hyperparameters using Bayes, the margin of error was reduced to 15% even at the beginning of the equivalent cycle (the first five equivalent cycles).

Finally, Table 8 explains the models developed by researchers working on the estimation status to ensure battery health, considering their boundaries. A means boundary conditions and B indicates parameters and material properties. Also, Spec. refers to specification.

E. SCOPE OF APPLICATION

It is a matter of curiosity in which operations of the batteries, prepared for repurpose according to the RUL and SOH, will be helpful. Considering the configurations such as direct package usage, package stack, direct module usage, package renewal with modules, and package renewal with cells, effective application areas that maximize profits were

TABLE 8. Parameters and material properties used considering SOH estimation model boundaries.

Ref.	Model	Spec.	Explanation
[238]	Three-dimensional thermal finite battery element modeling is used to analyze the temperature distribution under thermal abuse conditions and to perform furnace testing on more giant cells, considering their geometrical characteristics.	**A**	Charging was carried out in galvanostatic mode at a rate of 1 C at a voltage cut-off of 4.2 V and then in potentiostatic mode until the current dropped to 1000 mA. After boiling for 2 hours, the cell was placed in a preheated oven. The tests were performed on the cells at oven temperatures between 140°C and 160°C.
		B	Heat generation and rates, internal conduction and convection, external heat dissipation, heat transfer coupled with three-dimensional heat transfer elements, electrically conductive elements, and heat convection surface elements. Entropy is estimated from experimental measurements. The VLP 50/62/100S-Fe (3.2 V/55 Ah) cell, cathode, and anode are covered with aluminum and copper foils, and both electrodes use polyvinylidene fluoride and N-Methyl-2-pyrrolidone binder. A three-layer polypropylene, polyethylene, and polypropylene separator are available. Measurement of the internal pressure change is carried out with a pressure gauge. A 2 mm diameter thermocouple determines the internal and external temperature response. A thermally homogeneous cell body with thermophysical properties is considered.
[197]	SOC estimation is performed with an extended Kalman filter using a second-order RC model. The impact of battery aging on SOC estimation is considered. The recursive least squares algorithm is used with a parametric battery model.	**A**	Model parameters were obtained from other researchers by applying HPPC characteristics at various temperatures and determined using a genetic algorithm. Capacity estimation was performed at fixed time intervals of three and six months. Accelerated cycle life testing was conducted at 50°C with discharge under a maximum stress profile of 4C. The accuracy of the cell voltage measurement was ±5 mV, and the accuracy of the current measurement was 0.5% (>30 A) and ±0.1 A (<30 A).
		B	Determination of maximum charge and discharge power under voltage and current limits using SOC, definitions, and estimates based on OCV, internal resistance, coulomb efficiency, terminal voltage, estimated capacity, and OCV.
[251]	RUL estimation model based on support vector regression to determine the non-linear capacity degradation of triple LIB under coupling stress.	**A**	The orthogonal test is implemented with 1C. It is designed in two dimensions: temperature and discharge rate. The ambient temperature is limited to 25-45°C. EOL is assumed to be 80%.
		B	Number of cycles, voltage, capacity, internal resistance, and discharge capacity.
[252]	Considering the degradation effects in the Kalman filter-based online SOH forecasting model, the optimal SLB allocation approach is determined by an integrated method using short and long-term Gaussian process regression.	**A**	The voltage profiles obtained by another study after the external pulse test were used in the short-term SOH estimation model. SOH homogeneity for a single package is essential for high operational efficiency, but a standard cell count was adopted instead of various cell counts in different packages. SOC is between 20% and 80%, and the maximum DOD is limited to 60%. Under the same operating condition, 1000 homogeneous cells with similar initial SOH and degradation behavior were considered. Cell and pack SOHs are assumed to be the same.
		B	Cell voltage, number of cycles, charge/discharge efficiency, and maximum charge/discharge power.
[253]	Event-driven degradation model for second-life applications, including cell-to-pack cyclic battery aging, parameterized based on experimental open data and cycle depth, average SOC, and current.	**A**	Capacity loss is modeled as a classical exponential basis. The capacity loss in each cycle is assumed to be small and not directly linked to previous cycles. Calendar aging and temperature stress factors are not considered. High currents or DOD are not applied. Parameterization is performed by curve fitting for ±C/2, SOC 100%, and temperature 25°C. In addition, a control characterization cycle is performed every 50 cycles. The cells are assumed to have similar technology. Monte Carlo is used for cell-to-pack transition analysis. SOH starting at 80% and search interval 75-85% are considered.
		B	Cycle depth, average SOC, C-rate, experimental and unknown parameters, cumulative cycling capacity of the cell, and a function of our cycling stress factors.
[254]	The EOL of oversized pouch LIB cells was determined using a combination of several accelerated aging procedures.	**A**	It is assumed to be dismantled at 80% capacity. Once 4.4 V is reached, it cannot enter the constant voltage (CV) phase. It is charged with 55 A constant current, and a detailed charge/discharge procedure is available. A fundamental analysis, including capacity (50 A based on CCCV) and IR, is performed every 50 cycles.
		B	Cell charge/discharge current, OCV, power, and temperature—Nissan Leaf large-size pouch cell with LMO and lithium nickel oxide (LNO) cathode and graphite anode. The cell surface was painted with a tetanal camera Varnish Spray/Black. A customized cell holder made of POM-C acetal solid plastic material and aluminum plate is used.
[256]	The SOH assessment model is based on principal component regression, probability density function, selectivity concerning differential voltage and increasing current, and multicollinearity reduction by principal component analysis.	**A**	The two cyclically aged cells have SOHs of 82.6% and 93.8%. The first was used to determine the aging mechanism and build estimation models, and the other was used for validation. The cell has a cut-off voltage of 4.2 V and was applied for 1/25C and 1/2C charge and discharge. The EOL was set to 60% of capacity. The aging experiments were performed at a constant temperature (25 ± 1°C). The tester's sampling frequency is 1 s.
		B	Battery charge/discharge capacity, cell voltage, sampling accuracy, total capacity during full charge/discharge, and accumulated capacity near a given voltage point. Second-life NCR21700 triple lithium-ion battery.
[257]	The SOH estimation model is based on fundamental performance and cyclical aging tests, using linear regression and a support vector machine for non-linear health indicators and SOH correlation.	**A**	A second life assessment is performed for 24% and 71% of health indicators. The analysis is performed on 58 health indicators obtained from increasing capacity analysis, partial charging, CCCV testing, and internal resistance (four health indicator extraction methods). The modules' maximum, minimum, and nominal voltages are 8.3 V, 5 V, and 7.5 V. Since the manufacturer did not provide specific usage data, a process based on uncertainties was performed. The CCCV charge/discharge procedure applies C/3 and C/20. SOC levels of 90%, 70%, 50%, 30%, and 10% are considered. The test was performed in the temperature range -30°C to +180°C with a measurement accuracy of ±0.5°C. The IC curves' minimum distance between peaks and valleys was set to 30 points, and the minimum height was set to 5 points. The partial charging method considers 3.7 V to 4.15 V.
		B	Capacity and direct current internal resistance, cell voltage. LMO/LNO cathode and graphite anode Nissan Leaf modules with cell.
[258]	A model that determines suitable inputs and estimates useful capacity based on machine learning, considering the phenomenon of aging and renewal.	**A**	NASA prognostics uses 18650 LIB rechargeable battery data sets. At 24°C room temperature, the B0005 and B0006 LIB cells have been tested in charge-discharge and impedance operational analyses. The CCCV charge/discharge procedure involves applying a constant current of 1.5 A, considering a cut-off voltage of 4.2 V. The constant voltage charging continues until the current reaches 20 A. Discharge is performed with a constant current of 2 A up to 2.7 V.
		B	Charge and discharge profiles, charge and discharge current and voltage.

A: Boundary Conditions; **B:** Parameters and material properties.

determined [186]. In this way, the related curiosity could be alleviated to a small extent. However, it is possible to see the use of SLBs in almost every field to compensate for peak demand, especially in high electricity tariffs or other times. For this purpose, while the annual energy cost was minimized [267], the maximum demand was reduced by 60%, and the average energy use by 39% in commercial microgrid (MG), especially at peak times [268]. Another area is the energy arbitrage for the discharge at peak times and charging at off-peak times. In the related target, the usable energy capacity of the SLB was increased to $\geq$ 94% [269], and break-even results were obtained where the FB price fell to 60% and below [270], to 26% [271]. In addition, with the adoption of the target for SLBs, whose lifespan has been extended to 12.5 years, electricity bill savings have increased to 780 € [272]. Generating assets must meet frequency limits to be synchronized in the grid. In this context, generation assets need to be ramped up as fast as possible (from seconds to minutes) or to balance supply and demand. In this structure, which expresses frequency regulation and network flexibility, SLB is used frequently. SLB benefit increased by 2.6-fold [43], DC efficiency increased to 99% [273], and discounted payback period reduced to 5.5 years provided the internal rate of return was gradually reduced from 8% to 21% [274]. In [275], which focused on frequency response outside the energy market, high performance of 1,424 kWh/yr was achieved in the day ahead market. Especially in less demanding consumer applications (primarily residential), the C-rate is expected to be lower and SOC oscillation higher [109]. Therefore, in the middle segment (commercial), power generation and EV charging support, load following, and peak shaving will be appropriate, and grid management will be the right choice for high demands. In contrast, assets in generation units that deal with constant demand have frequent maintenance periods. After any interruption, it can be included in the system only with a specific initial power. It will be helpful to use in these applications such as maintenance, and black-start [51].

The use of SLB is beneficial in many areas. However, things sometimes went differently. Application areas such as PV smoothing (14%), renewable energy sources (RES) firming (11%), and peak demand shaving are not applicable for SLBs, based on the follow-up period in grid services [276]. In three different frequency reserve and demand response programs [277], fast EV charging support, area regulation, transmission delay, self-consumption [185], load balancing, energy reliability, peak demand shaving, and renewable energy system (RES) applications [52] did not yield beneficial results. However, the profitability of applications such as area regulation, PV firming, renewable energy time shift, transmission congestion compensation, and transmission support is debatable [52]. In transmission stabilization, however, each generator in the electrical grid must rotate at the same speed. In this way, it is ensured that the rated frequency remains within a specific range. A slight imbalance on the generation and load side causes voltage and frequency changes. It is desirable to exchange active and reactive power, area regulation, and provide the relevant power quickly to ensure power stability. In such a case, the charge/discharge capacities will be exceeded, and proper use will not be possible. Especially the slow response of battery technology cannot overcome this situation. A summary of all these application areas can be seen in Figure 10. Today, it is often possible to see ESS applications with MW/MWh capacity SLB. Companies such as BMW, Enel, Mercedes, and Nissan draw attention, as seen in Table 9. The user share is significant even at a low-capacity scale, especially in residences and rural areas. Although it is used in many applications as a stationary energy storage that provides demand support, it is possible to see its use in line with some targets. The US Energy Information Administration has evaluated the battery usage capacity over the years in different applications [278]. Based on the latest data in the first and second-life: frequency regulation, energy arbitrage, ramping or spinning reserve, utilization of residual and excess renewable energy, voltage or reactive power support, peak shaving, and load management, dominance proven.

F. MARKET AND CURRENT PROJECTS

The future of SLB, due to its benefits, is seen as bright by international organizations and researchers. Many studies have been made based on different capacities, markets, and sale prices estimations, as in Table 10. The global battery market in the projection of 2050 is seen in Figure 11 [3], [4], [5], [6].

IV. RECYCLING

Although the US Advanced Battery Commission plans a minimum standard life of 15 years for batteries [292], this can be as low as 8-12 years in operating conditions and driving profiles [52]. In the moments when the capacity loss drops by 40-50%, the second-life ends, and the recycling process (circular waste production) begins. In such a system, 30% of wasted CO_2 in transport and energy is eliminated by improving waste and continuous resource use while restoring the economic balance. Considering that 250,000 metric tons of lithium-ion batteries will enter waste management by 2025 [11], the attention of many organizations has turned to waste management. It is difficult to operate the circular economy system in a beneficial way under uncertain and variable operating conditions. Lithium-ion batteries, the system's first inputs, must be purged of residual energy that will trigger a short circuit or explosion risk before the pre-treatment phase. The batteries are sent to stabilization using brine or ohmic discharge to fix the problem [293], [294]. After the pre-treatment, the electrode materials are separated and collected in one place, while the metal elements and other by-products are recycled [295]. An indispensable recycling element is the extraction of metal oxides (lithium and

TABLE 9. Global applications of second-life and recycling in the last 10 years.

Company and Partnership	Location	Projects
Hyundai Motor Group SK On	Bartow, Georgia	Battery plant to supply US EV manufacturing facilities
Nissan	Cornwall, England	Designing the eVoyager, a small sea ferry
JR East	Eastern Japan	Emergency power supply at level crossings
Kia Europe Deutsche Bahn	Berlin EUREF-Campus, Germany	72 kWh capacity
Nissan	Paris, France	144 kW/192 kWh capacity
MINI BMW Group	United Kingdom	180 kWh capacity (off-grid mobile power units)
Nissan California Energy Commission	United Kingdom	300 kWh capacity for behind-the-meter
Volkswagen	Global	Portable EV charging station with 360 kWh capacity
Nuvation Energy ECO STOR	Norway	- 50 kW/150 kWh capacity for DSM. - 1 MW/700 kWh for transmission delay and distribution upgrades
UMICORE ENGIE	Olen, Belgium	1.2 MW/720 kWh capacity
BYD Itochu	China	1 MWh capacity
SAIC GM Wuling	Liuzhou, China	250 kW/1 MWh capacity
Toyota JERA	Japan	485 kW/1.26 MWh capacity
Bosch BMW Vattenfall	Hamburg, Germany	2 MWh capacity
BMW Vattenfall	Hamburg, Germany	2 MW capacity
Nissan & Eaton & BAM & The Mobility House	Johan Cruijff Arena, Holland	3 MW/2.8 MWh capacity
ENEL	Melilla, Spain	4 MW/1.7 MWh capacity
RWE AG Audi	Herdecke, Germany	4.5 MWh capacity
BAK China Southern Grid	Shenzhen, China	15 MW/7.27 MWh capacity
ENEL	Fiumicino Airport, Rome, Italy	10 MWh capacity
Daimler & The Mobility House &GETEC & REMONDIS	Vestfalya, Lunen, Germany	13 MWh capacity
Daimler Mercedes-Benz Energy	Elverlingsen, Germany	8.96 MW capacity
Daimler Beijing EV Co.	Global	40 MWh capacity
Mercedes	Germany	13 MW and 70 MW/60 MWh capacity for housing demand
China Tower & BYD & Guoxuan High Tech &YinLong New Energy, etc.	China	54 GWh capacity for 2 million telecommunications tower demand
Wrwick University & Jaguar Lan Rover & Videre Global & Connected Energy	United Kingdom	1.7m$ investment to create innovative BMS software for SLB
Nissan Sumitomo Corporation	Global	Initiate a business venture to "Reuse, Resell, Refabricate and Recycle"
LG Energy Solution & General Motors Co.	Ohio, ABD	Establishing Ultium Cells LLC, creating a value chain from raw material mining to battery production and disposal

TABLE 10. Interest and market for SLB.

Global Projection	Source
Lithium-ion battery capacity dismantled from EVs will reach 95 GWh, 25 GWh for stationary energy storage, and a cumulative total capacity of 185.5 GWh/year by 2025.	[162, 284]
34.75 billion $ by 2027.	[6]
7-92 GWh capacity in 2025 and 112-227 GWh in 2030.	[171]
More than 6 million battery packs per year will be removed from EVs, with a capacity exceeding 275 GWh annually by 2030	[163]
1.7 million EV batteries will be second-life, 5.1 billion $ by 2030.	[285]
The SLB price will drop to 73 $/kWh in 2030.	[286]
With 44.7% growth, 9.93 billion $ by 2031.	[287]
30% to 70% cheaper than a FB in 2025. In addition, up to 250 new EV models will be available using batteries from more than 15 manufacturers.	[171]
The FB costs 80 $/kWh, the direct reuse cost is 53 $/kWh, and the repurposed cost will drop to 77 $/kWh by 2030.	[235]
Each 1 million new EVs will add approximately 25 GWh of storage.	[288]
The selling price of the SLB is approximately 44 $/kWh, while the repurposed cost is 20 $/kWh.	[289]
The SLB selling price will drop to 43 $/kWh in 2030.	[290]
SLB use will be profitable until 2025. In the following years, while a stable profile is displayed, valuable results are obtained with a net recycling credit of 50 $/kWh.	[291]

transition metals), known as synthetic minerals (containing many separable components such as copper, aluminum, graphite, electrolyte, and plastic). A supercritical CO_2 solvent is obtained with tributyl phosphate-nitric acid and hydrogen peroxide admixture. Using the corresponding solvent for supercritical metal extraction, 90% of the four precious metals, such as cobalt, nickel, manganese, and lithium, are recovered [296]. Priority is given to these minerals in the pre-treatment phase, while metal oxides are enriched [297], [298]. Although the same task can be accomplished with alternatives such as heat treatment, solvent soaking, and mechanical treatment, it is easier to withdraw electrode

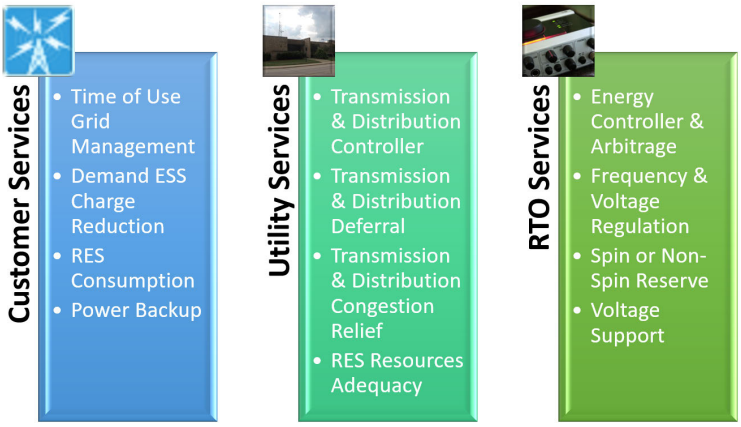

FIGURE 10. Battery capacity distribution in different application areas (grid management [276], demand response [277], RES consumption [279], power backup [280], transmission controller [13], transmission deferral [281], transmission congestion relief [282], RES resources adequacy [41], energy arbitrage [283], frequency regulation [273], spinning reserve [58], voltage support [46])).

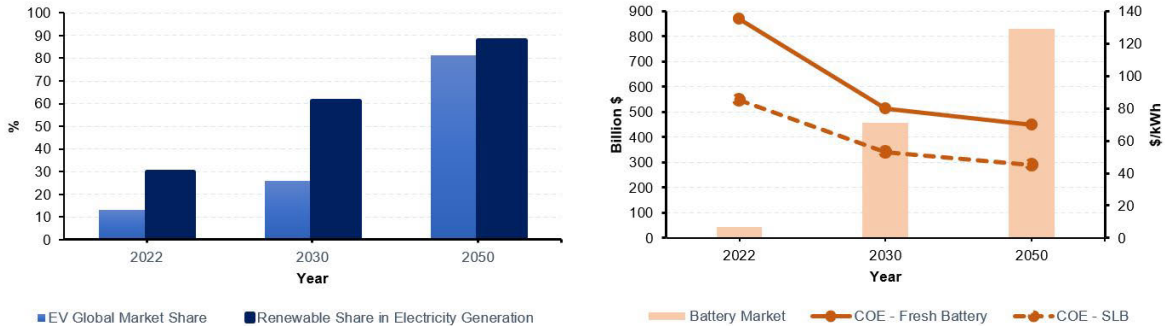

FIGURE 11. Destiny of batteries in future projection.

materials from the electrode sheets. In metal separation from the electrode, using soluble substances has proven the most effective way [295]. The purpose of acid/alkali leaching, bioleaching process, chlorination, and oxygen-free pyrolysis methods was fulfilled. Low-cost, high-safety, environmentally friendly bio-leach will become as common as acid leaching [299], [300]. On the other hand, the separated metals pass through chlorination and oxygen-free pyrolysis and come to the water filtration and evaporation steps. In the relevant step, metal recycling is completed by either chemical precipitation, solvent extraction, or electrochemical gathering. The first method, which performs complex operations by precipitation, is more widely used. The collected cathode electrodes interacted with filtered metal elements rather than recycled. Afterward, it is prepared for reuse by methods such as sintering and re-grinding. with such complex operational recycling strategies, only half of the economic value is recovered in the circular economy [295]. On the other hand, three heavy industrial processes are needed in the purification phase of recycling pyrometallurgy, hydrometallurgy, and direct, to refine the required chemistries such as lithium carbonate, cobalt, hydroxide, and nickel sulfate [66]. When using methods such as roasting or melting in pyrometallurgy, only some metals are recovered from the cathode, and high reaction rates are achieved. Generally, no mechanical pre-treatment is required, and it is mainly worked at high temperatures in the furnace and after stages. Most companies adopt it because of its lower cost and scalability [301]. However, in the mechanical process, where high energy costs are required to eliminate waste gas and slag, if there is no particle size control, metal loss (lithium, aluminum) increases, and the quality of lithium recovery decreases [295], [302]. While it requires more processing, in high-recovery hydrometallurgy, the cathode metals are first dissolved and purified with an acid, base or salt. In the final stage, it is introduced into solid-liquid reactions, such as ion exchange and precipitation, and liquid-liquid reactions, such as solvent extraction. Although toxicity and high chemical consumption may increase through ionic precipitation, crystallization, gas reduction, electrochemical reduction, or electrolytic reduction, high-purity quality products can be effectively recovered. Table 11 compares the heavy industrial methodologies used in the treatment phase.

TABLE 11. Comparison of industrial recycling methodologies.

Pyrometallurgy [303–305]		**Hydrometallurgy** [293, 306]		**Direct** [307, 308]	
Advantages	**Disadvantages**	**Advantages**	**Disadvantages**	**Advantages**	**Disadvantages**
Flexible	Li, Al, or organic materials cannot be recycled.	Flexible	Security concerns due to pressures	Preservation of the cathode structure	Complex mechanical pre-treatment and separation
No separation or other mechanical pre-treatment	Not available in LFP	Convenience in separation and recovery	Cathode deterioration due to acid	All battery materials are recoverable	Recovered material may not perform as well as raw material
High metal recovery	Expensive gas cleaning	High recovery rates	High volume waste production	Suitable for LFP	Mixing of cathode materials
Proven technology	Intense energy	Obtaining high purity material	Not economical for LFP	Efficient use of energy	The regeneration process is under development
Scalability	High capital cost	Efficient use of energy	Failure to recover anode material	Production residues can be recycled	Not at industrial level
High efficiency	Further refinement to recover the basic metal	Absence of air emissions	High operating cost	Attractive for high precious metal element cathodes	Low quality

The interest in recycling lags behind the second life, a certain momentum will be experienced, especially with the developments that will lead to financial improvement. Therefore, researchers are constantly developing circular closed systems and material flows that will benefit recycling now and in the future. For example, in [309], cumulative demand was reduced by 73-100% while improving financial profitability [310]. It was stated that 116 kt of lithium in China and 33 kt of lithium in the USA will be needed in 2030, and approximately 5-7 kt of lithium and 35-60 kt of nickel will be recovered [311]. It is estimated that 25-64% of product demand will disappear between 2040 and 2050 [312], while almost 1.7 GWh of SLB capacity (hence recycling) in Ireland will be reached by 2050 [313]. In Catalonia, cobalt, copper, and nickel recycling are predicted to increase by up to 80% and lithium by up to 60% [314].

A. PRODUCTION, COST, AND MARKET OF MINERALS

The usage rates of lithium, nickel, cobalt, graphite, and manganese minerals in different lithium-ion battery chemistries are variable, there is a common usage. In this context: lithium minerals are mined from salt water or hard rocks; from nickel minerals, sulfide, or laterite deposits; cobalt minerals from the by-product of copper and nickel mining; graphite is natural or synthetic can be obtained. Countries like Bolivia, Chile, and Argentina are famous lithium extraction points for salty waters and Australia for hard rock. It is mined from nickel sulfide/laterite deposits of high quality and content in Russia, Canada and Australia and low quality in Indonesia and the Philippines. Conversely, cobalt is extracted from the Democratic Republic of Congo at a rate of 70% from the refinery of hydrocarbons such as synthetic graphite and coke. Natural graphite is mined at 80% from China, while manganese is predominantly mined from South Africa, Australia, Gabon and China [66]. Lithium sells for 568.5 $/ton, a sevenfold increase in price compared to last year. Cobalt and nickel doubled and had a market value of 51.96 and 29.23 $/ton, respectively. For manganese, the situation is 31.25 $/ton. The yearly change in battery and metal prices can be accessed in [66]. Currently, 25% of the lithium-ion battery waste stream belongs to battery EVs, 36% to long-range PHEVs, and 39% to short-range PHEVs [315]. EV batteries account for 47% of total lithium demand, 24% of cobalt demand, and 7% of nickel. When the building blocks are evaluated, the cathode electrode, representing 40% of the total cost, has always been valuable [53]. The supply of cobalt, which has been used in the cathode until today, is high due to its price [12]. Cobalt-intensive cells, which account for 60% of the total cost, are mostly recycled rather than repurposed [316]. For this reason, studies continue to reduce the cobalt used in the cathode daily [162]. On the other hand, LFP is the only battery chemistry that provides financial incentives for recycling, and its use will become widespread. In EVs, China, with 75% of its current production volume, will play a significant role, given that lithium-ion battery purchases will reach 90% by 2025 [66]. In China, processing and refining facilities built on lithium, cobalt, and graphite minerals are vital in the global market. Considering that 70% of the 520 kt cathode demand and 85% of the 300 kt anode demand are met, more than 50% of global demand has been fulfilled (European share is 20%, US share is 7%). By 2030, it is estimated that China will undertake 70% of the battery production volume. In the relevant projection, EV battery demand will increase to 3.5 TWh, while cathode and anode demands will increase eight to 10 times. The cathode and anode productions will reach 5,200 kilotons (50 additional cathode facilities), and 2,500 kilotons (40 additional anode facilities). It is also predicted that demand will increase by 30% for lithium, 11% for nickel, and 9% for cobalt, while the recycling market will reach 19.3 from 1.6 billion $ [66]. 3.4 million kg of EV lithium battery cells, which make up 63% of EV batteries [317], are predicted to enter the waste cycle in 2040 [318].

TABLE 12. Battery pasaport.

General Information		
Information	**Value**	**Source**
Name and brand of battery	BMW i3 Samsung 94 Ah	Visual inspection
Battery identification number	6127 762506706	Visual inspection
Batch or serial number	170410 00728	Visual inspection
Place of manufacture	Germany	Visual inspection
Date of manufacture	04 / 2017	Visual inspection
Weight	28 kg	Visual inspection
Rated capacity	94 Ah	[319]
Date of manufacture of the battery	05 / 2017	Visual inspection
Chemistry	NMC111/C	[320]
Hazardous substances present in the battery	Cobalt, manganese, nickel, carbon, polyvinylidene fluoride, aluminium, copper	[321]
Usable extinguishing agent	Water	[322]
Critical raw materials present in the battery	Lithium, cobalt, copper, nickel, manganese, graphite	[321]
Size	410 x 300 x 150 mm	Visual inspection
Volume	18.4 L	Visual inspection
Configuration	12s1p	Visual inspection
Temperature range	[-40 ; 60°C]	[319]
Voltage range	[32.4 ; 49.8 V]	[319]
Rated voltage	44.2 V	[319]
Date end of first life	07/2021	Seller
Energy and Capacity Information		
Information	**Value**	**Source**
Rated capacity	94 Ah	[319]
Remaining capacity	91.8	Capacity and energy
Capacity lost	2.3%	Capacity and energy
Rated energy	4.1 kWh	[319]
Remaining energy	3.6 kWh	Capacity and energy
Rated energy densities	146 Wh/kg ; 222 Wh/L	[319]
Measured energy densities	114 Wh/kg ; 174 Wh/L	Capacity and energy
Energy/capacity of the worst cell	254.4 Wh / 84.2 Ah	Capacity and energy
Dispersion of energy/capacity	2.2% / 2.8%	Capacity and energy
Power Information		
Information	**Value**	**Source**
Ohmic resistance (SOC 50%, 10 s, 1C)	15.69 mΩ	Resistance and power
Rated power (SOC 50%, 10 s, 1C)	42 kW	Resistance and power
Measured power output (SOC 50%, 10 s, 1C)	38.6 kW	Resistance and power
Overall power loss	8%	Resistance and power
Charging power at SOC 80%	50.6 kW	Resistance and power
Discharging power at SOC 80%	12.7 kW	Resistance and power
Charging power at SOC 20%	31.5 kW	Resistance and power
Discharging power at SOC 20%	32.5 W	Resistance and power
Power/resistance of the worst cell	1488 W / 2.7 mohm	Resistance and power
Dispersion of rated power	24.4%	Resistance and power
Dispersion of rated resistance	43.3%	Resistance and power
Efficiency Information		
Information	**Value**	**Source**
Round-trip efficiency	90.7%	Efficiency and energy losses
Energy round trip fade	9%	Efficiency and energy losses
Cooling need	144 Wh	Efficiency and energy losses
Evolution of self-discharging rate	3.3% / 200 days	[319]

V. BARRIERS IN THE CIRCULAR BATTERY CHAIN

Since lithium-ion batteries are designed not to be disassembled, there are extra costs and procedures compared to older battery technologies (lead-acid, NiMH). Besides disassembly, even if it is possible to sort batteries with much different chemistry using robots automatically, the

TABLE 13. Timetable for the implementation of the European Parliament's regulation on the battery passport.

Timeline	EU Battery Regulation
July 28, 2023	Publication in the Official Journal of the European Union.
August 17, 2023	The official entry into force of the battery regulations.
February 18, 2024	Mandatory implementation of battery regulations.
August 18, 2024	Mandatory implementation of safety requirements for stationary battery energy storage systems, performance and durability requirements, conformity assessment procedures and economic operator obligations for rechargeable industrial batteries with a capacity greater than 2 kWh, light means of transport (LMT) and EV batteries.
February 18, 2025	Mandatory implementation of carbon footprint requirements for EV batteries.
August 18, 2025	Mandatory implementation of supply chain due diligence or waste battery management.
February 18, 2026	Mandatory implementation of carbon footprint requirements for industrial rechargeable batteries.
February 18, 2027	Mandatory implementation of battery passports for rechargeable industrial and EV batteries greater than 2 kWh and removable and replaceable portable and LMT batteries.
August 18, 2028	Mandatory implementation of requirements on recycled materials, conformity assessment procedures and economic operator obligations for rechargeable industrial batteries with a capacity over 2 kWh, except for those with external storage only, EV and starting/lighting/ignition (SLI) batteries.

TABLE 14. Offers and provisions on the EU regulation of the battery passport.

Offerings (Training, testing, verification, audit, certification)	Provisions in the Regulation (EU) 2023/1542 that are Relevant to the Offerings
Testing of hazardous substances in batteries	Article 6, Restrictions on substances Annex I: Restriction on substances
Calculation and verification of the life-cycle carbon footprint of batteries	Article 7 Carbon footprint Annex II: Carbon footprint
Verification of recycled content in batteries	Article 8, Recycled content
Battery performance and durability testing	Article 9 and 10, Performance and durability Annex III, Annex IV: Electrochemical performance and durability parameters
Verification and testing of removability and replaceability	Article 11, Removability and replaceability
Testing and certification of battery safety	Article 12, Safety Annex V: Safety parameters
Verification of Labelling, marking and information requirements	Article 13 and 14, Labelling, marking and battery management system information
Verification and audit of due diligence policies and its implementation	Article 48, Battery due diligence policies
Calculation and verification of battery-waste recycling and material-recovery efficiency	Articles 59, 60, 61, 71, Waste batteries collection, recycling efficiencies and material-recovery targets
Evaluation of second-life battery	Article 73, reuse or preparation for repurposing
Digital Battery passport verification and platform management	Article 77 and 78, digital battery passport Annex XIII: Information to be included in the battery passport
Verification of green public procurement	Article 85, 86, Green public procurement
EU conformity assessment, verification of EU declaration of conformity	CHAPTER IV Conformity of batteries

way to the recycling process is lengthy. In addition, the destruction of the descriptive label on the package over time or the lack of proper labeling creates difficulties in identifying the chemistry. Since every step of chemistry determination goes well and is complex, high efficiency can be achieved. However, when it comes to obtaining high-purity metal minerals, efficiency will be limited. Low-cost, closed-loop recycling management for the relevant purpose is still under development. As for financial gain, the revenue from selling critical minerals to be recycled is only between one-third and half of the recovery cost, reducing attractiveness [12]. Mineral ores based on lithium-ion, especially iron, and phosphorus, are widespread globally. For this reason, recycling the related minerals does not bring significant earnings and decreases incentives for recycling. In addition, recycling needs to be handled carefully, as recycling technologies are not developed to a high level and lack of standardisation prevails compared to reuse, high energy density and unique applications. Several problems need to be overcome, particularly cell dismantling and recycling. Due to the need for chemical recovery plants with sufficient technology, legislative shortcomings remain, such as sending the product abroad for recycling. Estimated costs of components may increase due to unforeseen problems in real applications. Non-selective sorting of cells and recycling all cells unnecessarily eliminates cells with good performance. In addition to assembly, the degree of automation of the battery disassembly process is another critical consideration [323], [324]. The lack of standardization and product diversity are the main reasons for manual disassembly processes. The main reason for the high cost of recycling is the increase in labor costs. Another challenge is the possibility of damage to components and fasteners after EOL. Thus, hybrid workstations, where robots and complex tasks are performed and more straightforward and repetitive by humans, may gradually transition to full

autonomy [325]. On the other hand, safety must be considered during disassembly. Batteries not fully discharged before disassembling can create safety hazards due to high voltage and chemicals in the cells. Further safety concerns include the lack of protective measures at workstations and the generation of fire and toxic gases if the electrolyte in the cells is damaged. Capacity limitations are due to several barriers to recycling. Difficulties in collection and transport, energy-intensive processes of advanced technologies requiring high temperatures such as pyrometallurgy are risky for some battery chemistries (LMO, LFP), diversity of battery designs due to lack of standardization, difficulty in disassembly due to adhesives and binders, uncertainty of recycling and low economic return are some of them. On the other hand, it is a common misconception that second-life starts in the range of 70-80% SOH. It is essential to define SLBs for the application in which they will be used rather than the performance threshold between the first and second-life [326], and it is assumed that SOH analysis can be trusted in most cases. In addition, whether EIS test data can be used to estimate the SOH of cells directly or whether it should be used whole or in part is a complicated issue. Especially for researchers using machine learning techniques, the minimum amount of conditioning information for SOH prediction is a criterion that should be emphasized [264]. Furthermore, regarding process speed, it is necessary to evaluate the feasibility of different chemical batteries under various operating conditions [327]. Using a representative second-life duty cycle in batteries has shown that the difference in the cause of deterioration in the first life makes the deterioration rates in the first and second-life inconsistent, emphasizing that SOH analysis alone is unreliable [328]. Contrary to the misconception that they will be retired with 80% SOH, it has been predicted in [329] that removed EV batteries can operate for 12 to 20 years in their second-life despite having only 60% to 67% remaining capacity. Instead of using disassembled cells after the first end-of-life thresholds, first-life end-of-test conditions must be considered, and second-life aging testing must be performed in limited cycles. In this approach, unnecessary battery cycles are reduced, ramp rate violations are eliminated, and the optimum SLB capacity is determined according to the minimum storage requirements for the second-life [330]. Thanks to DOD and SLB capacity optimization, throughput can be increased by up to 14% [279]. A different view is that the cell chemistries produced are unique and the cell forms are different, the cell equalization process to be applied in the characterization process cannot prevent the formation of heterogeneous structures. Additionally, most operations (such as automatic scanning and reassembly) are done manually during re-provisioning, which takes longer to prepare. For such reasons, widespread beliefs exist that RUL is estimated correctly while economic uncertainty persists. However, the operating conditions, and thus the user usage pattern and period, destroy the common opinion. Other vital issues are the need for a suitable SLB model, the techno-economically beneficial business model, and whether the relevant battery is purchased from a certified distributor. Likewise, especially during EV charging, the focus is on high energy density due to the increased range and power demand. The cyclical life, including SLB and recycling, is pushed into the background. While there are two different processes, batteries should be used as much as possible. The most common shortcoming is the absence of specific national or internationally accepted regulations or standards for recycling, repurposing, and datasets for initial use and production. Despite all these negativities, the dominant advantages should be addressed in line with the global goals.

VI. PROPOSALS TO OVERCOME BARRIERS IN THE CIRCULAR BATTERY CHAIN

When it comes to standards, the internationally accepted UL1974 stands out. The relevant procedure, which considers the monitoring of charge and discharge rates, suffers from the difficulty of identifying and mapping battery properties from different chemistries and designs. While the relevant procedure is detailed in Section III.B, to receive UL1974 certification, SLBs must also meet UL1973 criteria. To obtain accreditation in UL1974, analyses such as measuring open circuit voltage, insulation test against high input voltage, capacity test, internal resistance measurement, evaluation of BMS control algorithms and protection components, and self-discharge are indispensable. It is thought that most obstacles will be overcome with the battery passport mentioned in the relevant regulations becoming operational. Looking at the specifications of the relevant organization for the battery passport, capacity, impedance, and open circuit voltage measurement tests are required for batteries; each feature is examined experimentally. Although measurement conditions vary depending on the battery and its intended use, one prerequisite is obtaining the data sheet where safety limits such as voltage, current, and temperature are defined. Batteries produced after 2026 with a capacity of more than 2 kWh are required to obtain a passport by European legislation [55], [331], [332], [333]. It is recommended that the data sheet also include battery composition, performance and remaining life [334]. An example application for a battery passport suggested in [335] is shown in Table 12.

It can be stated that the missing information here was taken from the manufacturer's catalogs or the information regarding the battery chemistry in question in the literature. The EU's 2023 Battery Directive provides the data requirements that SLBs must meet. The new regulation has three goals: strengthening the EU internal market, promoting the circular economy, and reducing environmental and social impacts. The implementation timeline of the relevant regulation, including portable battery, starting, lighting and ignition battery, light transportation battery, industrial battery and EV battery, is given in Table 13 [336]. Table 14 shows the chronological list of the recommendations in the relevant

regulation and it is recommended that researchers interested in reuse and recycling follow the regulation [336], [337].

On the other hand, uncertainty continues in many technical and financial parameters resulting from the need for more data at each step. This problem can be eliminated by recording every related process and storing and sharing the data with the necessary places. Crypto-based blockchain data flow analysis is recommended. It manifests in all nodes in the decentralized network and can be verified with network participants, data is stored publicly, and transparency is ensured. In this way, battery price inflation can be prevented while the raw material content and quality used are always guaranteed. While it is always known who the manufacturer, user, and owner will be at different stages of its life, the qualities and quantities of the battery (manufacturer name, year of manufacture, brand/model, year of operation, logistics stages, etc.) are recorded and accessible. In this way, the primary responsibility for failure at any stage can be easily determined. The use of unnecessary and expensive tests that detect the second-life moment or EOL will be reduced. It allows one to rent to different business models securely and for a fixed fee. Also, supply chains will be predictable with accelerated decision-making, not day-to-day. In this way, it is easy for manufacturers to find the appropriate technology. It is undeniable that unplanned waste management will become history. A new method is required that accurately describes a system or product in the physical world, runs Multiphysics simulations in the cloud, and can easily monitor parameters that are difficult to measure (such as SOC and SOH) continuously. Industry 4.0 serves this purpose and offers the possibility of a digital twin that receives input from intelligent sensors.

Previous studies have investigated the use of blockchain technology in the energy sector, including e-mobility [338], [339]. In the e-mobility sector, blockchain has been effectively utilized for battery supply chain monitoring and battery trading, which are crucial tasks for ensuring the reliability and efficiency of EVs [340]. Blockchain technology, with its immutable ledger recording every battery transaction and interaction, significantly enhances the transparency and traceability of battery life cycles. This reliability instills a sense of security and trust among users. Integrating blockchain with second-life battery management can streamline the tracking of battery provenance, ensuring all stakeholders have access to accurate and tamper-proof data. Blockchain-based systems can also facilitate the certification of second-life batteries, verifying their performance and compliance with regulatory standards, thus building trust among users and manufacturers. Furthermore, by leveraging smart contracts, blockchain technology can automate the execution of warranty claims and recycling processes, ensuring efficient and prompt handling of end-of-life batteries and fostering optimism about the technology's potential.

The mandatory implementation of battery passports by February 18, 2027, aligns perfectly with the adoption of blockchain technology, ensuring each battery's history is securely recorded and easily accessible. This alignment with regulatory requirements reassures stakeholders about the technology's compliance. By utilizing blockchain, the carbon footprint requirements effective from February 18, 2025, can be accurately tracked and verified, enhancing transparency and compliance in the battery lifecycle.

OEMs find the recycling economy unsafe due to different chemistries and battery designs, the ability to monitor transparent and reliable data shared by stakeholders in blockchain management will reduce conflict of interest issues. Another proposed economic model is to collect batteries with performance that OEMs cannot use in EVs, prepare them for reuse, and rent them to customers [341]. Alternative economic architectures can also be created in which the logistics company or other energy storage companies act as intermediaries between the OEM and the customer, and data is partially shared with the intermediaries through the collaboration process. Online management of inventory according to SLB supply and demand, with a focus on sellers and customers, and designating the market operator as the battery trading intermediary will improve economic management [342]. However, excess energy use and data swelling can become significant problems due to increased nodes. A different view is that of a hybrid energy storage solution. This solution method reduces the shortcomings of each storage technology and perfectly matches the demand profile and energy balance in various operating periods. Thus, technical-financial performances are improved, such as efficiency, reliability, and lifetime. Also, intermittent renewable energy generation profiles are smoothed, improving poor power quality. In addition, frequency instability is overcome, and unbalanced loads are reduced. Moreover, the effective DC bus voltage dynamically provides high energy and power density. Thanks to the collaborative working strategy, battery degradation will be slowed when the instantaneous large power demand needs to be met. The efficiency of batteries with longer lifespans, with or without precious metals, will increase due to the reduced cost of expensive testing and labor.

VII. CONCLUSION

This review comprehensively examines the critical phases, economics, market dynamics, and challenges of new battery production and their reuse and recycling potential while addressing key criteria for defining the optimal battery throughout its lifecycle. Moreover, it explored the cradle-to-grave circular supply chain and the economics of batteries, highlighting current projects that illustrate the ongoing developments and the potential challenges and solutions within this field. The comparative analysis of different battery chemistries uses precise terminology, shedding light on their relative advantages and limitations. Additionally, addressed the trade-offs and variable performance characteristics between FB and SLB in stationary energy storage applications, supported by existing research. Three widely used battery models were mathematically compared in research, offering insights into their aging

mechanisms. Recent advancements in thermal modeling were discussed in mathematical terms, and a detailed look at experimental methodologies for SOH estimation and battery model parameterization was provided. The article also examined end-of-life estimation methods and highlighted the often-overlooked state-of-function phenomenon through mathematical expressions. Finally, key insights emerged from the discussions on the relevant standards and regulations, the potential areas for second-life battery applications, the recycling process, and the precious metal market. These aspects collectively contribute to a holistic understanding of battery technology's current and future directions. The proposed solutions (blockchain and hybrid ESS) could overcome the obstacles. With blockchain, a collaborative platform between stakeholders is created, and an environment of trust is provided with stored shared data. In addition, data on battery aging can be evaluated effectively, and investors and governments can make sound decisions. On the other hand, with hybrid energy storage systems, the aging process can be slowed down, and an effective supply-demand balance can be achieved. Ultimately, the review aimed to increase the interest of researchers and decision-makers in battery for lagging climate targets.

REFERENCES

[1] Int. Energy Agency. (2021). *Global EV Outlook 2021—Accelerating Ambitions Despite the Pandemic*. [Online]. Available: https://iea.blob.core.windows.net/assets/ed5f4484-f556-4110-8c5c-4ede8bcba637/GlobalEVOutlook2021.pdf

[2] *Renewable Power Generation Costs in 2021*, Int. Renew. Energy Agency, Masdar City, United Arab Emirates, 2022.

[3] Int. Energy Agency. (2021). *Net Zero by 2050: A Roadmap for the Global Energy Sector*. [Online]. Available: https://www.iea.org/reports/net-zero-by-2050

[4] BloombergNEF. *Global Battery Market*. Accessed: Mar. 25, 2024. [Online]. Available: https://dunyaenerji.org.tr/batarya-patlamasi-2040-yilina-kadar-12-trilyon-yatirim-gerektirecek/

[5] McKinsey Company. *Global Second-Life Battery Market*. Accessed: Mar. 25, 2024. [Online]. Available: https://www.mckinsey.com/industries/automotive-and-assembly/our-insights/second-life-ev-batteries-the-newest-value-pool-in-energy-storage

[6] Businesswire. (2022). *Second-life EV Batteries Market Intelligence Report—Global Forecast to 2027*. Res. Markets, Global. [Online]. Available: https://www.businesswire.com/news/home/20220728005693/en/

[7] C.-X. Zu and H. Li, "Thermodynamic analysis on energy densities of batteries," *Energy Environ. Sci.*, vol. 4, no. 8, p. 2614, 2011. [Online]. Available: http://xlink.rsc.org/?DOI=c0ee00777c

[8] S. D. Kurland, "Energy use for GWh-scale lithium-ion battery production," *Environ. Res. Commun.*, vol. 2, no. 1, Jan. 2020, Art. no. 012001. [Online]. Available: https://iopscience.iop.org/article/10.1088/2515-7620/ab5e1e/meta

[9] P. Meshram, B. D. Pandey, and T. R. Mankhand, "Extraction of lithium from primary and secondary sources by pre-treatment, leaching and separation: A comprehensive review," *Hydrometallurgy*, vol. 150, pp. 192–208, Dec. 2014, doi: 10.1016/j.hydromet.2014.10.012.

[10] A. Katwala. (2018). *The Spiralling Environmental Cost of Our Lithium Battery Addiction*. Wired U.K. [Online]. Available: https://www.wecanfigurethisout.org/ENERGY/Webnotes/EnergyConsumption/GreenerCarsandTrucksSupportingFiles/Spiralling%20environmental%20cost%20of%20our%20lithium%20battery%20addiction%20-%20WIRED%20UK%20-%202018.pdf

[11] T. Chen, L. Cai, X. Wen, and X. Zhang, "Experimental research and energy consumption analysis on the economic performance of a hybrid-power gas engine heat pump with $LiFePO_4$ battery," *Energy*, vol. 214, Jan. 2021, Art. no. 118913, doi: 10.1016/j.energy.2020.118913.

[12] D. Deshwal, P. Sangwan, and N. Dahiya, "Economic analysis of lithium ion battery recycling in India," *Wireless Pers. Commun.*, vol. 124, no. 4, pp. 3263–3286, Jun. 2022, doi: 10.1007/s11277-022-09512-5.

[13] Z. Song, M. S. Nazir, X. Cui, I. A. Hiskens, and H. Hofmann, "Benefit assessment of second-life electric vehicle lithium-ion batteries in distributed power grid applications," *J. Energy Storage*, vol. 56, Dec. 2022, Art. no. 105939, doi: 10.1016/j.est.2022.105939.

[14] Y. Yang, J. Qiu, C. Zhang, J. Zhao, and G. Wang, "Flexible integrated network planning considering echelon utilization of second life of used electric vehicle batteries," *IEEE Trans. Transport. Electrific.*, vol. 8, no. 1, pp. 263–276, Mar. 2022, doi: 10.1109/TTE.2021.3068121.

[15] Y. Al-Wreikat, E. K. Attfield, and J. R. Sodré, "Model for payback time of using retired electric vehicle batteries in residential energy storage systems," *Energy*, vol. 259, Nov. 2022, Art. no. 124975, doi: 10.1016/j.energy.2022.124975.

[16] L. Colarullo and J. Thakur, "Second-life EV batteries for stationary storage applications in local energy communities," *Renew. Sustain. Energy Rev.*, vol. 169, Nov. 2022, Art. no. 112913, doi: 10.1016/j.rser.2022.112913.

[17] Y. Wu, Z. Liu, J. Liu, H. Xiao, R. Liu, and L. Zhang, "Optimal battery capacity of grid-connected PV-battery systems considering battery degradation," *Renew. Energy*, vol. 181, pp. 10–23, Jan. 2022, doi: 10.1016/j.renene.2021.09.036.

[18] J. Falk, A. Nedjalkov, M. Angelmahr, and W. Schade, "Applying lithium-ion second life batteries for off-grid solar powered system—A socio-economic case study for rural development," *Zeitschrift für Energiewirtschaft*, vol. 44, no. 1, pp. 47–60, Mar. 2020. [Online]. Available: https://hdl.handle.net/10419/289044

[19] M. D'Arpino and M. Cancian, "Lifetime optimization for a grid-friendly DC fast charge station with second life batteries," *ASME Lett. Dyn. Syst. Control*, vol. 1, no. 1, p. 11014, Jan. 2021, doi: 10.1115/1.4046579.

[20] H. Ekhteraei Toosi, A. Merabet, and A. Swingler, "Impact of battery degradation on energy cost and carbon footprint of smart homes," *Electr. Power Syst. Res.*, vol. 209, Aug. 2022, Art. no. 107955, doi: 10.1016/j.epsr.2022.107955.

[21] X. Deng, F. Wang, X. Lin, B. Hu, K. Arash, and X. Hu, "Distributed energy management of home-vehicle Nexus with stationary battery energy storage," *Renew. Sustain. Energy Rev.*, vol. 168, Oct. 2022, Art. no. 112837, doi: 10.1016/j.rser.2022.112837.

[22] Y. Deng, Y. Zhang, F. Luo, and Y. Mu, "Hierarchical energy management for community microgrids with integration of second-life battery energy storage systems and photovoltaic solar energy," *IET Energy Syst. Integr.*, vol. 4, no. 2, pp. 206–219, Jun. 2022, doi: 10.1049/esi2.12055.

[23] Y. Deng, Y. Zhang, F. Luo, and Y. Mu, "Operational planning of centralized charging stations utilizing second-life battery energy storage systems," *IEEE Trans. Sustain. Energy*, vol. 12, no. 1, pp. 387–399, Jan. 2021, doi: 10.1109/TSTE.2020.3001015.

[24] L. Bartolucci, S. Cordiner, V. Mulone, M. Santarelli, F. Ortenzi, and M. Pasquali, "PV assisted electric vehicle charging station considering the integration of stationary first- or second-life battery storage," *J. Cleaner Prod.*, vol. 383, Jan. 2023, Art. no. 135426. [Online]. Available: https://www.sciencedirect.com/science/article/pii/S0959652622050004

[25] Y. Gao, Y. Cai, and C. Liu, "Annual operating characteristics analysis of photovoltaic-energy storage microgrid based on retired lithium iron phosphate batteries," *J. Energy Storage*, vol. 45, Jan. 2022, Art. no. 103769, doi: 10.1016/j.est.2021.103769.

[26] C. Ioakimidis, A. Murillo-Marrodán, A. Bagheri, D. Thomas, and K. Genikomsakis, "Life cycle assessment of a lithium iron phosphate (LFP) electric vehicle battery in second life application scenarios," *Sustainability*, vol. 11, no. 9, p. 2527, May 2019, doi: 10.3390/su11092527.

[27] D. Kamath, R. Arsenault, H. C. Kim, and A. Anctil, "Economic and environmental feasibility of second-life lithium-ion batteries as fast-charging energy storage," *Environ. Sci. Technol.*, vol. 54, no. 11, pp. 6878–6887, Jun. 2020.

[28] J. Thakur, C. Martins Leite de Almeida, and A. G. Baskar, "Electric vehicle batteries for a circular economy: Second life batteries as residential stationary storage," *J. Cleaner Prod.*, vol. 375, Nov. 2022, Art. no. 134066, doi: 10.1016/j.jclepro.2022.134066.

[29] J. W. Li, S. C. He, Q. Q. Yang, H. W. He, W. T. Zou, and W. K. Cao, "An energy management system for second-life battery in renewable energy systems considering battery degradation costs," 2022, pp. 1–10, doi: 10.21203/rs.3.rs-952412/v1.

[30] A. Nedjalkov, J. Meyer, H. Göken, M. V. Reimer, and W. Schade, "Blueprint and implementation of rural stand-alone power grids with second-life lithium ion vehicle traction battery systems for resilient energy supply of tropical or remote regions," *Materials*, vol. 12, no. 16, p. 2642, Aug. 2019, doi: 10.3390/ma12162642.

[31] N. Kebir, A. Leonard, M. Downey, B. Jones, K. Rabie, S. M. Bhagavathy, and S. A. Hirmer, "Second-life battery systems for affordable energy access in Kenyan primary schools," *Sci. Rep.*, vol. 13, no. 1, p. 1374, Jan. 2023, doi: 10.1038/s41598-023-28377-7.

[32] A. Bhatt, W. Ongsakul, and N. Madhu M., "Optimal techno-economic feasibility study of net-zero carbon emission microgrid integrating second-life battery energy storage system," *Energy Convers. Manage.*, vol. 266, Aug. 2022, Art. no. 115825, doi: 10.1016/j.enconman.2022.115825.

[33] X. Han, Y. Liang, Y. Ai, and J. Li, "Economic evaluation of a PV combined energy storage charging station based on cost estimation of second-use batteries," *Energy*, vol. 165, pp. 326–339, Dec. 2018, doi: 10.1016/j.energy.2018.09.022.

[34] J. Li, S. He, Q. Yang, T. Ma, and Z. Wei, "Optimal design of the EV charging station with retired battery systems against charging demand uncertainty," *IEEE Trans. Ind. Informat.*, vol. 19, no. 3, pp. 3262–3273, Mar. 2023, doi: 10.1109/TII.2022.3175718.

[35] F. Tao, Y. Kishita, C. Scheller, S. Blömeke, and Y. Umeda, "Designing a sustainable circulation system of second-life traction batteries: A scenario-based simulation approach," *Proc. CIRP*, vol. 105, pp. 733–738, Jan. 2022, doi: 10.1016/j.procir.2022.02.122.

[36] J. Sindha, J. Thakur, and M. Khalid, "The economic value of hybrid battery swapping stations with second life of batteries," *Cleaner Energy Syst.*, vol. 5, Aug. 2023, Art. no. 100066. [Online]. Available: https://www.sciencedirect.com/science/article/pii/S277278312300016X

[37] A. Demirci, "Optimal sizing and techno-economic evaluation of microgrids based on 100% renewable energy powered by second-life battery," *IEEE Access*, vol. 11, pp. 113291–113306, 2023, doi: 10.1109/ACCESS.2023.3324547.

[38] Z. Song, S. Feng, L. Zhang, Z. Hu, X. Hu, and R. Yao, "Economy analysis of second-life battery in wind power systems considering battery degradation in dynamic processes: Real case scenarios," *Appl. Energy*, vol. 251, Oct. 2019, Art. no. 113411, doi: 10.1016/j.apenergy.2019.113411.

[39] M. Philippot, D. Costa, M. S. Hosen, A. Senécat, E. Brouwers, E. Nanini-Maury, J. Van Mierlo, and M. Messagie, "Environmental impact of the second life of an automotive battery: Reuse and repurpose based on ageing tests," *J. Cleaner Prod.*, vol. 366, Sep. 2022, Art. no. 132872, doi: 10.1016/j.jclepro.2022.132872.

[40] A. Khowaja, M. D. Dean, and K. M. Kockelman, "Quantifying the emissions impact of repurposed electric vehicle battery packs in residential settings," *J. Energy Storage*, vol. 47, Mar. 2022, Art. no. 103628, doi: 10.1016/j.est.2021.103628.

[41] M. Terkes, O. Arikan, and E. Gokalp, "The effect of electric vehicle charging demand variability on optimal hybrid power systems with second-life lithium-ion or fresh Na–S batteries considering power quality," *Energy*, vol. 288, Jan. 2024, Art. no. 129760. [Online]. Available: https://www.sciencedirect.com/science/article/pii/S0360544223031547

[42] S. Lieskoski, J. Tuuf, and M. Björklund-Sänkiaho, "Techno-economic analysis of the business potential of second-life batteries in ostrobothnia, Finland," *Batteries*, vol. 10, no. 1, p. 36, Jan. 2024. [Online]. Available: https://www.mdpi.com/2313-0105/10/1/36

[43] H. Tang and S. Wang, "Life-cycle economic analysis of thermal energy storage, new and second-life batteries in buildings for providing multiple flexibility services in electricity markets," *Energy*, vol. 264, Feb. 2023, Art. no. 126270, doi: 10.1016/j.energy.2022.126270.

[44] A. Wangsupphaphol, S. Chaitusaney, and M. Salem, "A techno-economic assessment of a second-life battery and photovoltaics hybrid power source for sustainable electric vehicle home charging," *Sustainability*, vol. 15, no. 7, p. 5866, Mar. 2023, doi: 10.3390/su15075866.

[45] A. I. López, A. Ramírez-Díaz, I. Castilla-Rodríguez, J. Gurriarán, and J. A. Mendez-Perez, "Wind farm energy surplus storage solution with second-life vehicle batteries in isolated grids," *Energy Policy*, vol. 173, Feb. 2023, Art. no. 113373. [Online]. Available: https://www.sciencedirect.com/science/article/pii/S0301421522005924

[46] M. Terkes, Z. Öztürk, A. Demirci, and S. M. Tercan, "Optimal sizing and feasibility analysis of second-life battery energy storage systems for community microgrids considering carbon reduction," *J. Cleaner Prod.*, vol. 421, Oct. 2023, Art. no. 138507, doi: 10.1016/j.jclepro.2023.138507.

[47] T. Steckel, A. Kendall, and H. Ambrose, "Applying levelized cost of storage methodology to utility-scale second-life lithium-ion battery energy storage systems," *Appl. Energy*, vol. 300, Oct. 2021, Art. no. 117309, doi: 10.1016/j.apenergy.2021.117309.

[48] H. Lee, D. Lim, B. Lee, J. Gu, Y. Choi, and H. Lim, "What is the optimized cost for a used battery? Economic analysis in case of energy storage system as 2nd life of battery," *J. Cleaner Prod.*, vol. 374, Nov. 2022, Art. no. 133669. [Online]. Available: https://www.sciencedirect.com/science/article/pii/S0959652622032474

[49] F. Salek, S. Resalati, D. Morrey, P. Henshall, and A. Azizi, "Technical energy assessment and sizing of a second life battery energy storage system for a residential building equipped with EV charging station," *Appl. Sci.*, vol. 12, no. 21, p. 11103, Nov. 2022. [Online]. Available: https://www.mdpi.com/2076-3417/12/21/11103

[50] C. Zhang, Y. Yang, Y. Wang, J. Qiu, and J. Zhao, "Auction-based peer-to-peer energy trading considering echelon utilization of retired electric vehicle second-life batteries," *Appl. Energy*, vol. 358, Mar. 2024, Art. no. 122592, doi: 10.1016/j.apenergy.2023.122592.

[51] E. Hossain, D. Murtaugh, J. Mody, H. M. R. Faruque, M. S. H. Sunny, and N. Mohammad, "A comprehensive review on second-life batteries: Current state, manufacturing considerations, applications, impacts, barriers & potential solutions, business strategies, and policies," *IEEE Access*, vol. 7, pp. 73215–73252, 2019, doi: 10.1109/ACCESS.2019.2917859.

[52] Y. Zhao, O. Pohl, A. I. Bhatt, G. E. Collis, P. J. Mahon, T. Rüther, and A. F. Hollenkamp, "A review on battery market trends, second-life reuse, and recycling," *Sustain. Chem.*, vol. 2, no. 1, pp. 167–205, Mar. 2021, doi: 10.3390/suschem2010011.

[53] M. Shahjalal, P. K. Roy, T. Shams, A. Fly, J. I. Chowdhury, M. R. Ahmed, and K. Liu, "A review on second-life of Li-ion batteries: Prospects, challenges, and issues," *Energy*, vol. 241, Feb. 2022, Art. no. 122881, doi: 10.1016/j.energy.2021.122881.

[54] E. Martinez-Laserna, I. Gandiaga, E. Sarasketa-Zabala, J. Badeda, D.-I. Stroe, M. Swierczynski, and A. Goikoetxea, "Battery second life: Hype, hope or reality? A critical review of the state of the art," *Renew. Sustain. Energy Rev.*, vol. 93, pp. 701–718, Oct. 2018. [Online]. Available: https://www.sciencedirect.com/science/article/pii/S1364032118302491

[55] X. Gu, H. Bai, X. Cui, J. Zhu, W. Zhuang, Z. Li, X. Hu, and Z. Song, "Challenges and opportunities for second-life batteries: Key technologies and economy," *Renew. Sustain. Energy Rev.*, vol. 192, Mar. 2024, Art. no. 114191, doi: 10.1016/j.rser.2023.114191.

[56] A. Kampker, H. H. Heimes, C. Offermanns, J. Vienenkötter, M. Frank, and D. Holz, "Identification of challenges for second-life battery systems—A literature review," *World Electr. Vehicle J.*, vol. 14, no. 4, p. 80, Mar. 2023. [Online]. Available: https://www.mdpi.com/2032-6653/14/4/80

[57] H. Iqbal, S. Sarwar, D. Kirli, J. K. H. Shek, and A. E. Kiprakis, "A survey of second-life batteries based on techno-economic perspective and applications-based analysis," *Carbon Neutrality*, vol. 2, no. 1, p. 8, Apr. 2023. [Online]. Available: https://link.springer.com/10.1007/s43979-023-00049-5

[58] M. K. Al-Alawi, J. Cugley, and H. Hassanin, "Techno-economic feasibility of retired electric-vehicle batteries repurpose/reuse in second-life applications: A systematic review," *Energy Climate Change*, vol. 3, Dec. 2022, Art. no. 100086. [Online]. Available: https://www.sciencedirect.com/science/article/pii/S2666278722000162

[59] C. A. R. Júnior, E. R. Sanseverino, P. Gallo, D. Koch, Y. Kotak, H.-G. Schweiger, and H. Zanin, "Towards a business model for second-life batteries: Barriers, opportunities, uncertainties, and technologies," *J. Energy Chem.*, vol. 78, pp. 507–525, Mar. 2023. [Online]. Available: https://www.sciencedirect.com/science/article/pii/S2095495622006842

[60] J. Li, S. He, Q. Yang, Z. Wei, Y. Li, and H. He, "A comprehensive review of second life batteries towards sustainable mechanisms: Potential, challenges, and future prospects," *IEEE Trans. Transport. Electrific.*, vol. 9, no. 4, pp. 4824–4845, May 2023, doi: 10.1109/TTE.2022.3220411.

[61] F. Salek, S. Resalati, M. Babaie, P. Henshall, D. Morrey, and L. Yao, "A review of the technical challenges and solutions in maximising the potential use of second life batteries from electric vehicles," *Batteries*, vol. 10, no. 3, p. 79, Feb. 2024. [Online]. Available: https://www.mdpi.com/2313-0105/10/3/79

[62] A. Hassan, S. Khan, R. Li, W. Su, X. Zhou, M. Wang, and B. Wang, "Second-life batteries: A review on power grid applications, degradation mechanisms, and power electronics interface architectures," *Batteries*, vol. 9, no. 12, p. 571, Nov. 2023. [Online]. Available: https://www.mdpi.com/2313-0105/9/12/571

[63] P. Eleftheriadis, S. Leva, M. Gangi, A. V. Rey, A. Borgo, G. Coslop, E. Groppo, L. Grande, and M. Sedzik, "Second life batteries: Current regulatory framework, evaluation methods, and economic assessment: Reuse, refurbish, or recycle," *IEEE Ind. Appl. Mag.*, vol. 30, no. 1, pp. 46–58, Jan. 2024, doi: 10.1109/MIAS.2023.3325091.

[64] S. Ansari, A. Ayob, M. S. Hossain Lipu, A. Hussain, and M. H. M. Saad, "Remaining useful life prediction for lithium-ion battery storage system: A comprehensive review of methods, key factors, issues and future outlook," *Energy Rep.*, vol. 8, pp. 12153–12185, Nov. 2022, doi: 10.1016/j.egyr.2022.09.043.

[65] S. Wang, S. Jin, D. Bai, Y. Fan, H. Shi, and C. Fernandez, "A critical review of improved deep learning methods for the remaining useful life prediction of lithium-ion batteries," *Energy Rep.*, vol. 7, pp. 5562–5574, Nov. 2021, doi: 10.1016/j.egyr.2021.08.182.

[66] Int. Energy Agency. (2022). *Global Supply Chains of EV Batteries*. [Online]. Available: http://www.iea.org/t&c/

[67] J. W. Lee, M. H. S. M. Haram, G. Ramasamy, S. P. Thiagarajah, E. E. Ngu, and Y. H. Lee, "Technical feasibility and economics of repurposed electric vehicles batteries for power peak shaving," *J. Energy Storage*, vol. 40, Aug. 2021, Art. no. 102752, doi: 10.1016/j.est.2021.102752.

[68] D. Wolff, L. Canals Casals, G. Benveniste, C. Corchero, and L. Trilla, "The effects of lithium sulfur battery ageing on second-life possibilities and environmental life cycle assessment studies," *Energies*, vol. 12, no. 12, p. 2440, Jun. 2019, doi: 10.3390/en12122440.

[69] C. White and L. G. Swan, "Pack-level performance of electric vehicle batteries in second-life electricity grid energy services," *J. Energy Storage*, vol. 57, Jan. 2023, Art. no. 106265. [Online]. Available: https://www.sciencedirect.com/science/article/pii/S2352152X2202254X

[70] T. Placke, R. Kloepsch, S. Dühnen, and M. Winter, "Lithium ion, lithium metal, and alternative rechargeable battery technologies: The Odyssey for high energy density," *J. Solid State Electrochem.*, vol. 21, no. 7, pp. 1939–1964, Jul. 2017. [Online]. Available: http://link.springer.com/10.1007/s10008-017-3610-7

[71] D. Deng, "Li-ion batteries: Basics, progress, and challenges," *Energy Sci. Eng.*, vol. 3, no. 5, pp. 385–418, Sep. 2015. [Online]. Available: https://onlinelibrary.wiley.com/doi/10.1002/ese3.95

[72] T. Bashir, S. A. Ismail, Y. Song, R. M. Irfan, S. Yang, S. Zhou, J. Zhao, and L. Gao, "A review of the energy storage aspects of chemical elements for lithium-ion based batteries," *Energy Mater.*, vol. 1, no. 2, 2022, Art. no. 100019, doi: 10.20517/energymater.2021.20.

[73] C. Chen, K. Matsumoto, K. Kubota, R. Hagiwara, and Q. Xu, "An energy-dense solvent-free dual-ion battery," *Adv. Funct. Mater.*, vol. 30, no. 39, pp. 1–10, Sep. 2020, doi: 10.1002/adfm.202003557.

[74] Battery Univ. *The Secrets of Battery Runtime*. Accessed: Mar. 25, 2024. [Online]. Available: https://batteryuniversity.com/article/the-secrets-of-battery-runtime

[75] N. Schweikert, R. Heinzmann, A. Eichhöfer, H. Hahn, and S. Indris, "Electrochemical impedance spectroscopy of $Li_4Ti_5O_{12}$ and $LiCoO_2$ based half-cells and $Li_4Ti_5O_{12}/LiCoO_2$ cells: Internal interfaces and influence of state-of-charge and cycle number," *Solid State Ionics*, vol. 226, pp. 15–23, Oct. 2012. [Online]. Available: https://linkinghub.elsevier.com/retrieve/pii/S0167273812004596

[76] Y. Bai, L. Li, Y. Li, G. Chen, H. Zhao, Z. Wang, C. Wu, H. Ma, X. Wang, H. Cui, and J. Zhou, "Reversible and irreversible heat generation of NCA/Si–C pouch cell during electrochemical energy-storage process," *J. Energy Chem.*, vol. 29, pp. 95–102, Feb. 2019. [Online]. Available: https://linkinghub.elsevier.com/retrieve/pii/S2095495618300767

[77] J. Wang, S. Liu, C. Lin, F. Wang, C. Liu, Y. Su, S. Chen, and F. Wu, "Experimental study on the internal resistance and heat generation characteristics of lithium ion power battery with NCM/C material system," *SAE Int. J. Passenger Cars-Electron. Electr. Syst.*, vol. 11, no. 2, pp. 131–138, Apr. 2018, doi: 10.4271/07-11-02-0012.

[78] (2021). *Understanding Different Battery Chemistry*. [Online]. Available: https://skill-lync.com/student-projects/week-1-understanding-different-battery-chemistry-176

[79] Fortress Power. (2021). *How to Calculate the Energy Cost of Different Battery Chemistries?* [Online]. Available: https://www.fortresspower.com/how-to-calculate-the-energy-cost-of-different-battery-chemistries/

[80] Battery Univ. (2021). *BU-107: Comparison Table of Secondary Batteries*. [Online]. Available: https://batteryuniversity.com/article/bu-107-comparison-table-of-secondary-batteries

[81] T. Le Varlet, O. Schmidt, A. Gambhir, S. Few, and I. Staffell, "Comparative life cycle assessment of lithium-ion battery chemistries for residential storage," *J. Energy Storage*, vol. 28, Apr. 2020, Art. no. 101230. [Online]. Available: https://linkinghub.elsevier.com/retrieve/pii/S2352152X19309880

[82] Z. Wang, J. Yuan, X. Zhu, H. Wang, L. Huang, Y. Wang, and S. Xu, "Overcharge-to-thermal-runaway behavior and safety assessment of commercial lithium-ion cells with different cathode materials: A comparison study," *J. Energy Chem.*, vol. 55, pp. 484–498, Apr. 2021. [Online]. Available: https://linkinghub.elsevier.com/retrieve/pii/S2095495620305234

[83] R. A. Leising, M. J. Palazzo, E. S. Takeuchi, and K. J. Takeuchi, "A study of the overcharge reaction of lithium-ion batteries," *J. Power Sources*, vols. 97–98, pp. 681–683, Jul. 2001. [Online]. Available: https://linkinghub.elsevier.com/retrieve/pii/S0378775301005985

[84] J. Shepard. (2023). *Why Self-discharge is Important in Batteries*. [Online]. Available: https://www.batterypowertips.com/why-self-discharge-is-important-in-batteries/

[85] M. Swierczynski, D.-I. Stroe, A.-I. Stan, R. Teodorescu, and S. K. Kær, "Investigation on the self-discharge of the $LiFePO_4$/C nanophosphate battery chemistry at different conditions," in *Proc. IEEE Conf. Expo Transp. Electrific. Asia–Pacific (ITEC Asia–Pacific)*, Aug. 2014, pp. 1–6, doi: 10.1109/ITEC-AP.2014.6940762.

[86] J. Warner, "Second life and recycling of lithium-ion batteries," in *The Handbook of Lithium-Ion Battery Pack Design*, J. Warner, Ed., Amsterdam, The Netherlands: Elsevier, 2015, ch. 14, pp. 169–176. [Online]. Available: https://www.sciencedirect.com/science/article/pii/B9780128014561000142

[87] S. Mothilal Bhagavathy, H. Budnitz, T. Schwanen, and M. McCulloch. (Mar. 2021). *Impact of Charging Rates on Electric Vehicle Battery Life*. Findings. [Online]. Available: https://findingspress.org/article/21459-impact-of-charging-rates-on-electric-vehicle-battery-life

[88] Battery Univ. (2022). *BU-410: Charging at High and Low Temperatures*. [Online]. Available: https://batteryuniversity.com/article/bu-410-charging-at-high-and-low-temperatures

[89] E. Catenaro and S. Onori, "Experimental data of lithium-ion batteries under galvanostatic discharge tests at different rates and temperatures of operation," *Data Brief*, vol. 35, Apr. 2021, Art. no. 106894. [Online]. Available: https://linkinghub.elsevier.com/retrieve/pii/S2352340921001785

[90] H. Wang, J. Liu, D. Xia, Y. Fu, Y. Zhu, B. Hu, Z. Tao, H. Xiao, and S. Deng, "Effect of low temperatures on battery recharge and discharge voltage," *IOP Conf. Ser., Earth Environ. Sci.*, vol. 571, no. 1, Nov. 2020, Art. no. 012011. [Online]. Available: https://iopscience.iop.org/article/10.1088/1755-1315/571/1/012011

[91] A. M. Aris and B. Shabani, "An experimental study of a lithium ion cell operation at low temperature conditions," *Energy Proc.*, vol. 110, pp. 128–135, Mar. 2017. [Online]. Available: https://linkinghub.elsevier.com/retrieve/pii/S1876610217301479

[92] Battery Univ. (2021). *BU-502: Discharging at High and Low Temperatures*. [Online]. Available: https://batteryuniversity.com/article/bu-502-discharging-at-high-and-low-temperatures

[93] Modern Survival Blog. (2019). *Which Off-Grid Battery Chemistry Costs Less?* [Online]. Available: https://modernsurvivalblog.com/alternative-energy/solar-battery-comparison-chart/

[94] A. K. Barnes, J. C. Balda, S. O. Geurin, and A. Escobar-Mejía, "Optimal battery chemistry, capacity selection, charge/discharge schedule, and lifetime of energy storage under time-of-use pricing," in *Proc. 2nd IEEE PES Int. Conf. Exhib. Innov. Smart Grid Technol.*, Dec. 2011, pp. 1–7, doi: 10.1109/ISGTEUROPE.2011.6162702.

[95] Y. Qiao, S. Wang, F. Gao, X. Li, M. Fan, and R. Yang, "Toxicity analysis of second use lithium-ion battery separator and electrolyte," *Polym. Test.*, vol. 81, Jan. 2020, Art. no. 106175. [Online]. Available: https://linkinghub.elsevier.com/retrieve/pii/S0142941819313534

[96] W. Mrozik, M. A. Rajaeifar, O. Heidrich, and P. Christensen, "Environmental impacts, pollution sources and pathways of spent lithium-ion batteries," *Energy Environ. Sci.*, vol. 14, no. 12, pp. 6099–6121, 2021, doi: 10.1039/d1ee00691f.

[97] N. P. Lebedeva and L. Boon-Brett, "Considerations on the chemical toxicity of contemporary Li-ion battery electrolytes and their components," *J. Electrochemical Soc.*, vol. 163, no. 6, pp. A821–A830, Feb. 2016. [Online]. Available: https://iopscience.iop.org/article/10.1149/2.0171606jes

[98] M. Zackrisson and S. Schellenberger, "Toxicity of lithium ion battery chemicals-overview with focus on recycling," RISE Res. Institutes Sweden, Product Realisation Methodology, Gothenburg, Sweden, Project Rep. 28132/1, 2020. [Online]. Available: https://www.diva-portal.org/smash/record.jsf?pid=diva2%3A1787697dswid=1821

[99] L. Deguenon, D. Yamegueu, S. Moussa Kadri, and A. Gomna, "Overcoming the challenges of integrating variable renewable energy to the grid: A comprehensive review of electrochemical battery storage systems," *J. Power Sources*, vol. 580, Oct. 2023, Art. no. 233343. [Online]. Available: https://linkinghub.elsevier.com/retrieve/pii/S037877532300719X

[100] L. Li, B. Wang, K. Jiao, M. Ni, Q. Du, Y. Liu, B. Li, G. Ling, and C. Wang, "Comparative techno-economic analysis of large-scale renewable energy storage technologies," *Energy AI*, vol. 14, Oct. 2023, Art. no. 100282. [Online]. Available: https://linkinghub.elsevier.com/retrieve/pii/S266654682300054X

[101] S. U.-D. Khan, I. Wazeer, Z. Almutairi, and M. Alanazi, "Techno-economic analysis of solar photovoltaic powered electrical energy storage (EES) system," *Alexandria Eng. J.*, vol. 61, no. 9, pp. 6739–6753, Sep. 2022. [Online]. Available: https://www.sciencedirect.com/science/article/pii/S1110016821008334

[102] T. Thien, H. Axelsen, M. Merten, and D. U. Sauer, "Energy management of stationary hybrid battery energy storage systems using the example of a real-world 5 MW hybrid battery storage project in Germany," *J. Energy Storage*, vol. 51, Jul. 2022, Art. no. 104257. [Online]. Available: https://linkinghub.elsevier.com/retrieve/pii/S2352152X22002857

[103] J. Shepard. (2021). *The Difference Between Lithium Ion and Lithium Polymer Batteries*. [Online]. Available: https://www.batterypowertips.com/difference-between-lithium-ion-lithium-polymer-batteries-faq/

[104] S. Bhowmick. (2022). *A Detailed Comparison of Popular Li-Ion Battery Chemistries Used in Electric Vehicles*. [Online]. Available: https://circuitdigest.com/article/a-detailed-comparision-of-popular-li-ion-battery-chemistries-used-in-evs

[105] H. Hesse, R. Martins, P. Musilek, M. Naumann, C. Truong, and A. Jossen, "Economic optimization of component sizing for residential battery storage systems," *Energies*, vol. 10, no. 7, p. 835, Jun. 2017, doi: 10.3390/en10070835.

[106] C. Sun, F. Sun, and S. J. Moura, "Nonlinear predictive energy management of residential buildings with photovoltaics & batteries," *J. Power Sources*, vol. 325, pp. 723–731, Sep. 2016, doi: 10.1016/j.jpowsour.2016.06.076.

[107] S. J. Tong, A. Same, M. A. Kootstra, and J. W. Park, "Off-grid photovoltaic vehicle charge using second life lithium batteries: An experimental and numerical investigation," *Appl. Energy*, vol. 104, pp. 740–750, Apr. 2013, doi: 10.1016/j.apenergy.2012.11.046.

[108] S. Tong and M. Klein, "Second life battery pack as stationary energy storage for smart grid," SAE Tech. Paper 2014-01-0342, 2014, doi: 10.4271/2014-01-0342.

[109] X. Hu, X. Deng, F. Wang, Z. Deng, X. Lin, R. Teodorescu, and M. G. Pecht, "A review of second-life lithium-ion batteries for stationary energy storage applications," *Proc. IEEE*, vol. 110, no. 6, pp. 735–753, Jun. 2022, doi: 10.1109/JPROC.2022.3175614.

[110] C. R. Birkl, M. R. Roberts, E. McTurk, P. G. Bruce, and D. A. Howey, "Degradation diagnostics for lithium ion cells," *J. Power Sources*, vol. 341, pp. 373–386, Feb. 2017, doi: 10.1016/j.jpowsour.2016.12.011.

[111] X.-G. Yang, Y. Leng, G. Zhang, S. Ge, and C.-Y. Wang, "Modeling of lithium plating induced aging of lithium-ion batteries: Transition from linear to nonlinear aging," *J. Power Sources*, vol. 360, pp. 28–40, Aug. 2017, doi: 10.1016/j.jpowsour.2017.05.110.

[112] U. Krewer, F. Röder, E. Harinath, R. D. Braatz, B. Bedürftig, and R. Findeisen, "Review—Dynamic models of Li-ion batteries for diagnosis and operation: A review and perspective," *J. Electrochem. Soc.*, vol. 165, no. 16, pp. A3656–A3673, Nov. 2018, doi: 10.1149/2.1061814jes.

[113] T. Morstyn, B. Hredzak, R. P. Aguilera, and V. G. Agelidis, "Model predictive control for distributed microgrid battery energy storage systems," *IEEE Trans. Control Syst. Technol.*, vol. 26, no. 3, pp. 1107–1114, May 2018, doi: 10.1109/TCST.2017.2699159.

[114] J. Cao, D. Harrold, Z. Fan, T. Morstyn, D. Healey, and K. Li, "Deep reinforcement learning-based energy storage arbitrage with accurate lithium-ion battery degradation model," *IEEE Trans. Smart Grid*, vol. 11, no. 5, pp. 4513–4521, Sep. 2020, doi: 10.1109/TSG.2020.2986333.

[115] M. Chen and G. A. Rincon-Mora, "Accurate electrical battery model capable of predicting runtime and I–V performance," *IEEE Trans. Energy Convers.*, vol. 21, no. 2, pp. 504–511, Jun. 2006, doi: 10.1109/TEC.2006.874229.

[116] R. Xiong, J. Cao, Q. Yu, H. He, and F. Sun, "Critical review on the battery state of charge estimation methods for electric vehicles," *IEEE Access*, vol. 6, pp. 1832–1843, 2018, doi: 10.1109/ACCESS.2017.2780258.

[117] D. M. Rosewater, D. A. Copp, T. A. Nguyen, R. H. Byrne, and S. Santoso, "Battery energy storage models for optimal control," *IEEE Access*, vol. 7, pp. 178357–178391, 2019, doi: 10.1109/ACCESS.2019.2957698.

[118] B. Schweighofer, K. M. Raab, and G. Brasseur, "Modeling of high power automotive batteries by the use of an automated test system," *IEEE Trans. Instrum. Meas.*, vol. 52, no. 4, pp. 1087–1091, Aug. 2003, doi: 10.1109/TIM.2003.814827.

[119] S. Abu-Sharkh and D. Doerffel, "Rapid test and non-linear model characterisation of solid-state lithium-ion batteries," *J. Power Sources*, vol. 130, nos. 1–2, pp. 266–274, May 2004, doi: 10.1016/j.jpowsour.2003.12.001.

[120] A. Hentunen, T. Lehmuspelto, and J. Suomela, "Time-domain parameter extraction method for Thévenin-equivalent circuit battery models," *IEEE Trans. Energy Convers.*, vol. 29, no. 3, pp. 558–566, Sep. 2014, doi: 10.1109/TEC.2014.2318205.

[121] M. Abaspour, K. R. Pattipati, B. Shahrrava, and B. Balasingam, "Robust approach to battery equivalent-circuit-model parameter extraction using electrochemical impedance spectroscopy," *Energies*, vol. 15, no. 23, p. 9251, Dec. 2022. [Online]. Available: https://www.mdpi.com/1996-1073/15/23/9251

[122] S. M. R. Islam, S.-Y. Park, and B. Balasingam, "Circuit parameters extraction algorithm for a lithium-ion battery charging system incorporated with electrochemical impedance spectroscopy," in *Proc. IEEE Appl. Power Electron. Conf. Expo. (APEC)*, Mar. 2018, pp. 3353–3358, doi: 10.1109/APEC.2018.8341584.

[123] X. Zhang, J. Lu, S. Yuan, J. Yang, and X. Zhou, "A novel method for identification of lithium-ion battery equivalent circuit model parameters considering electrochemical properties," *J. Power Sources*, vol. 345, pp. 21–29, Mar. 2017, doi: 10.1016/j.jpowsour.2017.01.126.

[124] M. Hossain, S. Saha, M. E. Haque, M. T. Arif, and A. Oo, "A parameter extraction method for the Thevenin equivalent circuit model of Li-ion batteries," in *Proc. IEEE Ind. Appl. Soc. Annu. Meeting*, Sep. 2019, pp. 1–7, doi: 10.1109/IAS.2019.8912326.

[125] M. Hossain, S. Saha, M. T. Arif, A. M. T. Oo, N. Mendis, and M. E. Haque, "A parameter extraction method for the Li-ion batteries with wide-range temperature compensation," *IEEE Trans. Ind. Appl.*, vol. 56, no. 5, pp. 5625–5636, Sep. 2020, doi: 10.1109/TIA.2020.3011385.

[126] M.-K. Tran, M. Mathew, S. Janhunen, S. Panchal, K. Raahemifar, R. Fraser, and M. Fowler, "A comprehensive equivalent circuit model for lithium-ion batteries, incorporating the effects of state of health, state of charge, and temperature on model parameters," *J. Energy Storage*, vol. 43, Nov. 2021, Art. no. 103252, doi: 10.1016/j.est.2021.103252.

[127] W. Merrouche, B. Lekouaghet, E. Bouguenna, and Y. Himeur, "Parameter estimation of ECM model for Li-ion battery using the weighted mean of vectors algorithm," *J. Energy Storage*, vol. 76, Jan. 2024, Art. no. 109891, doi: 10.1016/j.est.2023.109891.

[128] N. Tian, Y. Wang, J. Chen, and H. Fang, "One-shot parameter identification of the Thevenin's model for batteries: Methods and validation," *J. Energy Storage*, vol. 29, Jun. 2020, Art. no. 101282, doi: 10.1016/j.est.2020.101282.

[129] "PNGV battery test manual," U.S. Dept. Energy Office Sci. Tech. Inf. (OSTI), USA, Tech. Rep., Jul. 1997, doi: 10.2172/578702. [Online]. Available: https://www.osti.gov/biblio/578702

[130] H. Miniguano, A. Barrado, A. Lázaro, P. Zumel, and C. Fernández, "General parameter identification procedure and comparative study of Li-ion battery models," *IEEE Trans. Veh. Technol.*, vol. 69, no. 1, pp. 235–245, Jan. 2020, doi: 10.1109/TVT.2019.2952970.

[131] Z. Li, X. Shi, M. Shi, C. Wei, F. Di, and H. Sun, "Investigation on the impact of the HPPC profile on the battery ECM parameters' offline identification," in *Proc. Asia Energy Electr. Eng. Symp. (AEEES)*, May 2020, pp. 753–757, doi: 10.1109/AEEES48850.2020.9121487.

[132] T. Biało , R. Niestrój, W. Skarka, and W. Korski, "HPPC test methodology using LFP battery cell identification tests as an example," *Energies*, vol. 16, no. 17, p. 6239, 2023. [Online]. Available: https://www.mdpi.com/1996-1073/16/17/6239

[133] H. Zhang, C. Deng, Y. Zong, Q. Zuo, H. Guo, S. Song, and L. Jiang, "Effect of sample interval on the parameter identification results of RC equivalent circuit models of Li-ion battery: An investigation based on HPPC test data," *Batteries*, vol. 9, no. 1, p. 1, Dec. 2022. [Online]. Available: https://www.mdpi.com/2313-0105/9/1/1

[134] I. M. Monirul, L. Qiu, and R. Ruby, "Accurate SOC estimation of ternary lithium-ion batteries by HPPC test-based extended Kalman filter," *J. Energy Storage*, vol. 92, Jul. 2024, Art. no. 112304, doi: 10.1016/j.est.2024.112304.

[135] Z. Chen, X. Shu, R. Xiao, W. Yan, Y. Liu, and J. Shen, "Optimal charging strategy design for lithium-ion batteries considering minimization of temperature rise and energy loss," *Int. J. Energy Res.*, vol. 43, no. 9, pp. 4344–4358, Jul. 2019, doi: 10.1002/er.4560.

[136] X. Zeng, Y. Zhang, B. Guo, L. Huang, and C. Li, "Optimal day-ahead dispatch of air-conditioning load under dynamic carbon emission factors," in *Proc. 5th Asia Energy Electr. Eng. Symp. (AEEES)*, Mar. 2023, pp. 1–6.

[137] J. Smekens, O. Hegazy, N. Omar, D. Widanage, A. Hubin, J. Van Mierlo, and P. Van den Bossche, "Influence of pulse variations on the parameters of first order empirical Li-ion battery model," in *Proc. World Electr. Vehicle Symp. Exhib. (EVS)*, Nov. 2013, pp. 1–6.

[138] J. Sun and J. Kainz, "Optimization of hybrid pulse power characterization profile for equivalent circuit model parameter identification of Li-ion battery based on Taguchi method," *J. Energy Storage*, vol. 70, Oct. 2023, Art. no. 108034, doi: 10.1016/j.est.2023.108034.

[139] *Oleochemistry Data*, Maruzen, Tokyo, Japan, 2012, p. 90.

[140] L. He, M. Hu, Y. Wei, B. Liu, and Q. Shi, "State of charge estimation by finite difference extended Kalman filter with HPPC parameters identification," *Sci. China Technol. Sci.*, vol. 63, no. 3, pp. 410–421, Mar. 2020, doi: 10.1007/s11431-019-1467-9.

[141] D. Cadar, D. Petreus, I. Ciocan, and P. Dobra, "An improvement on empirical modelling of the batteries," in *Proc. 32nd Int. Spring Seminar Electron. Technol.*, 2009, pp. 1–6, doi: 10.1109/ISSE.2009.5207015.

[142] A. R. Sparacino, G. F. Reed, R. J. Kerestes, B. M. Grainger, and Z. T. Smith, "Survey of battery energy storage systems and modeling techniques," in *Proc. IEEE Power Energy Soc. Gen. Meeting*, Jul. 2012, pp. 1–8, doi: 10.1109/PESGM.2012.6345071.

[143] M. T. Lawder, V. Viswanathan, and V. R. Subramanian, "Balancing autonomy and utilization of solar power and battery storage for demand based microgrids," *J. Power Sources*, vol. 279, pp. 645–655, Apr. 2015. [Online]. Available: https://linkinghub.elsevier.com/retrieve/pii/S0378775315000166

[144] M. Doyle, T. F. Fuller, and J. Newman, "Modeling of galvanostatic charge and discharge of the lithium/polymer/insertion cell," *J. Electrochem. Soc.*, vol. 140, no. 6, pp. 1526–1533, Jun. 1993. [Online]. Available: https://iopscience.iop.org/article/10.1149/1.2221597

[145] G. Ning and B. N. Popov, "Cycle life modeling of lithium-ion batteries," *J. Electrochem. Soc.*, vol. 151, no. 10, p. A1584, 2004. [Online]. Available: https://iopscience.iop.org/article/10.1149/1.1787631/meta

[146] C. Y. Wang, W. B. Gu, and B. Y. Liaw, "Micro-macroscopic coupled modeling of batteries and fuel cells: I. Model development," *J. Electrochem. Soc.*, vol. 145, no. 10, pp. 3407–3417, Oct. 1998. [Online]. Available: https://iopscience.iop.org/article/10.1149/1.1838820

[147] J. M. Reniers, G. Mulder, S. Ober-Blöbaum, and D. A. Howey, "Improving optimal control of grid-connected lithium-ion batteries through more accurate battery and degradation modelling," *J. Power Sources*, vol. 379, pp. 91–102, Mar. 2018. [Online]. Available: https://linkinghub.elsevier.com/retrieve/pii/S0378775318300041

[148] S. Marelli and M. Corno, "Model-based estimation of lithium concentrations and temperature in batteries using soft-constrained dual unscented Kalman filtering," *IEEE Trans. Control Syst. Technol.*, vol. 29, no. 2, pp. 926–933, Mar. 2021, doi: 10.1109/TCST.2020.2974176.

[149] E. Samadani, S. Panchal, M. Mastali, and R. Fraser, "Battery life cycle management for plug-in hybrid electric vehicle (PHEVs) and electric vehicles (EVs)," Transp. Canada Annu. Rep., Univ. Waterloo, Waterloo, ON, Canada, Tech. Rep. 2012, 2012, vol. 88.

[150] H. Najafi Khaboshan, F. Jaliliantabar, A. A. Abdullah, S. Panchal, and A. Azarinia, "Parametric investigation of battery thermal management system with phase change material, metal foam, and fins; utilizing CFD and ANN models," *Appl. Thermal Eng.*, vol. 247, Jun. 2024, Art. no. 123080. [Online]. Available: https://www.sciencedirect.com/science/article/pii/S1359431124007488

[151] V. Talele, U. Moralı, H. Najafi Khaboshan, M. S. Patil, S. Panchal, R. Fraser, and M. Fowler, "Improving battery safety by utilizing composite phase change material to delay the occurrence of thermal runaway event," *Int. Commun. Heat Mass Transf.*, vol. 155, Jun. 2024, Art. no. 107527. [Online]. Available: https://www.sciencedirect.com/science/article/pii/S0735193324002896

[152] A. H. Vakilzadeh, A. B. Sarvestani, K. Javaherdeh, R. Kamali, and S. Panchal, "Heat transfer and fluid flow in a PCM-filled enclosure: Effect of heated wall configuration," *J. Energy Storage*, vol. 87, May 2024, Art. no. 111448. [Online]. Available: https://www.sciencedirect.com/science/article/pii/S2352152X24010338

[153] A. R. Bais, D. Subhedar, and S. Panchal, "Experimental investigations of a novel phase change material and nano enhanced phase change material based passive battery thermal management system for Li-ion battery discharged at a high C rate," SSRN 4743339, doi: 10.2139/ssrn.4743339.

[154] J. Pu, X.-F. Ping, S. Panchal, N. Hua, R. Fraser, M. Fowler, and X. K. Zhang, "Structural optimization of a serpentine-channel cold plate for thermal management of lithium-ion battery based on the field synergy principle," SSRN 4795285, 2024, doi: 10.2139/ssrn.4795285.

[155] S. Zhang, M. S. Ding, K. Xu, J. Allen, and T. R. Jow, "Understanding solid electrolyte interface film formation on graphite electrodes," *Electrochem. Solid-State Lett.*, vol. 4, no. 12, p. A206, 2001. [Online]. Available: https://iopscience.iop.org/article/10.1149/1.1414946/meta

[156] E. Coron, S. Geniès, M. Cugnet, and P. X. Thivel, "Impact of lithium-ion cell condition on its second life viability," *J. Electrochem. Soc.*, vol. 167, no. 11, Jul. 2020, Art. no. 110556. [Online]. Available: https://iopscience.iop.org/article/10.1149/1945-7111/aba703/meta

[157] P. V. H. Seger, E. Coron, P.-X. Thivel, D. Riu, M. Cugnet, and S. Genies, "Open data model parameterization of a second-life Li-ion battery," *J. Energy Storage*, vol. 47, Mar. 2022, Art. no. 103546, doi: 10.1016/j.est.2021.103546.

[158] A. Barré, B. Deguilhem, S. Grolleau, M. Gérard, F. Suard, and D. Riu, "A review on lithium-ion battery ageing mechanisms and estimations for automotive applications," *J. Power Sources*, vol. 241, pp. 680–689, Nov. 2013, doi: 10.1016/j.jpowsour.2013.05.040.

[159] Z. Li, J. Huang, B. Yann Liaw, V. Metzler, and J. Zhang, "A review of lithium deposition in lithium-ion and lithium metal secondary batteries," *J. Power Sources*, vol. 254, pp. 168–182, May 2014, doi: 10.1016/j.jpowsour.2013.12.099.

[160] X. Han, L. Lu, Y. Zheng, X. Feng, Z. Li, J. Li, and M. Ouyang, "A review on the key issues of the lithium ion battery degradation among the whole life cycle," *eTransportation*, vol. 1, Aug. 2019, Art. no. 100005, doi: 10.1016/j.etran.2019.100005.

[161] X. Hu, L. Xu, X. Lin, and M. Pecht, "Battery lifetime prognostics," *Joule*, vol. 4, no. 2, pp. 310–346, Feb. 2020, doi: 10.1016/j.joule.2019.11.018.

[162] M. H. S. M. Haram, J. W. Lee, G. Ramasamy, E. E. Ngu, S. P. Thiagarajah, and Y. H. Lee, "Feasibility of utilising second life EV batteries: Applications, lifespan, economics, environmental impact, assessment, and challenges," *Alexandria Eng. J.*, vol. 60, no. 5, pp. 4517–4536, Oct. 2021. [Online]. Available: https://www.sciencedirect.com/science/article/pii/S1110016821001757

[163] "Second-life electric vehicle batteries 2020–2030 and 2023–2033," IDTechEx, Tech. Rep. [Online]. Available: https://www.idtechex.com/en/research-report/second-life-electric-vehicle-batteries-2020-2030/681

[164] Res. Markets, Global. (2023). *Global Electric Vehicle (EV) Battery Market 2023–2027*. [Online]. Available: https://www.researchandmarkets.com/reports/5017669/global-electric-vehicle-ev-battery-market-2023

[165] Int. Energy Agengy. (2023). *Global EV Outlook 2023*. [Online]. Available: https://www.iea.org/reports/global-ev-outlook-2023

[166] World Economic Forum; Global Battery Alliance. (Sep. 2019). *A Vision for a Sustainable Battery Value Chain in 2030*. [Online]. Available: https://www.weforum.org/publications/a-vision-for-a-sustainable-battery-value-chain-in-2030/

[167] Int. Renew. Energy Agency. (2019). *International Renewable Energy Agency. Utility-Scale Batteries Innovation Landscape Brief*. [Online]. Available: https://www.irena.org/-/media/Files/IRENA/Agency/Publication/2019/Sep/IRENAUtility-scale-batteries2019.pdf

[168] International Renewable Energy Agency (IRENA). (2017). *Electricity Storage Renewables: Costs Markets to 2030*. [Online]. Available: https://www.irena.org/-/media/Files/IRENA/Agency/Publication/2017/Oct/IRENAElectricityStorageCosts2017.pdf

[169] BloombergNEF. (2023). *Electric Vehicle Outlook 2023*. [Online]. Available: https://about.bnef.com/electric-vehicle-outlook/
[170] BloombergNEF. (Nov. 2023). *Zero-Emission Vehicles Factbook a BloombergNEF Special Report Prepared for COP27*. [Online]. Available: https://assets.bbhub.io/dotorg/sites/64/2022/11/2022-COP27-ZEV-TransitionFactbook.pdf
[171] H. Engel, P. Hertzke, and G. Siccardo. (Apr. 2019). *Second-Life EV Batteries: The Newest Value Pool in Energy Storage*. McKinsey Company. [Online]. Available: https://www.mckinsey.com/industries/automotive-and-assembly/our-insights/second-life-ev-batteries-the-newest-value-pool-in-energy-storage
[172] European Union. (2008). *Directive 2008/98/EC of the European Parliament, and of the Council of 19 Novmber 2008 on Waste and Repealing Certain Directives*. [Online]. Available: https://eur-lex.europa.eu/legal-content/EN/TXT/?uri=celex%3A32008L0098
[173] J. Eur. Union. (2012). *Directive 2012/19/EU of the European Parliament and of the Council of 4*. [Online]. Available: https://eur-lex.europa.eu/legal-content/EN/TXT/?uri=celex%3A32012L0019
[174] H. C. Spelman. (2014). *Triple Win: The Economic, Social and Environmental Case for Remanufacturing*. [Online]. Available: https://www.policyconnect.org.uk/research/report-triple-win-social-economic-and-environmental-case-remanufacturing
[175] I. Hartwell and J. Marco, "Management of intellectual property uncertainty in a remanufacturing strategy for automotive energy storage systems," *J. Remanufacturing*, vol. 6, no. 1, p. 3, Dec. 2016. [Online]. Available: http://link.springer.com/10.1186/s13243-016-0025-z
[176] G. Hunt, "USABC electric vehicle battery test procedures manual, revision 2," US Dept. Energy Idaho Field Office, Idaho Nat. Eng. Lab. (INEL), Idaho Falls, ID, USA, Tech. Rep. DOE/ID-10479, Rev, 1996, p. 39, vol. 2.
[177] Kelleher Environ. (2019). *Research Study on Reuse and Recycling of Batteries Employed in Electric Vehicles: The Technical, Environmental, Economic, Energy and Cost Implications of Reusing and Recycling EV Batteries*. [Online]. Available: https://www.api.org/-/media/files/oil-and-natural-gas/fuels/ev%20battery%20reuse%20recyc%20api%20summary%20report%2024nov2020.pdf
[178] L. Ahmadi, S. B. Young, M. Fowler, R. A. Fraser, and M. A. Achachlouei, "A cascaded life cycle: Reuse of electric vehicle lithium-ion battery packs in energy storage systems," *Int. J. Life Cycle Assessment*, vol. 22, no. 1, pp. 111–124, Jan. 2017, doi: 10.1007/s11367-015-0959-7.
[179] K. Venkatapathy, E. Tazelaar, and B. Veenhuizen, "A systematic identification of first to second life shift-point of lithium-ion batteries," in *Proc. IEEE Vehicle Power Propuls. Conf. (VPPC)*, Oct. 2015, pp. 1–4, doi: 10.1109/VPPC.2015.7352885.
[180] B. Gohla-Neudecker, M. Bowler, and S. Mohr, "Battery 2nd life: Leveraging the sustainability potential of EVs and renewable energy grid integration," in *Proc. Int. Conf. Clean Electr. Power (ICCEP)*, Jun. 2015, pp. 311–318, doi: 10.1109/ICCEP.2015.7177641.
[181] Y. Tang, Q. Zhang, H. Li, Y. Li, and B. Liu, "Economic analysis on repurposed EV batteries in a distributed PV system under sharing business models," *Energy Proc.*, vol. 158, pp. 4304–4310, Feb. 2019, doi: 10.1016/j.egypro.2019.01.793.
[182] M. A. Cusenza, F. Guarino, S. Longo, M. Mistretta, and M. Cellura, "Reuse of electric vehicle batteries in buildings: An integrated load match analysis and life cycle assessment approach," *Energy Buildings*, vol. 186, pp. 339–354, Mar. 2019, doi: 10.1016/j.enbuild.2019.01.032.
[183] I. Mathews, B. Xu, W. He, V. Barreto, T. Buonassisi, and I. M. Peters, "Technoeconomic model of second-life batteries for utility-scale solar considering calendar and cycle aging," *Appl. Energy*, vol. 269, Jul. 2020, Art. no. 115127, doi: 10.1016/j.apenergy.2020.115127.
[184] E. Winarno, W. Hadikurniawati, and R. N. Rosso, "Location based service for presence system using haversine method," in *Proc. Int. Conf. Innov. Creative Inf. Technol. (ICITech)*, Nov. 2017, pp. 1–4, doi: 10.1109/INNOCIT.2017.8319153.
[185] L. C. Casals, B. Amante García, and C. Canal, "Second life batteries lifespan: Rest of useful life and environmental analysis," *J. Environ. Manage.*, vol. 232, pp. 354–363, Feb. 2019, doi: 10.1016/j.jenvman.2018.11.046.
[186] T. Montes, M. Etxandi-Santolaya, J. Eichman, V. J. Ferreira, L. Trilla, and C. Corchero, "Procedure for assessing the suitability of battery second life applications after EV first life," *Batteries*, vol. 8, no. 9, p. 122, Sep. 2022, doi: 10.3390/batteries8090122.
[187] M. Etxandi-Santolaya, L. Canals Casals, and C. Corchero, "Extending the electric vehicle battery first life: Performance beyond the current end of life threshold," *Heliyon*, vol. 10, no. 4, Feb. 2024, Art. no. e26066. [Online]. Available: https://linkinghub.elsevier.com/retrieve/pii/S2405844024020978
[188] G. Richter, "Method and device for determining the state of function of an energy storage battery," U.S. Patent 6 885 951, Apr. 26, 2005.
[189] S. M. Rezvanizaniani, Z. Liu, Y. Chen, and J. Lee, "Review and recent advances in battery health monitoring and prognostics technologies for electric vehicle (EV) safety and mobility," *J. Power Sources*, vol. 256, pp. 110–124, Jun. 2014. [Online]. Available: https://linkinghub.elsevier.com/retrieve/pii/S0378775314001098
[190] M. Dubarry, N. Vuillaume, and B. Y. Liaw, "Origins and accommodation of cell variations in Li-ion battery pack modeling," *Int. J. Energy Res.*, vol. 34, no. 2, pp. 216–231, Feb. 2010. [Online]. Available: https://onlinelibrary.wiley.com/doi/10.1002/er.1668
[191] J.-H. Park, "Photochemical degradation and toxicity reduction of methyl 1-[(butylamino)carbonyl]-1H-benzimidazol-2-ylcarbamate in agricultural wastewater: Comparative study of photocatalysis and sonophotocatalysis," *Desalination*, vol. 249, no. 2, pp. 480–485, Dec. 2009. [Online]. Available: https://linkinghub.elsevier.com/retrieve/pii/S0011916409007516
[192] T. Yamazaki, K. Sakurai, and K. Muramoto, "Estimation of the residual capacity of sealed lead-acid batteries by neural network," in *Proc. 20th Int. Telecommun. Energy Conf.*, 1998, pp. 210–214, doi: 10.1109/intlec.1998.793500.
[193] P. Ramadass, B. Haran, R. White, and B. N. Popov, "Capacity fade of Sony 18650 cells cycled at elevated temperatures," *J. Power Sources*, vol. 112, no. 2, pp. 606–613, Nov. 2002. [Online]. Available: https://www.sciencedirect.com/science/article/pii/S0378775302004743
[194] K. Qian, C. Zhou, Y. Yuan, and M. Allan, "Temperature effect on electric vehicle battery cycle life in vehicle-to-grid applications," in *CICED Proc.*, Sep. 2010, pp. 1–6.
[195] M. Etxandi-Santolaya, L. Canals Casals, T. Montes, and C. Corchero, "Are electric vehicle batteries being underused? A review of current practices and sources of circularity," *J. Environ. Manage.*, vol. 338, Jul. 2023, Art. no. 117814. [Online]. Available: https://linkinghub.elsevier.com/retrieve/pii/S0301479723006023
[196] G. Dong, J. Wei, and Z. Chen, "Kalman filter for onboard state of charge estimation and peak power capability analysis of lithium-ion batteries," *J. Power Sources*, vol. 328, pp. 615–626, Oct. 2016. [Online]. Available: https://linkinghub.elsevier.com/retrieve/pii/S0378775316310746
[197] P. Shen, M. Ouyang, L. Lu, J. Li, and X. Feng, "The co-estimation of state of charge, state of health, and state of function for lithium-ion batteries in electric vehicles," *IEEE Trans. Veh. Technol.*, vol. 67, no. 1, pp. 92–103, Jan. 2018, doi: 10.1109/TVT.2017.2751613.
[198] E. Meissner and G. Richter, "Battery monitoring and electrical energy management: Precondition for future vehicle electric power systems," *J. Power Sources*, vol. 116, no. 1, pp. 79–98, 2003. [Online]. Available: https://www.sciencedirect.com/science/article/pii/S0378775302007139
[199] G. L. Plet, *Battery Management Systems, Volume II: Equivalent-Circuit Methods*, 1st ed., Norwood, MA, USA: Artech House, 2015.
[200] M. Etxandi-Santolaya, L. C. Casals, and C. Corchero, "Limitations of the state of health and health indicators for electric vehicle batteries," in *Proc. IEEE Vehicle Power Propuls. Conf. (VPPC)*, Oct. 2023, pp. 1–6, doi: 10.1109/vppc60535.2023.10403249.
[201] M. Etxandi-Santolaya, L. Canals Casals, B. Amante García, and C. Corchero, "Circular economy-based alternatives beyond second-life applications: Maximizing the electric vehicle battery first life," *World Electr. Vehicle J.*, vol. 14, no. 3, p. 66, Mar. 2023, doi: 10.3390/wevj14030066.
[202] J. Zhu, I. Mathews, D. Ren, W. Li, D. Cogswell, B. Xing, T. Sedlatschek, S. N. R. Kantareddy, M. Yi, T. Gao, Y. Xia, Q. Zhou, T. Wierzbicki, and M. Z. Bazant, "End-of-life or second-life options for retired electric vehicle batteries," *Cell Rep. Phys. Sci.*, vol. 2, no. 8, Aug. 2021, Art. no. 100537, doi: 10.1016/j.xcrp.2021.100537.
[203] C. A. Rufino Júnior, E. R. Sanseverino, P. Gallo, D. Koch, Y. Kotak, H.-G. Schweiger, and H. Zanin. (Jun. 2023). *Reviewing Regulations and Standards for Second-Life Batteries*. [Online]. Available: https://www.preprints.org/manuscript/202306.0711/v1
[204] M. H. S. M. Haram, M. T. Sarker, G. Ramasamy, and E. E. Ngu, "Second life EV batteries: Technical evaluation, design framework, and case analysis," *IEEE Access*, vol. 11, pp. 138799–138812, 2023, doi: 10.1109/ACCESS.2023.3340044.

[205] H.-G. Schweiger, O. Obeidi, O. Komesker, A. Raschke, M. Schiemann, C. Zehner, M. Gehnen, M. Keller, and P. Birke, "Comparison of several methods for determining the internal resistance of lithium ion cells," *Sensors*, vol. 10, no. 6, pp. 5604–5625, Jun. 2010. [Online]. Available: http://www.mdpi.com/1424-8220/10/6/5604

[206] W. Waag, C. Fleischer, C. Schaeper, B. Gmbh, and D. U. Sauer, "Self-adapting on-board diagnostic algorithms for lithium-ion batteries," in *Advanced Battery Development for Automotive and Utility Applications and Their Electric Power Grid Integration*. Aachen, Germany: Haus der Technik e.V., Mar. 2011. [Online]. Available: https://www.researchgate.net/profile/Dirk-Uwe-Sauer/publication/297712781

[207] M. M. Hoque, M. A. Hannan, A. Mohamed, and A. Ayob, "Battery charge equalization controller in electric vehicle applications: A review," *Renew. Sustain. Energy Rev.*, vol. 75, pp. 1363–1385, Aug. 2017. [Online]. Available: https://linkinghub.elsevier.com/retrieve/pii/S1364032116308681

[208] S. Bhattarai and N. S. Mubenga, "Review of equalization techniques applied to second-life EV battery packs and their efficiency," in *Proc. IEEE Nat. Aerosp. Electron. Conf.*, Aug. 2023, pp. 10–15, doi: 10.1109/naecon58068.2023.10365787.

[209] R. Di Rienzo, A. Verani, N. Nicodemo, F. Baronti, R. Roncella, and R. Saletti, "Comparison of active energy-balance architectures for second-life battery dynamic equalization," in *Proc. IEEE 2nd Ind. Electron. Soc. Annu. On-Line Conf. (ONCON)*, Dec. 2023, pp. 1–6, doi: 10.1109/oncon60463.2023.10431394.

[210] R. Di Rienzo, N. Nicodemo, A. Verani, F. Baronti, R. Roncella, and R. Saletti, "A novel methodology to study and compare active energy-balance architectures with dynamic equalization for second-life battery applications," *J. Energy Storage*, vol. 73, Dec. 2023, Art. no. 108772. [Online]. Available: https://www.sciencedirect.com/science/article/pii/S2352152X23021692

[211] M. Rasheed, R. Hassan, M. Kamel, H. Wang, R. Zane, S. Tong, and K. Smith, "Active reconditioning of retired lithium-ion battery packs from electric vehicles for second-life applications," *IEEE J. Emerg. Sel. Topics Power Electron.*, vol. 12, no. 1, pp. 388–404, Feb. 2024, doi: 10.1109/JESTPE.2023.3325251.

[212] D. Galatro, D. A. Romero, C. Da Silva, O. Trescases, and C. H. Amon, "Impact of cell spreading on second-life of lithium-ion batteries," *Can. J. Chem. Eng.*, vol. 101, no. 3, pp. 1114–1122, 2023.

[213] N. S. Mubenga, K. Sharma, and T. Stuart, "A bilevel equalizer to boost the capacity of second life Li ion batteries," *Batteries*, vol. 5, no. 3, p. 55, Aug. 2019, doi: 10.3390/batteries5030055.

[214] X. Cui, A. Ramyar, J. B. Siegel, P. Mohtat, A. G. Stefanopoulou, and A.-T. Avestruz, "Comparing power processing system approaches in second-use battery energy buffering for electric vehicle charging," *J. Energy Storage*, vol. 49, May 2022, Art. no. 104017, doi: 10.1016/j.est.2022.104017.

[215] D. Kehl, T. Jennert, F. Lienesch, and M. Kurrat, "Electrical characterization of Li-ion battery modules for second-life applications," *Batteries*, vol. 7, no. 2, p. 32, May 2021, doi: 10.3390/batteries7020032.

[216] M. M. Camboim, A. C. Moreira, M. D. F. N. C. Rosolem, R. F. Beck, V. T. Arioli, C. Omae, and H. Ding, "State of health estimation of second-life batteries through electrochemical impedance spectroscopy and dimensionality reduction," *J. Energy Storage*, vol. 78, Feb. 2024, Art. no. 110063. [Online]. Available: https://www.sciencedirect.com/science/article/pii/S2352152X2303462X

[217] E. Braco, I. San Martín, P. Sanchis, and A. Ursúa, "Fast capacity and internal resistance estimation method for second-life batteries from electric vehicles," *Appl. Energy*, vol. 329, May 2023, Art. no. 120235. [Online]. Available: https://www.sciencedirect.com/science/article/pii/S0306261922014921

[218] H. Quinard, E. Redondo-Iglesias, S. Pelissier, and P. Venet, "Fast electrical characterizations of high-energy second life lithium-ion batteries for embedded and stationary applications," *Batteries*, vol. 5, no. 1, p. 33, Mar. 2019, doi: 10.3390/batteries5010033.

[219] F. Salek, A. Azizi, S. Resalati, P. Henshall, and D. Morrey, "Mathematical modelling and simulation of second life battery pack with heterogeneous state of health," *Mathematics*, vol. 10, no. 20, p. 3843, Oct. 2022, doi: 10.3390/math10203843.

[220] R. Vaidya, V. Selvan, P. Badami, K. Knoop, and A. M. Kannan, "Plug-in hybrid vehicle and second-life applications of lithium-ion batteries at elevated temperature," *Batteries Supercaps*, vol. 1, no. 2, pp. 75–82, Aug. 2018, doi: 10.1002/batt.201700002.

[221] E. Martinez-Laserna, E. Sarasketa-Zabala, I. V. Sarria, D.-I. Stroe, M. Swierczynski, A. Warnecke, J.-M. Timmermans, S. Goutam, N. Omar, and P. Rodriguez, "Technical viability of battery second life: A study from the ageing perspective," *IEEE Trans. Ind. Appl.*, vol. 54, no. 3, pp. 2703–2713, May 2018, doi: 10.1109/TIA.2018.2801262.

[222] F. Mandrile, M. Pastorelli, S. Musumeci, I. A. Urkiri, and A. Remirez, "Second life management from battery storage system of electric waterborne transport applications: Perspectives and solutions," *IEEE Access*, vol. 11, pp. 35122–35139, 2023, doi: 10.1109/ACCESS.2023.3265168.

[223] N. Kumar, S. M. Ramakrishnan, K. Panchapakesan, D. Subramaniam, I. Masters, M. Dowson, and A. Das, "In-depth evaluation of micro-resistance spot welding for connecting tab to 18,650 Li-ion cells for electric vehicle battery application," *Int. J. Adv. Manuf. Technol.*, vol. 121, nos. 9–10, pp. 6581–6597, Aug. 2022, doi: 10.1007/s00170-022-09775-z.

[224] M. F. R. Zwicker, M. Moghadam, W. Zhang, and C. V. Nielsen, "Automotive battery pack manufacturing—A review of battery to tab joining," *J. Adv. Joining Processes*, vol. 1, Mar. 2020, Art. no. 100017. [Online]. Available: https://linkinghub.elsevier.com/retrieve/pii/S2666330920300157

[225] M. B. Sai, S. C. Mondal, and V. Kumar, "Optimization of battery tab interconnects by micro-TIG welding using simulated annealing algorithm and response surface method," in *Design in the Era of Industry 4.0*, vol. 3, A. Chakrabarti and V. Singh, Eds., Singapore: Springer, 2023, pp. 283–293.

[226] A. Das, I. Masters, and P. Haney, "Modelling the impact of laser micro-joint shape and size on resistance and temperature for electric vehicle battery joining application," *J. Energy Storage*, vol. 52, Aug. 2022, Art. no. 104868. [Online]. Available: https://linkinghub.elsevier.com/retrieve/pii/S2352152X22008751

[227] R. Palanivel, "A contemporary review of the advancements in joining technologies for battery applications," *Mater. Technol.*, vol. 57, no. 3, pp. 275–281, May 2023, doi: 10.17222/mit.2023.797. [Online]. Available: https://mater-tehnol.si/index.php/MatTech/article/view/797

[228] K. Bieliszczuk, J. Zr da, and T. Chmielewski, "Selected properties of aluminum ultrasonic wire bonded joints with nickel-plated steel substrate for 18650 cylindrical cells," *J. Adv. Joining Processes*, vol. 9, Jun. 2024, Art. no. 100197. [Online]. Available: https://linkinghub.elsevier.com/retrieve/pii/S2666330924000141

[229] H. Rallo, G. Benveniste, I. Gestoso, and B. Amante, "Economic analysis of the disassembling activities to the reuse of electric vehicles Li-ion batteries," *Resour., Conservation Recycling*, vol. 159, Aug. 2020, Art. no. 104785. [Online]. Available: https://linkinghub.elsevier.com/retrieve/pii/S0921344920301063

[230] R. V. Nanditta and N. R. B, "Review on comparative study of various automotive cell joining techniques and challenges," in *Proc. Int. Conf. Electron. Renew. Syst. (ICEARS)*, Mar. 2022, pp. 136–141, doi: 10.1109/ICEARS53579.2022.9752335.

[231] S. Sathyan and D. Mukherjee, "Assessment of joining technologies for automotive battery system manufacturing," *Indian Weld. J.*, vol. 55, no. 4, Oct. 2022. [Online]. Available: https://research.ebsco.com/c/d7qe3y/search/details/3ahofqbdkf?db=obo

[232] Y. Zhou, C. Li, T. Shen, D. Chen, X. Wang, and Y. Ma, "Interfacial microstructure of multi-layered Al–Cu joint by electromagnetic pulse welding," *J. Mater. Res. Technol.*, vol. 25, pp. 2446–2454, Jul. 2023. [Online]. Available: https://linkinghub.elsevier.com/retrieve/pii/

[233] A. Das, D. Li, D. Williams, and D. Greenwood, "Joining technologies for automotive battery systems manufacturing," *World Electr. Vehicle J.*, vol. 9, no. 2, p. 22, Jul. 2018. [Online]. Available: http://www.mdpi.com/2032-6653/9/2/22

[234] H. Ambrose, A. Kendall, M. Slattery, and T. Steckel. (2016). *Battery Second-Life: Unpacking Opportunities and Barries for the Reuse of Electric Vehicle Batteries*. [Online]. Available: https://pdfslide.net/documents/battery-second-life-unpacking-opportunities-and-2020-05-27-battery-second-life.html?page=2

[235] P. Salza and P. R. Thomas. (Feb. 2021). *2nd Life Batteries*. [Online]. Available: https://www.globalelectricity.org/wp-content/uploads/2022/09/GSEPSecondLifeBatteries.pdf

[236] W. Waag and D. U. Sauer, "Adaptive estimation of the electromotive force of the lithium-ion battery after current interruption for an accurate state-of-charge and capacity determination," *Appl. Energy*, vol. 111, pp. 416–427, Nov. 2013, doi: 10.1016/j.apenergy.2013.05.001.

[237] M.-F. Ge, Y. Liu, X. Jiang, and J. Liu, "A review on state of health estimations and remaining useful life prognostics of lithium-ion batteries," *Measurement*, vol. 174, Apr. 2021, Art. no. 109057, doi: 10.1016/j.measurement.2021.109057.

[238] G. Guo, B. Long, B. Cheng, S. Zhou, P. Xu, and B. Cao, "Three-dimensional thermal finite element modeling of lithium-ion battery in thermal abuse application," *J. Power Sources*, vol. 195, no. 8, pp. 2393–2398, Apr. 2010. [Online]. Available: https://linkinghub.elsevier.com/retrieve/pii/S0378775309019417

[239] G.-H. Kim, A. Pesaran, and R. Spotnitz, "A three-dimensional thermal abuse model for lithium-ion cells," *J. Power Sources*, vol. 170, no. 2, pp. 476–489, Jul. 2007. [Online]. Available: https://linkinghub.elsevier.com/retrieve/pii/S0378775307007082

[240] R. Tschirschwitz, C. Bernardy, P. Wagner, T. Rappsilber, C. Liebner, S.-K. Hahn, and U. Krause, "Harmful effects of lithium-ion battery thermal runaway: Scale-up tests from cell to second-life modules," *RSC Adv.*, vol. 13, no. 30, pp. 20761–20779, Jul. 2023, doi: 10.1039/d3ra02881j.

[241] J. N. C. Sekhar, B. Domathoti, and E. D. R. Santibanez Gonzalez, "Prediction of battery remaining useful life using machine learning algorithms," *Sustainability*, vol. 15, no. 21, p. 15283, Oct. 2023. [Online]. Available: https://www.mdpi.com/2071-1050/15/21/15283

[242] L. Chen, Y. Ding, B. Liu, S. Wu, Y. Wang, and H. Pan, "Remaining useful life prediction of lithium-ion battery using a novel particle filter framework with grey neural network," *Energy*, vol. 244, Apr. 2022, Art. no. 122581. [Online]. Available: https://linkinghub.elsevier.com/retrieve/pii/S0360544221028309

[243] B. Zraibi, M. Mansouri, and S. E. Loukili, "Comparing deep learning methods to predict the remaining useful life of lithium-ion batteries," *Mater. Today: Proc.*, vol. 62, pp. 6298–6304, 2022. [Online]. Available: https://linkinghub.elsevier.com/retrieve/pii/S2214785322022143

[244] D. Chen, J. Meng, H. Huang, J. Wu, P. Liu, J. Lu, and T. Liu, "An empirical-data hybrid driven approach for remaining useful life prediction of lithium-ion batteries considering capacity diving," *Energy*, vol. 245, Apr. 2022, Art. no. 123222. [Online]. Available: https://linkinghub.elsevier.com/retrieve/pii/S0360544222001256

[245] E. Walker, S. Rayman, and R. E. White, "Comparison of a particle filter and other state estimation methods for prognostics of lithium-ion batteries," *J. Power Sources*, vol. 287, pp. 1–12, Aug. 2015. [Online]. Available: https://linkinghub.elsevier.com/retrieve/pii/S037877531500659X

[246] X. Lai, Y. Zheng, and T. Sun, "A comparative study of different equivalent circuit models for estimating state-of-charge of lithium-ion batteries," *Electrochimica Acta*, vol. 259, pp. 566–577, Jan. 2018. [Online]. Available: https://linkinghub.elsevier.com/retrieve/pii/S0013468617322880

[247] M. Elmahallawy, T. Elfouly, A. Alouani, and A. M. Massoud, "A comprehensive review of lithium-ion batteries modeling, and state of health and remaining useful lifetime prediction," *IEEE Access*, vol. 10, pp. 119040–119070, 2022, doi: 10.1109/ACCESS.2022.3221137.

[248] X. Li, Y. Ma, and J. Zhu, "An online dual filters RUL prediction method of lithium-ion battery based on unscented particle filter and least squares support vector machine," *Measurement*, vol. 184, Nov. 2021, Art. no. 109935. [Online]. Available: https://linkinghub.elsevier.com/retrieve/pii/S0263224121008708

[249] Z. Xue, Y. Zhang, C. Cheng, and G. Ma, "Remaining useful life prediction of lithium-ion batteries with adaptive unscented Kalman filter and optimized support vector regression," *Neurocomputing*, vol. 376, pp. 95–102, Feb. 2020. [Online]. Available: https://linkinghub.elsevier.com/retrieve/pii/S0925231219313426

[250] J. He, Y. Tian, and L. Wu, "A hybrid data-driven method for rapid prediction of lithium-ion battery capacity," *Rel. Eng. Syst. Saf.*, vol. 226, Oct. 2022, Art. no. 108674. [Online]. Available: https://linkinghub.elsevier.com/retrieve/pii/S0951832022003088

[251] J. Du, W. Zhang, C. Zhang, and X. Zhou, "Battery remaining useful life prediction under coupling stress based on support vector regression," *Energy Proc.*, vol. 152, pp. 538–543, Oct. 2018, doi: 10.1016/j.egypro.2018.09.207.

[252] M. Cheng, X. Zhang, A. Ran, G. Wei, and H. Sun, "Optimal dispatch approach for second-life batteries considering degradation with online SoH estimation," *Renew. Sustain. Energy Rev.*, vol. 173, Mar. 2023, Art. no. 113053. [Online]. Available: https://www.sciencedirect.com/science/article/pii/S1364032122009340

[253] P. V. H. Seger, P.-X. Thivel, and D. Riu, "A second life Li-ion battery ageing model with uncertainties: From cell to pack analysis," *J. Power Sources*, vol. 541, Sep. 2022, Art. no. 231663. [Online]. Available: https://linkinghub.elsevier.com/retrieve/pii/S0378775322006619

[254] P. S. Attidekou, Z. Milojevic, M. Muhammad, M. Ahmeid, S. Lambert, and P. K. Das, "Methodologies for large-size pouch lithium-ion batteries end-of-life gateway detection in the second-life application," *J. Electrochem. Soc.*, vol. 167, no. 16, Dec. 2020, Art. no. 160534.

[255] E. Braco, I. San Martín, P. Sanchis, A. Ursúa, and D.-I. Stroe, "State of health estimation of second-life lithium-ion batteries under real profile operation," *Appl. Energy*, vol. 326, Nov. 2022, Art. no. 119992, doi: 10.1016/j.apenergy.2022.119992.

[256] C. Liu, X. Wen, J. Zhong, W. Liu, J. Chen, J. Zhang, Z. Wang, and Q. Liao, "Characterization of aging mechanisms and state of health for second-life 21700 ternary lithium-ion battery," *J. Energy Storage*, vol. 55, Nov. 2022, Art. no. 105511, doi: 10.1016/j.est.2022.105511.

[257] E. Braco, I. San Martin, P. Sanchis, A. Ursúa, and D.-I. Stroe, "Health indicator selection for state of health estimation of second-life lithium-ion batteries under extended ageing," *J. Energy Storage*, vol. 55, Nov. 2022, Art. no. 105366, doi: 10.1016/j.est.2022.105366.

[258] A. Bhatt, W. Ongsakul, N. Madhu, and J. G. Singh, "Machinelearning-basedapproach for useful capacity prediction ofsecond-lifebatteries employing appropriate input selection," *Int. J. Energy Res.*, vol. 45, no. 15, pp. 21023–21049, Dec. 2021, doi: 10.1002/er.7160.

[259] I. Sanz-Gorrachategui, P. Pastor-Flores, M. Pajovic, Y. Wang, P. V. Orlik, C. Bernal-Ruiz, A. Bono-Nuez, and J. S. Artal-Sevil, "Remaining useful life estimation for LFP cells in second-life applications," *IEEE Trans. Instrum. Meas.*, vol. 70, pp. 1–10, 2021, doi: 10.1109/TIM.2021.3055791.

[260] Y. Jiang, J. Jiang, C. Zhang, W. Zhang, Y. Gao, and N. Li, "State of health estimation of second-life $LiFePO_4$ batteries for energy storage applications," *J. Cleaner Prod.*, vol. 205, pp. 754–762, Dec. 2018, doi: 10.1016/j.jclepro.2018.09.149.

[261] L. Ma, C. Zhang, J. Wang, K. Wang, and J. Chen, "Study on capacity estimation methods of second-life application batteries," *World Electr. Vehicle J.*, vol. 12, no. 4, p. 163, Sep. 2021, doi: 10.3390/wevj12040163.

[262] B. Du, Z. Yu, S. Yi, Y. He, and Y. Luo, "State-of-charge estimation for second-life lithium-ion batteries based on cell difference model and adaptive fading unscented Kalman filter algorithm," *Int. J. Low-Carbon Technol.*, vol. 16, no. 3, pp. 927–939, Sep. 2021, doi: 10.1093/ijlct/ctab019.

[263] M. Tran, J. Sihvo, and T. Roinila, "Internal impedance in determining usability of used lithium-ion batteries in second-life applications," *IEEE Trans. Ind. Appl.*, vol. 59, no. 5, pp. 6513–6521, Sep. 2023, doi: 10.1109/TIA.2023.3280466.

[264] M. Faraji-Niri, M. Rashid, J. Sansom, M. Sheikh, D. Widanage, and J. Marco, "Accelerated state of health estimation of second life lithium-ion batteries via electrochemical impedance spectroscopy tests and machine learning techniques," *J. Energy Storage*, vol. 58, Feb. 2023, Art. no. 106295. [Online]. Available: https://www.sciencedirect.com/science/article/pii/S2352152X22022848

[265] T. Wang, Y. Jiang, L. Kang, and Y. Liu, "Determination of retirement points by using a multi-objective optimization to compromise the first and second life of electric vehicle batteries," *J. Cleaner Prod.*, vol. 275, Dec. 2020, Art. no. 123128, doi: 10.1016/j.jclepro.2020.123128.

[266] C. Zhang, H. Wang, and L. Wu, "Life prediction model for lithium-ion battery considering fast-charging protocol," *Energy*, vol. 263, Apr. 2023, Art. no. 126109. [Online]. Available: https://www.sciencedirect.com/science/article/pii/S0360544222029954

[267] G. Graber, V. Calderaro, V. Galdi, and A. Piccolo, "Battery second-life for dedicated and shared energy storage systems supporting EV charging stations," *Electronics*, vol. 9, no. 6, p. 939, Jun. 2020, doi: 10.3390/electronics9060939.

[268] J. Lacap, J. W. Park, and L. Beslow, "Development and demonstration of microgrid system utilizing second-life electric vehicle batteries," *J. Energy Storage*, vol. 41, Sep. 2021, Art. no. 102837. [Online]. Available: https://www.sciencedirect.com/science/article/pii/S2352152X21005594

[269] C. White, B. Thompson, and L. G. Swan, "Comparative performance study of electric vehicle batteries repurposed for electricity grid energy arbitrage," *Appl. Energy*, vol. 288, Apr. 2021, Art. no. 116637. [Online]. Available: https://www.sciencedirect.com/science/article/pii/S0306261921001720

[270] N. Fallah and C. Fitzpatrick, "Techno-financial investigation of second-life of electric vehicle batteries for energy imbalance services in the Irish electricity market," *Proc. CIRP*, vol. 105, pp. 164–170, Jan. 2022, doi: 10.1016/j.procir.2022.02.028.

[271] N. Fallah and C. Fitzpatrick, "How will retired electric vehicle batteries perform in grid-based second-life applications? A comparative techno-economic evaluation of used batteries in different scenarios," *J. Cleaner Prod.*, vol. 361, Aug. 2022, Art. no. 132281, doi: 10.1016/j.jclepro.2022.132281.

[272] H. Rallo, L. Canals Casals, D. De La Torre, R. Reinhardt, C. Marchante, and B. Amante, "Lithium-ion battery 2nd life used as a stationary energy storage system: Ageing and economic analysis in two real cases," *J. Cleaner Prod.*, vol. 272, Nov. 2020, Art. no. 122584, doi: 10.1016/j.jclepro.2020.122584.

[273] C. White, B. Thompson, and L. G. Swan, "Repurposed electric vehicle battery performance in second-life electricity grid frequency regulation service," *J. Energy Storage*, vol. 28, Apr. 2020, Art. no. 101278. [Online]. Available: https://www.sciencedirect.com/science/article/pii/S2352152X19315919

[274] L. Janota, T. Králík, and J. Knápek, "Second life batteries used in energy storage for frequency containment reserve service," *Energies*, vol. 13, no. 23, p. 6396, Dec. 2020, doi: 10.3390/en13236396.

[275] M. A. Varnosfaderani, D. Strickland, M. Ruse, and E. B. Castillo, "Sweat testing cycles of batteries for different electrical power applications," *IEEE Access*, vol. 7, pp. 132333–132342, 2019, doi: 10.1109/ACCESS.2019.2940846.

[276] A. Rahil, E. Partenie, M. Bowkett, M. H. Nazir, and M. M. Hussain, "Investigating the possibility of using second-life batteries for grid applications," *Battery Energy*, vol. 1, no. 3, Jul. 2022, Art. no. 20210001, doi: 10.1002/bte2.20210001.

[277] L. Canals Casals, M. Barbero, and C. Corchero, "Reused second life batteries for aggregated demand response services," *J. Cleaner Prod.*, vol. 212, pp. 99–108, Mar. 2019, doi: 10.1016/j.jclepro.2018.12.005.

[278] Energy Information Administration (EIA). *Battery Storage Use Cases 2016-2021*. Accessed: Mar. 25, 2024. [Online]. Available: https://www.eia.gov/analysis/studies/electricity/batterystorage/

[279] M. Terkes, A. Demirci, and E. Gokalp, "An evaluation of optimal sized second-life electric vehicle batteries improving technical, economic, and environmental effects of hybrid power systems," *Energy Convers. Manage.*, vol. 291, Sep. 2023, Art. no. 117272. [Online]. Available: https://www.sciencedirect.com/science/article/pii/S0196890423006180

[280] C. Zhu, J. Xu, K. Liu, and X. Li, "Feasibility analysis of transportation battery second life used in backup power for communication base station," in *Proc. IEEE Transp. Electrific. Conf. Expo, Asia–Pacific (ITEC Asia–Pacific)*, Aug. 2017, pp. 1–4, doi: 10.1109/ITEC-AP.2017.8080810.

[281] K. Nováková, A. Pražanová, D.-I. Stroe, and V. Knap, "Second-life of lithium-ion batteries from electric vehicles: Concept, aging, testing, and applications," *Energies*, vol. 16, no. 5, p. 2345, Feb. 2023. [Online]. Available: https://www.mdpi.com/1996-1073/16/5/2345

[282] S. Narayana Gowda, H. Nazaripouya, and R. Gadh, "Congestion relief services by vehicle-to-grid enabled electric vehicles considering battery degradation," *Sustainability*, vol. 15, no. 24, p. 16733, Dec. 2023. [Online]. Available: https://www.mdpi.com/2071-1050/15/24/16733

[283] N. Horesh, C. Quinn, H. Wang, R. Zane, M. Ferry, S. Tong, and J. C. Quinn, "Driving to the future of energy storage: Techno-economic analysis of a novel method to recondition second life electric vehicle batteries," *Appl. Energy*, vol. 295, Aug. 2021, Art. no. 117007, doi: 10.1016/j.apenergy.2021.117007.

[284] D. Stringer and J. Ma. (2018). *Where 3 Million Electric Vehicle Batteries Will Go When They Retire*. Bloomberg Businessweek. [Online]. Available: https://www.bloomberg.com/news/features/2018-06-27/where-3-million-electric-vehicle-batteries-will-go-when-they-retire

[285] Circular Energy Storage Research and Consulting. (2024). *Lithium-Ion Battery Recycling Capacity and Market Outlook 2024*. [Online]. Available: https://circularenergystorage.com/

[286] Capgemini. (2021). *World Energy Markets Observatory*. Enerdata, vaasaETT, Global. [Online]. Available: https://www.capgemini.com/au-en/wp-content/uploads/sites/9/2021/10/WEMO2021.pdf

[287] Transparency Market Research Inc. (2023). *Second-life EV Battery Market*. GlobeNewswire, Global. [Online]. Available: https://www.globenewswire.com/news-release/2023/11/30/2788582/32656/en/Second-life-EV-Battery-Market

[288] G. Reid and J. Julve. (2016). *Second Life-Batterien Als Flexible Speicher Für Erneuerbare Energien*. [Online]. Available: https://www.acamedia.info/sciences/sciliterature/globalw/reference/bee/SecondLife-BatterienalsflexibleEE-Speicher

[289] E. Cready, J. Lippert, J. Pihl, I. Weinstock, and P. Symons, "Technical and economic feasibility of applying used Ev batteries in stationary applications," Tech. Rep. [Online]. Available: https://www.osti.gov/biblio/809607

[290] H. E. Melin, "The lithium-ion battery end-of-life market—A baseline study," World Econ. Forum, Cologny, Switzerland, 2018. [Online]. Available: https://coilink.org/20.500.12592/kr041t

[291] S. I. Sun, A. J. Chipperfield, M. Kiaee, and R. G. A. Wills, "Effects of market dynamics on the time-evolving price of second-life electric vehicle batteries," *J. Energy Storage*, vol. 19, pp. 41–51, Oct. 2018, doi: 10.1016/j.est.2018.06.012.

[292] M. R. Palacín and A. de Guibert, "Why do batteries fail?" *Science*, vol. 351, no. 6273, Feb. 2016, Art. no. 1253292. [Online]. Available: https://www.science.org/doi/abs/10.1126/science.1253292

[293] G. Harper, R. Sommerville, E. Kendrick, L. Driscoll, P. Slater, R. Stolkin, A. Walton, P. Christensen, O. Heidrich, S. Lambert, A. Abbott, K. Ryder, L. Gaines, and P. Anderson, "Recycling lithium-ion batteries from electric vehicles," *Nature*, vol. 575, no. 7781, pp. 75–86, Nov. 2019, doi: 10.1038/s41586-019-1682-5.

[294] X. Zeng, J. Li, and N. Singh, "Recycling of spent lithium-ion battery: A critical review," *Crit. Rev. Environ. Sci. Technol.*, vol. 44, no. 10, pp. 1129–1165, May 2014, doi: 10.1080/10643389.2013.763578.

[295] J. Xiao, J. Li, and Z. Xu, "Challenges to future development of spent lithium ion batteries recovery from environmental and technological perspectives," *Environ. Sci. Technol.*, vol. 54, no. 1, pp. 9–25, Jan. 2020, doi: 10.1021/acs.est.9b03725.

[296] J. Zhang and G. Azimi, "Recycling of lithium, cobalt, nickel, and manganese from end-of-life lithium-ion battery of an electric vehicle using supercritical carbon dioxide," *Resour., Conservation Recycling*, vol. 187, Dec. 2022, Art. no. 106628, doi: 10.1016/j.resconrec.2022.106628.

[297] S. Al-Thyabat, T. Nakamura, E. Shibata, and A. Iizuka, "Adaptation of minerals processing operations for lithium-ion (LiBs) and nickel metal hydride (NiMH) batteries recycling: Critical review," *Minerals Eng.*, vol. 45, pp. 4–17, May 2013, doi: 10.1016/j.mineng.2012.12.005.

[298] J. Ordoñez, E. J. Gago, and A. Girard, "Processes and technologies for the recycling and recovery of spent lithium-ion batteries," *Renew. Sustain. Energy Rev.*, vol. 60, pp. 195–205, Jul. 2016, doi: 10.1016/j.rser.2015.12.363.

[299] B. Xin, D. Zhang, X. Zhang, Y. Xia, F. Wu, S. Chen, and L. Li, "Bioleaching mechanism of Co and Li from spent lithium-ion battery by the mixed culture of acidophilic sulfur-oxidizing and iron-oxidizing bacteria," *Bioresource Technol.*, vol. 100, no. 24, pp. 6163–6169, Dec. 2009, doi: 10.1016/j.biortech.2009.06.086.

[300] Y. Hong and M. Valix, "Bioleaching of electronic waste using acidophilic sulfur oxidising bacteria," *J. Cleaner Prod.*, vol. 65, pp. 465–472, Feb. 2014, doi: 10.1016/j.jclepro.2013.08.043.

[301] F. He, D. Tamberrino, V. Yang, H. Elder, F. He, M. Chu, and V. Yang. (2017). *China's Battery Challenge: A New Solution to a Growth Problem*. [Online]. Available: https://knowen-production.s3.amazonaws.com/uploads/attachment/file/3453/ChinaE28099s%2BBattery%2BChallenge%2BA%2Bnew%2Bsolution%2Bto%2Ba%2Bgrowth%2Bproblem.pdf

[302] Y. Choi and S.-W. Rhee, "Current status and perspectives on recycling of end-of-life battery of electric vehicle in Korea (republic of)," *Waste Manage.*, vol. 106, pp. 261–270, Apr. 2020, doi: 10.1016/j.wasman.2020.03.015.

[303] M. Kaya, "State-of-the-art lithium-ion battery recycling technologies," *Circular Economy*, vol. 1, no. 2, Dec. 2022, Art. no. 100015. [Online]. Available: https://linkinghub.elsevier.com/retrieve/pii/S2773167722000152

[304] N. Antuñano and I. Careaga. (2021). *Analysis of the Major Recycling Processes in the Battery Industry*. [Online]. Available: https://cicenergigune.com/en/blog/major-recycling-processes-battery-industry

[305] F. Arshad, L. Li, K. Amin, E. Fan, N. Manurkar, A. Ahmad, J. Yang, F. Wu, and R. Chen, "A comprehensive review of the advancement in recycling the anode and electrolyte from spent lithium ion batteries," *ACS Sustain. Chem. Eng.*, vol. 8, no. 36, pp. 13527–13554, Sep. 2020. [Online]. Available: https://pubs.acs.org/doi/10.1021/acssuschemeng.0c04940

[306] H. Ali, H. A. Khan, and M. Pecht, "Preprocessing of spent lithium-ion batteries for recycling: Need, methods, and trends," *Renew. Sustain. Energy Rev.*, vol. 168, Oct. 2022, Art. no. 112809. [Online]. Available: https://linkinghub.elsevier.com/retrieve/pii/S136403212200692X
[307] Z. J. Baum, R. E. Bird, X. Yu, and J. Ma, "Lithium-ion battery recycling overview of techniques and trends," *ACS Energy Lett.*, vol. 7, no. 2, pp. 712–719, Feb. 2022. [Online]. Available: https://pubs.acs.org/doi/10.1021/acsenergylett.1c02602
[308] M. Chen, X. Ma, B. Chen, R. Arsenault, P. Karlson, N. Simon, and Y. Wang, "Recycling end-of-life electric vehicle lithium-ion batteries," *Joule*, vol. 3, no. 11, pp. 2622–2646, Nov. 2019. [Online]. Available: https://linkinghub.elsevier.com/retrieve/pii/S254243511930474X
[309] C. Zhang, Y.-X. Chen, and Y.-X. Tian, "Collection and recycling decisions for electric vehicle end-of-life power batteries in the context of carbon emissions reduction," *Comput. Ind. Eng.*, vol. 175, Jan. 2023, Art. no. 108869. [Online]. Available: https://www.sciencedirect.com/science/article/pii/S0360835222008579
[310] J. Geng, S. Gao, X. Sun, Z. Liu, F. Zhao, and H. Hao, "Potential of electric vehicle batteries second use in energy storage systems: The case of China," *Energy*, vol. 253, Aug. 2022, Art. no. 124159. [Online]. Available: https://www.sciencedirect.com/science/article/pii/S0360544222010623
[311] M. Shafique, M. Rafiq, A. Azam, and X. Luo, "Material flow analysis for end-of-life lithium-ion batteries from battery electric vehicles in the USA and China," *Resour., Conservation Recycling*, vol. 178, Mar. 2022, Art. no. 106061, doi: 10.1016/j.resconrec.2021.106061.
[312] A. Nurdiawati and T. K. Agrawal, "Creating a circular EV battery value chain: End-of-life strategies and future perspective," *Resour., Conservation Recycling*, vol. 185, Oct. 2022, Art. no. 106484, doi: 10.1016/j.resconrec.2022.106484.
[313] N. Fallah, C. Fitzpatrick, S. Killian, and M. Johnson, "End-of-life electric vehicle battery stock estimation in Ireland through integrated energy and circular economy modelling," *Resour., Conservation Recycling*, vol. 174, Nov. 2021, Art. no. 105753, doi: 10.1016/j.resconrec.2021.105753.
[314] M. S. Crespo, M. Van Ginkel González, and L. T. Peiró, "Prospects on end of life electric vehicle batteries through 2050 in Catalonia," *Resour., Conservation Recycling*, vol. 180, May 2022, Art. no. 106133. [Online]. Available: https://www.sciencedirect.com/science/article/pii/S0921344921007412
[315] K. Richa, C. W. Babbitt, and G. Gaustad, "Eco-efficiency analysis of a lithium-ion battery waste hierarchy inspired by circular economy," *J. Ind. Ecology*, vol. 21, no. 3, pp. 715–730, Jun. 2017, doi: 10.1111/jiec.12607.
[316] L. Gaines, "Lithium-ion battery recycling processes: Research towards a sustainable course," *Sustain. Mater. Technol.*, vol. 17, Sep. 2018, Art. no. e00068, doi: 10.1016/j.susmat.2018.e00068.
[317] C. Liu, J. Lin, H. Cao, Y. Zhang, and Z. Sun, "Recycling of spent lithium-ion batteries in view of lithium recovery: A critical review," *J. Cleaner Prod.*, vol. 228, pp. 801–813, Aug. 2019, doi: 10.1016/j.jclepro.2019.04.304.
[318] K. M. Winslow, S. J. Laux, and T. G. Townsend, "A review on the growing concern and potential management strategies of waste lithium-ion batteries," *Resour., Conservation Recycling*, vol. 129, pp. 263–277, Feb. 2018, doi: 10.1016/j.resconrec.2017.11.001.
[319] PushEV. *Samsung SDI 94Ah Battery Cell Full Specifications*. Accessed: Jan. 13, 2024. [Online]. Available: https://pushevs.com/2018/04/05/samsung-sdi-94-ah-battery-cell-full-specifications/
[320] A. U. Schmid, M. Kurka, and K. P. Birke, "Reproducibility of Li-ion cell reassembling processes and their influence on coin cell aging," *J. Energy Storage*, vol. 24, Aug. 2019, Art. no. 100732. [Online]. Available: https://linkinghub.elsevier.com/retrieve/pii/S2352152X19300106
[321] Samsung SDI. (2016). *Safety Data Sheet*. [Online]. Available: https://www.powr-flite.com/media/pf/documentation/sds-sheets/sds-x1200-samsung-sdi.pdf
[322] BMW. (2016). *The BMW I3 Rescue Guideline*. [Online]. Available: https://www.press.bmwgroup.com/global/article/attachment/T0143924EN/222601
[323] S. Blankemeyer, D. Wiens, T. Wiese, A. Raatz, and S. Kara, "Investigation of the potential for an automated disassembly process of BEV batteries," *Proc. CIRP*, vol. 98, pp. 559–564, Jan. 2021. [Online]. Available: https://linkinghub.elsevier.com/retrieve/pii/S2212827121001815
[324] R. D'Souza, J. Patsavellas, and K. Salonitis, "Automated assembly of Li-ion vehicle batteries: A feasibility study," *Proc. CIRP*, vol. 93, pp. 131–136, Jan. 2020. [Online]. Available: https://linkinghub.elsevier.com/retrieve/pii/S2212827120307460
[325] K. Wegener, W. H. Chen, F. Dietrich, K. Dröder, and S. Kara, "Robot assisted disassembly for the recycling of electric vehicle batteries," *Proc. CIRP*, vol. 29, pp. 716–721, Jan. 2015. [Online]. Available: https://linkinghub.elsevier.com/retrieve/pii/S2212827115000931
[326] M. Hassini, E. Redondo-Iglesias, and P. Venet, "Second-life batteries modeling for performance tracking in a mobile charging station," *World Electr. Vehicle J.*, vol. 14, no. 4, p. 94, Apr. 2023. [Online]. Available: https://www.mdpi.com/2032-6653/14/4/94
[327] A. Takahashi, A. Allam, and S. Onori, "Evaluating the feasibility of batteries for second-life applications using machine learning," *iScience*, vol. 26, no. 4, Apr. 2023, Art. no. 106547, doi: 10.1016/j.isci.2023.106547.
[328] S. Tasnim Mowri, A. Barai, S. Moharana, A. Gupta, and J. Marco, "Assessing the impact of first-life lithium-ion battery degradation on second-life performance," *Energies*, vol. 17, no. 2, p. 501, Jan. 2024. [Online]. Available: https://www.mdpi.com/1996-1073/17/2/501
[329] W. Gao, Z. Cao, N. V. Kurdkandi, Y. Fu, and C. Mi, "Evaluation of the second-life potential of the first-generation Nissan leaf battery packs in energy storage systems," *eTransportation*, vol. 20, May 2024, Art. no. 100313. [Online]. Available: https://www.sciencedirect.com/science/article/pii/S2590116824000031
[330] A. A. Kebede, M. S. Hosen, T. Kalogiannis, H. A. Behabtu, M. Z. Assefa, T. Jemal, V. Ramayya, J. Van Mierlo, T. Coosemans, and M. Berecibar, "Optimal sizing and lifetime investigation of second life lithium-ion battery for grid-scale stationary application," *J. Energy Storage*, vol. 72, Nov. 2023, Art. no. 108541, doi: 10.1016/j.est.2023.108541.
[331] M. F. Börner, M. H. Frieges, B. Späth, K. Spütz, H. H. Heimes, D. U. Sauer, and W. Li, "Challenges of second-life concepts for retired electric vehicle batteries," *Cell Rep. Phys. Sci.*, vol. 3, no. 10, Oct. 2022, Art. no. 101095, doi: 10.1016/j.xcrp.2022.101095.
[332] R. H. E. M. Koppelaar, S. Pamidi, E. Hajósi, L. Herreras, P. Leroy, H.-Y. Jung, A. Concheso, R. Daniel, F. B. Francisco, C. Parrado, S. Dell'Ambrogio, F. Guggiari, D. Leone, and A. Fontana, "A digital product passport for critical raw materials reuse and recycling," *Sustainability*, vol. 15, no. 2, p. 1405, Jan. 2023, doi: 10.3390/su15021405.
[333] A. Weng, E. Dufek, and A. Stefanopoulou, "Battery passports for promoting electric vehicle resale and repurposing," *Joule*, vol. 7, no. 5, pp. 837–842, May 2023, doi: 10.1016/j.joule.2023.04.002.
[334] M. Zorn, C. Ionescu, D. Klohs, K. Zähl, N. Kisseler, A. Daldrup, S. Hams, Y. Zheng, C. Offermanns, S. Flamme, C. Henke, A. Kampker, and B. Friedrich, "An approach for automated disassembly of lithium-ion battery packs and high-quality recycling using computer vision, labeling, and material characterization," *Recycling*, vol. 7, no. 4, p. 48, Jul. 2022, doi: 10.3390/recycling7040048.
[335] M. Hassini, E. Redondo-Iglesias, and P. Venet, "Battery passports for second-life batteries: An experimental assessment of suitability for mobile applications," *Batteries*, vol. 10, no. 5, p. 153, 2024. [Online]. Available: https://www.mdpi.com/2313-0105/10/5/153
[336] TÜV Rheinland. (2023). *EU New Battery Regulation (EU) 2023/1542*. [Online]. Available: https://www.tuv.com/landingpage/en/eu-new-battery-regulation-eu-2023-1542/
[337] European Commission. (2023). *Regulation (EU) 2023/1542 of the European Parliament and of the Council Concerning Batteries and Waste Batteries*. [Online]. Available: https://eur-lex.europa.eu/eli/reg/2023/1542/oj
[338] U. Cali, M. Deveci, S. S. Saha, U. Halden, and F. Smarandache, "Prioritizing energy blockchain use cases using type-2 neutrosophic number-based EDAS," *IEEE Access*, vol. 10, pp. 34260–34276, 2022, doi: 10.1109/ACCESS.2022.3162190.
[339] M. Andoni, V. Robu, D. Flynn, S. Abram, D. Geach, D. Jenkins, P. McCallum, and A. Peacock, "Blockchain technology in the energy sector: A systematic review of challenges and opportunities," *Renew. Sustain. Energy Rev.*, vol. 100, pp. 143–174, Feb. 2019, doi: 10.1016/j.rser.2018.10.014.
[340] C. A. R. Júnior, E. R. Sanseverino, P. Gallo, D. Koch, H.-G. Schweiger, and H. Zanin, "Blockchain review for battery supply chain monitoring and battery trading," *Renew. Sustain. Energy Rev.*, vol. 157, Apr. 2022, Art. no. 112078, doi: 10.1016/j.rser.2022.112078.
[341] M. M. B. Klör, D. Beverungen, S. Bräuer, and F. Plenter, "A market for trading used electric vehicle batteries," in *Proc. 23rd Eur. Conf. Inf. Syst. (ECIS)*, 2015, pp. 1–15. [Online]. Available: https://web.archive.org/web/20200321143815id/https://aisel.aisnet.org/cgi/viewcontent.cgi?article=1104context=ecis2015cr
[342] M. E. Peck and D. Wagman, "Energy trading for fun and profit buy your neighbor's rooftop solar power or sell your own-it'll all be on a blockchain," *IEEE Spectr.*, vol. 54, no. 10, pp. 56–61, Oct. 2017, doi: 10.1109/MSPEC.2017.8048842.

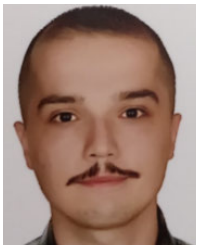

MUSA TERKES received the B.Sc. degree in electrical engineering from Yildiz Technical University (YTU), Istanbul, Türkiye, in 2019, and the M.Sc. degree in electrical power systems from the Graduate School of Science and Engineering, YTU, in 2022, where he is currently pursuing the Ph.D. degree in electrical power systems with the Graduate School of Science and Engineering. He assists in power systems, fault analysis, energy transmission, distribution systems course and teaches electrical power systems, lighting, electrical internal installation, and high voltage laboratories. His research interests include optimal sizing of hybrid power systems, control methods for energy storage systems, energy economics, benefits of renewable energy systems, grid effects of electric vehicles, energy management allocation of microgrids, second-life battery feasibility, and aging. He has published several articles related his research areas.

ALPASLAN DEMIRCI (Member, IEEE) received the B.Sc. degree in electrical and electronics engineering from Sakarya University, Türkiye, the B.Sc. and M.Sc. degrees in electrical education from Marmara University, stanbul, Türkiye, in 2007 and 2011, respectively, and the Ph.D. degree in electrical engineering from the Graduate School of Science and Engineering, Yildiz Technical University (YTU), stanbul, in 2023. He is currently an Associate Professor with the Department of Electrical Engineering, YTU. His research interests include power system optimization methods, distributed renewable energy systems, energy economics, electric vehicles, and energy storage systems. He has published several articles related his research areas.

ERDIN GOKALP received the B.Sc., M.Sc., and Ph.D. degrees in electrical engineering from Yildiz Technical University, Istanbul, Türkiye, in 1986, 1988, and 1994, respectively. He has been an Associate Professor with the Department of Electrical Engineering, Yildiz Technical University, since 2022. He is the author of several articles and conference papers. His research interests include power system analysis, renewable energy, power transmission and distribution, and smart grids.

UMIT CALI (Senior Member, IEEE) received the B.E. degree in electrical engineering from Yildiz Technical University, Istanbul, Türkiye, in 2000, and the M.Sc. degree in electrical communication engineering and the Ph.D. degree in electrical engineering and computer science from the University of Kassel, Germany, in 2005 and 2010, respectively. He is currently a Professor in digital engineering for future technologies with the University of York, U.K. He joined the Department of Electric Power Engineering, Norwegian University of Science and Technology, Norway, in 2020, as an Associate Professor and was promoted to a Full Professor, in 2023. He was with the University of Wisconsin-Platteville and University of North Carolina at Charlotte as an Assistant Professor, between 2013 and 2020, respectively. His current research interests include energy informatics, artificial intelligence, blockchain technology, renewable energy systems, and energy economics. He is serving as the active Vice Chair for the IEEE Blockchain in Energy Standards WG (P2418.5).